UNIVERSIDAD DE LA FRONTERA

Facultad de Ingeniería, Ciencias y Administración
Programa Doctorado y Magíster en Recursos Naturales

"BIOFERTILIZERS BASED ON THE COMPLEX PHOSPHATASE-NANOCLAYS FROM AN ANDISOL AND AEROBIC STABILIZED CATTLE DUNG"

TESIS PARA OPTAR AL GRADO DE
DOCTOR EN CIENCIAS DE RECURSOS
NATURALES

MARCELA CALABI FLOODY

TEMUCO – CHILE
2011

"BIOFERTILIZERS BASED ON THE COMPLEX PHOSPHATASE-NANOCLAYS FROM AN ANDISOL AND AEROBIC STABILIZED CATTLE DUNG"

Esta Tesis es realizada bajo la supervisión de la Directora de Tesis, Dra. MARÍA DE LA LUZ MORA GIL, del Departamento de Ciencias Químicas y ha sido aprobada por los miembros de la comisión examinadora.

MARCELA CALABY FLOODY

DIRECTOR PROGRAMA DE POSTGRADO EN CIENCIAS DE RECURSOS NATURALES

Dra. MARÍA DE LA LUZ MORA

Dr. FERNANDO BORIE B.

DIRECCIÓN DE POSTGRADO UNIVERSIDAD DE LA FRONTERA

Dra. MARYSOL ALVEAR Z.

DR. GERARDO GALINDO G.

DR. PATRICIO REYES NÚÑEZ

Papas les dedico mí tesis por su incondicional amor, apoyo, y todo lo que me han enseñado en la vida, los adoro…

Agradecimientos/ Acknowledgements

Quisiera agradecer a mi tutora de tesis la Dra. María de la Luz Mora, por haberme permitido desarrollar la tesis doctoral junto a su equipo de trabajo, y por haber contribuido en mi formación profesional y científica; a los docentes del programa de Doctorado en Ciencias de Recursos Naturales, especialmente a la Dra. Alejandra Jara y al Dr. Milko Jorquera por su apoyo y conocimientos entregados.

I gratefully acknowledge to the Prof. Dr. Mark Welland for allowing me to do a research stay in his group at the Nanoscience Centre, University of Cambridge, UK. I would thank colleagues at the Nanoscience Centre for their assistance and input especially from Dr James Bendall. I wish to acknowledge the help that I received from Prof. Dr. Cornelia Rumpel, her disposition and kindness every time I needed and also for allowed me to do a research stay in her group at the Laboratoire de Biogéochimie et Ecologie des Milieux Continentaux (BIOEMCO) Centre INRA Versailles-Grignon, France.

Mis mayores agradecimientos son para mi familia, quienes son el motor de mi vida y de quienes me enorgullezco. Agradezco a Dios por haberme dado la familia que tengo, que con el tiempo ha ido creciendo y enriqueciendose, gracias a todos y cada uno de ustedes por acompañarme en cada momento, sobre todo en los momentos difíciles, por enseñarme y malcriarme, por todo el amor que me brindan. Ale gracias especialmente por siempre preocuparte de mi y más allá de ser mi hermana ser mi amiga. Amor, gracias por formar parte de mi vida, por tu amor, apoyo, preocupación y toda felicidad que me has dado.

Con mucho cariño quiero agradecer a todas las personas y compañeros que han hecho posible el desarrollo de esta tesis, por su amistad, por su ayuda, consejos y compañía, agradezco a todo el personal del Laboratorio de Suelo de la Universidad de la Fontera, quienes me brindaron un grato lugar de trabajo en estos años especialmente a Juanita, Olguita, y a mis amigas Ale y Fanny. A mi gran amigo Oscar que ha sido un pilar fundamental para alcanzar este momento, mis más sinceros agradecimientos por tu compañía, e incondicional apoyo y ayuda. También quiero agradecer a mis amigas Marce y Mali por sus consejos, hospitalidad cuando me han recibido en sus hogares y sobre todo por su amistad.

Finalmente quiero agradecer a la Comisión de Investigación Científica y Tecnológica (Conicyt) quien me brindo la posibilidad de poder desarrollarme personal y profesionalmente, gracias por las becas otorgadas espcialmente para manutención la cual me

permitió dedicarme por completo a mi doctorado, apoyo de tesis (AT-24080106) y pasantías en el extranjero. Quiero agradecer también por el financiamiento a través del proyecto ECOSSUD-CONICYT C08U01 y a los proyectos FONDECYT 1061262, 1100625 y 11070241.

Abstract

Andisols of Southern Chile support around 60% of the Chilean agriculture. However these soils have a high phosphorus fixation capacity. In these soils, large amounts of P applied to soil as inorganic fertilizer, around 80% of the added total P, are rapidly become unavailable to the plants and incorporated into organic matter or relatively insoluble inorganic P minerals. Thus, the use of these fertilizers leads a high cost and environmental damage. Another P reservoir for plant nutrition could be organic wastes P-rich with low P bioavailable, such as cattle dung, which are a highly produced in our country. For these reason it is necessary to find new alternatives to dispose these P reserves. Phosphohydrolases are essential in P cycle in soils. However, phosphohydrolases, such as phosphatases, are naturally immobilized obtaining stabilization and protection against environmental factors, but their catalytic activity can be decreased. In this context, the nanotechnology applied to enzyme immobilization can be a suitable alternative to release P from cattle dung and Andisols, because enzyme immobilization in nanomaterials has reported improvement in its catalytic activity. Recent studies have showed that acid phosphatase immobilized on allophanic clays from Andisols of Southern Chile, increased its catalytic activity respect to the free enzyme, but major efforts are required to know if immobilized acid phosphatase could increase the P bioavailability contained in animal wastes and Andisol reserves. The main aims of this work were: i) To extract natural nanoclays from an Andisol of the Southern Chile to evaluate its role like agent in the carbon stabilization, and study as support material for acid phosphatase immobilization, and ii) To produce a biofertilizer based in allophanic nanoclay-phosphatase complexes and aerobic stabilized cattle dung in order to increase the phosphate availability.

An Andisol, from Piedras Negras Series, taken from Southern Chile was sampled within 0–20 cm of depth, sieved to 2 mm mesh and air-dried. One part of the soil was treated with 30% hydrogen peroxide to remove the soil organic matter. The separation of particle-size < 2 μm fractions was performed by sedimentation procedures based on Stoke's law. The nanoclays were extracted from allophanic and montmorillonite clays (AppliChem A6918, LOT 7W007719). The clays and nanoclays were characterized by elemental analysis, pyrolysis GC/MS, electron and atomic force microscopy, infrared spectroscopy, and electrophoresis. The complexes were formed by interaction between acid phosphatase and allophanic and montmorillonite nanoclays, and used as model systems to simulate enzymatic reactions in heterogeneous environment. The enzymatic activities of free and immobilised phosphatase were assayed with 6 mM *p*-nitrophenylphosphate (*p*-NPP) and the concentration

of *p*-nitrophenol was determined by spectrophotometer at 405 nm. The kinetics parameters (V_{max} and K_m values) were calculated according to Michaelis–Menten equation. The phosphorous mineralization was determinate by colorimetric analysis.

The microscopy analysis showed that our modified methodology for nanoclays extraction allowed obtain aggregates with the high proportions of mesoporous, which are suitable to enzymatic immobilization. The natural nanoclay was dominantly consists of hollow allophane spherules forming globular aggregates of about 100 nm in diameter. And this fraction showed that organic matter governs the feature behavior and the aggregates of allophane nanoparticles retain a significant amount (~12 %) of carbon against intensive peroxide treatment, suggesting that this nano-fraction play an important role in carbon stabilization.

Our results show that acid phosphatase stabilization increased the specific activity (between 4 to 48 %) and V_{max} (between 38 and 28 %). These studies confirm that allophanic and montmorillonite clay and nanoclay support materials were suitable for acid phosphatase stabilization. However among these support materials, clay and nanoclay from Andisol were better than montmotillonite materials, showing a high increasing compared to free enzyme.

The P mineralization was governed by water-soluble P present on cattle dung. Therefore the high P_i initial concentration in degraded dung and large variability in P_i concentrations suggests a little influence on organic P mineralization by addition of free or support immobilized enzyme. However, more research involving initially low P_i containing organic materials is required to further assess the effectiveness of free or support material immobilized enzyme addition on P mineralization in animal wastes their implications on bioavailability of P_i in the rhizosphere.

Table of contents

Chapter 7 Appendix

Figure Indesx

Table Index

1

Introduction

1. Introduction

One of the main constraints to the Chilean agricultural production on Andisols is their low P availability. In Chile, Andisols cover around 60% (5.1 million ha) of agricultural land (Mora, 1992; Escudey et al., 2001; Matus et al., 2006) between latitude 19 ° to 56 ° supporting the bulk of agricultural production. Its mineralogy is dominated by allophane, and between 35 to 60% from the soil are clays (Escudey et al., 2001). Allophane is an aluminosilicate with spherical morphology, with an outer diameter of 3.5–5.0 nm (Abidin et al., 2007; Creton et al., 2008), capable to generate stable microaggregates with pore sizes in the nanoscale range. These soils have a high capacity of specific and nonspecific anion adsorption, and a high cation exchange capacity. It has been reported that essential nutrients (such as, phosphates and sulphates) to the plant are easily absorbed on these soil types (Escudey et al., 2001; Mora et al, 2005). More than 50% of fixed P is like organic-P unavailability to the plants (Borie y Rubio, 2003) resulting in nutritional deficit. However, these soils have a high P content, between 923 a 3000 mg kg^{-1} (Escudey et al., 2001), of which between 33 to 64 % corresponds to monoester-phosphate (Borie and Rubio, 2003, Briceño et al., 2005).

Agricultural wastes are suitable for organic fertilization by its high content of essential nutrients (N, P and S) (Baeza, 2002). Cattle dung is a organic waste rich in P because around 70% of ingested P by cattle is excreted (Rebollar y Mateos, 1999). In general, I animal dungs the P is found in inorganic (orthophosphate and pyrophosphate) and organic forms (phospholipids, DNA, phosphonates and phytate) (Fuentes et al., 2006). It has been reported that around 50% of P from the dung is in organic forms (Barnett, 1994). Previous at its application on the soil, this waste must be stabilized due to pathogen and seed contents (Fuentes et al., 2009a). In this context, the simpler and inexpensive technology used to stabilize organic wastes is the aerobic composting (Traoré et al., 1999; Garrido et al., 2002; Speir et al., 2004). This waste, added to the potentially P available in Andisols of Southern Chile might contribute to the plant nutrition, reducing the application of chemical fertilizers (100 - 150 kg P ha^{-1} yr^{-1}) in productive systems. Therefore, it is necessary find new ways to improve the organic P availability for plant nutrition.

Extracellular enzymes such as phosphatases and proteases secreted by microorganisms are important on biogeochemical cycles in soil (Allison, 2006). Enzymes have high affinity by clay minerals (<2 μm). Thus, a high proportion of they are naturally immobilized in soils, giving them protection against denaturation, and improving their thermal and chemical

stability (Ensminger and Gieseking, 1942; Gianfreda and Bollag, 2002). However, its catalytic efficiency can be decreased (Rao and Gianfreda, 2000, Kelleher et al., 2004, Huang et al., 2005).

The allophane aggregates have similar physical characteristics to silica nanomaterials (Woignier et al., 2007) which are very important in biocatalysis (Kim et al. 2006). Studies on acid phosphatase immobilization in natural and synthetic mineral clays have reported low enzyme load and loss in their catalytic efficiency (Rao and Gianfreda, 2000, Kelleher et al., 2004, Huang et al., 2005). However, acid phosphatase immobilized on silica nanopores showed an increase in their activity and catalytic efficiency (Wei et al., 2001). Preliminary researches in our group showed that acid phosphatase immobilized in allophanic clays increase its activity respect to the free enzyme (Rosas et al., 2008, Calabi-Floody et al., 2008). Based on our results, and enzyme catalytic activity improvement reported in the enzymatic immobilization on nanomaterials (Wang et al., 2006, Kim et al., 2006, Li and Hu, 2003, Liu et al., 2005), more studies are required to know if immobilized acid phosphatase on nanoclays could increase the P bioavailability contained in animal wastes and Andisol reserves.

1.1 Hypotheses

The black carbon has a strong interaction with the nano-fraction in Andisols of the southern Chile playing an important role in the carbon stabilization.

The catalytic efficiency and V_{max} of the acid phosphatase immobilized on nanoclay from an Andisol will increase due to the specific structure and physicochemical characteristics of these nanoclays.

The phosphorus availability will be increase in the aerobic stabilized cattle dung by application of phosphatase-nanoclay complexes.

1.2 General objective

To extract natural nanoclays from an Andisol of the Southern Chile to evaluate its role like agent in the carbon stabilization, and study as support material for acid phosphatase immobilization.

To produce a biofertilizer based in allophanic nanoclay-phosphatase complexes and aerobic stabilized cattle dung in order to increase the phosphate availability.

1.3 Specific objectives

1. To determine the operational conditions for the extraction of nanoclays from an Andisol of the southern Chile and their structural and physicochemical characteristics (heterogeneity and relation with the superficial activity).
2. To determine the carbon content and chemical compounds in the nanoclay fraction from an Andisol of the southern Chile.
3. To determine the catalytic properties and stability of phosphatase when is immobilized in natural nanoclays (allophane) and identify related mechanisms.
4. To compare the nanometric scale effect of the support materials in the catalytic properties of phosphatase immobilized in nanoclays (allophane and montmorillionite).
5. To evaluate the capacity of the phosphatase-nanoclay complex on phosphate mineralization in aerobic stabilized cattle dung to produce biofertilizers.

2

Theoretical Background

Natural nanoclays: applications and future trends – a Chilean perspective

Marcela Calabi Floody[1], Benny K.G.Theng[2], Patricio Reyes[3] and María de la Luz Mora[4*]

[1]*Programa de Doctorado en Ciencias de Recursos Naturales Universidad de La Frontera, Temuco, Chile,* [2]*Landcare Research, Private Bag 11052, Palmerston North 4442, New Zealand,* [3]*Departamento de Físico Química, Universidad de Concepción, Concepción, Chile,* [4]*Departamento de Ciencias Química, Universidad de La Frontera, Casilla 54-D, Temuco, Chile*

2.1 Abstract

Because of their large potential for agricultural, industrial, and medicinal applications**,** nanomaterials have been the focus of much research during the past few decades. Nanoclays are natural nanomaterials that occur in the clay fraction of soil, among which montmorillonite and allophane are the most important species. Montmorillonite is a crystalline hydrous phyllosilicate (layer silicate). Organically modified montmorillonites or 'organoclays', formed by intercalation of quaternary ammonium cations, have long been used as rheological modifiers and additives in paints, inks, greases and cosmetics, and as carriers and delivery systems for the controlled release of drugs. Perhaps the largest, single usage of organoclays over recent years has been in the manufacture of polymer-clay nanocomposites. These organic-inorganic hybrid materials show superior mechanical, thermal, and gas barrier properties. Organoclays are also useful in pollution control and water treatment. Allophane is a non-crystalline aluminosilicate derived from the weathering of volcanic ash. A large proportion of the agricultural land in Chile is covered by volcanic soils whose clay fraction is dominated by allophane. Consisting of nanosize (3.5–5.0 nm) hollow spherules, allophane is a suitable support material for enzyme immobilization. Allophane is also effective in adsorbing phenolic compounds and colour from kraft mill effluents, and phosphate from water and wastewater.

Keywords: nanoclay, nanomaterials, polymer-clay nanocomposites, organoclays, allophane, volcanic soils, Chile

2.2 Introduction

Nanotechnology is concerned with the design, synthesis, and use of materials at the nanoscale level, ranging from 1 to 100 nanometres (EPA, 2007). The term 'nano' comes from the Greek *nanos*, meaning dwarf, and when used as a prefix indicates 10^{-9}. A widely accepted definition for nanomaterials is that their particles have at least one dimension smaller than 100 nanometres (Holister et al., 2003). The width of one nanometre (nm) is around 100 000 times smaller than the diameter of a single human hair, while its length is in the range of individual molecules (Macilwain, 1999; Qian and Hinestroza, 2004).

Because of their nanoscale dimensions and large surface area/volume ratio, nanomaterials have properties (electronic, kinetic, magnetic, optical) that are very different from those of their bulk counterparts. For example, nanomaterials are transparent since their particles are smaller than the wavelength of light. We might add that some properties of nanoparticles may not be predictable due to the increased influence of superficial atoms or quantum effects (Holister et al., 2003). The peculiar properties of nanomaterials are useful and important to the manufacture of packaging, cosmetic, biomedical, and electronic materials (Kim et al., 2006; Nowack and Bucheli, 2007). Thus, cell phones, computers, cosmetics, paints, pharmaceuticals, sporting goods, and textiles all contain nanomaterials of one kind or another. (Medina et al., 2007). Indeed, the impact of nanotechnology on society has been referred to as the "second industrial revolution" (Qian and Hinestroza, 2004). The developed countries have allocated sizeable funds to developing nanomaterials for industrial and household applications. The World Technology Division estimated that in 1997 the USA alone spent US$116 million, while Japan and Western Europe separately spent about US$120 million on nanotechnological research and development. Worldwide expenditure on nanotechnology has since increased by leaps and bounds (Macilwain, 1999).

Some nanomaterials (e.g., carbon black, soot), have long been known and used by humans. Humans are also exposed to a range of engineered and anthropogenic nanoparticles (e.g., carbon nanotubes, fullerenes, photocatalysts, vehicle exhaust emissions) in the ambient environment (air, water, soil), raising concerns about their potential adverse effects on health (Nowack and Bucheli, 2007). Here we review information on the use and potential applications of natural nanoclays with particular reference to allophane, the dominant nanoclay constituent of volcanic soils.

2.3 Clays as natural nanomaterials

In soil science, the term ’clay fraction’ (or simply ‘clay’) refers to a class of materials whose particles are smaller than 2 μm in equivalent spherical diameter. The clay fraction would therefore include ‘nanoclays’ the particles of which are smaller than 100 nm. Soil nanoclays are commonly dominated by phyllosilicates, and often contain metal (hydr) oxides and organic matter (Tan, 1998; Porta et al., 2003; Theng and Yuan, 2008). Nanoclays may be separated from the clay fraction or the bulk clay material by a variety of methods (Table 2.1).

Table 2.1. Methods used for extracting and processing nanoclays.

Method	***Reference***
Energetic stirring, centrifugation and freeze-drying	Liu *et al*. (2005); Li & Hu (2003)
Ultracentrifugation	*Joussein* et al. *(2007)*
Ultrasonication (to disperse or exfoliate nanoclays)	*Jeon* et al. *(2003) ; Dean* et al. *(2007) ; Sun* et al. *(2007)*
Centrifugation and cross-flow filtration	*Tang* et al. *(2008)*

The basic structural unit of phyllosilicates (clay minerals) is a layer comprising a silica tetrahedral sheet and an alumina octahedral sheet. (Fig. 2.1). In 1:1 type phyllosilicates (e.g., kaolinite), each layer is made up of one tetrahedral and one octahedral sheet, while individual layers in 2:1 type phyllosilicates (e.g., montmorillonite) consist of an octahedral sheet sandwiched between two tetrahedral sheets. Because of isomorphous substitution (e.g., Al^{3+} for Si^{4+} in the tetrahedral sheet and Mg^{2+} for Al^{3+} in the octahedral sheet), the layers of many clay minerals (e.g., montmorillonite) carry a permanent negative charge which is balanced by exchangeable inorganic cations (Na^{+}, Ca^{2+}) occupying interlayer sites. The cation exchange capacity (CEC) of these minerals is, therefore, independent of medium pH. On the other hand, some nanoclays (e.g., allophane) have little, if any, isomorphous substitution within their structure. Thus, the surface charge and CEC of such materials vary with the pH of the ambient solution.

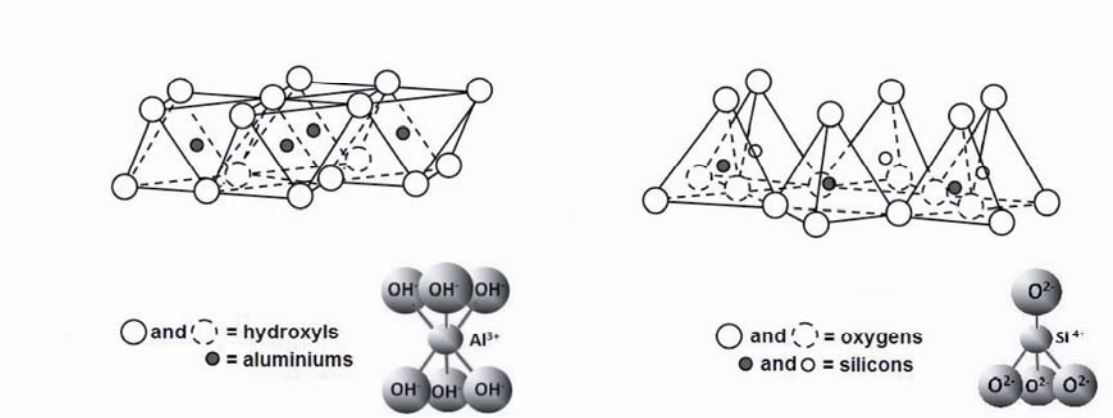

Figure 2.1. Structure of an alumina octahedral sheet (left) and a silica tetrahedral sheet (right) (adapted from McLaren & Cameron, 2000).

The clay fraction of soils may contain both crystalline (e.g., phyllosilicates) and non-crystalline (e.g., allophane, imogolite) minerals. Table 2.2 gives a simplified classification scheme for phyllosilicates (Guggenheim et al., 2006) and non-crystalline clays.

Because of their abundance (in soils and sediments), low cost, and environmentally friendly nature, clays and clay minerals (allophane, kaolinite, montmorillonite) have found applications in many fields, including medicine, pharmacy (Carretero et al., 2006; Droy-Lefaix and Tateo, 2006; Gomes and Silva, 2007), and catalysis (Causserand et al., 2001; Lojou et al., 2005; Biondi et al., 2007; Villegas et al., 2007) as well as in the manufacture of cosmetics, paint, and ink (Burgentzlé et al., 2004). These materials are also useful for environmental protection and remediation such as the removal of grease, oil and nitrogen from water and wastewater, and the sequestration of heavy metals in contaminated soils (Lee et al., 2003; Zhou et al., 2003; Khider et al., 2004; Rahman et al., 2005; Churchman et al., 2006; Shahwan et al., 2006; Volzone, 2007; Yuan and Wu, 2007).

Table 2.2. Classification of crystalline phyllosilicates and non-crystalline clays

Class	Layer type	Species*
Planar hydrous Phyllosilicates	1:1	Kaolinite, halloysite (planar), cronstedtite, lizardite, amesite
	2:1	Talc, kerolite, pyrophyllite, saponite, hectorite,sauconite, montmorillonite, beidellite, nontronite, vermiculite, phlogopite, muscovite, paragonite, wonesite, bityite, margarite, clinochlore, donbassite
Non-planar hydrous phyllosilicates	1:1	Antigorite, bementite, greenalite, pyrosmalite, friedelite, schallerite, megillite
	2:1	Palygorskite, sepiolite, falcondoite, minnesotaite, stilpnomelane, ganophyllite, zussmanite, gonyerite, parsettensite.
Non-crystalline clays		Allophane, imogolite†

*not an exhaustive list of species; †imogolite has long-range order along the tubule axis

2.4 Nanoclays and organoclays

The term ‘nanoclays’ is used here to denote clays and clay minerals whose particles have at least one dimension in the nanoscale range (1–100 nm). The classic and most well-known example of a nanoclay is montmorillonite (Lepoittevin et al., 2002; Jeon et al., 2003; Wang et al., 2007), a species of the smectite group of hydrous phyllosilicates (Guggenheim et al., 2006). Other species in the group include hectorite and saponite (Table 2.2). Although a montmorillonite particle is several hundred nanometers long (and wide), its thickness is in the

nanoscale range (< 10 nm). Montmorillonite is naturally hydrophilic because of the presence of hydrated inorganic counterions (Na^+ or Ca^{2+}) in the interlayer space. Since many applications involve intimate mixing of mineral with an organic or polymer phase, the montmorillonite surface must first be rendered hydrophobic. This may be achieved by replacing the counterions with organic cations, commonly long-chain quaternary ammonium or phosphonium cations (Hedley et al., 2007). Montmorillonites intercalated with quaternary ammonium cations (QACs) are known as 'organoclays' (Churchman et al., 2006). Another nanoclay of importance is allophane, consisting of spheroidal particles with a diameter of 3.5–5.0 nm. The structure, properties, and applications of allophane are summarized below.

2.5 Applications of nanoclays and organoclays

2.5.1 Polymer-clay nanocomposites

Perhaps the single most important application of (hydrophobic) organoclays is in the formulation and synthesis of polymer-clay nanocomposites. As the name suggests, these 'hybrid' materials consist of a continuous (polymer) phase or matrix and a dispersed (organoclay) phase. The incorporation into polymers of fine-grained solids ('microfillers'), such as cellulose, calcium carbonate, coal, metal oxides, and silica as reinforcing agents has been practised for a long time (Deshmane et al., 2007; Subramani et al., 2007). The use of (organoclay) nanofillers, however, is a relatively recent development (Lepoittevin et al., 2002; Jeon et al., 2003; Cotterell et al., 2007; Deshmane et al., 2007; Wang et al., 2007). Since the nanofiller particles have a high aspect (length/thickness) ratio, the dispersion of a small amount (< 10%) in the polymer matrix can lead to marked improvements in physical properties compared with the corresponding original, unfilled polymers or conventional microcomposites. In a pioneering work, scientists at Toyota Central Research Laboratories prepared a nylon-clay nanocomposite by intercalating ε-caprolactam into an organoclay, and polymerizing the monomer by heating (Fukushima and Inagaki, 1987). The resultant nylon-6 nancomposite has superior mechanical and thermal properties relative to the pristine polymer (Table 2.3).

Table 2.3. Comparing some physical properties of pristine nylon-6 polymer with those of nylon-6-organoclay nanocomposites and the polymer filled with mineral or glass fibres (Patel *et al*., 2006).

Materials property	Pristine nylon-6	3–6% Organoclay	30% Mineral	30% Glass fibre
Tensile strength ($\times 10^4$ kPa)*	4.999	8.136	5.516	15.8585
Flexural modulus (kPa)	827	344.75	4481.75	6895
Notched izod impact strength (J)	1.2	1.2	1.6	1.8
Heat deflection temperature (°C)	66	110	120	194
Specific gravity (g/cc)	1.3	1.14	1.36	1.35

Apart from showing superior tensile, flexural, and impact strengths as well as heat distortion (deflection) temperature, polymer-clay nanocomposites generally display significant improvements in break elongation, storage stability, flame retardancy, solvent resistance, and gas barrier properties over the corresponding neat polymers (Yasmin et al., 2003; Burgentzlé et al., 2004; Kashiwagi et al., 2005; Dean et al., 2007; Deshmane et al., 2007; Huang and Netravali, 2007; Ludueña et al., 2007; Maharsia and Jerro, 2007;.Malucelli et al., 2007; Subramani et al., 2007; Wang et al., 2007) (Table 2.4). Some strain-related properties, such as notched impact strength, however, may be inferior to those of the starting polymers. This problem may be overcome by incorporating a second polymer species to yield ternary nanocomposites (Drozdov and Christiansen, 2007; Wang et al., 2007).

Because of their huge potential for industrial and technological applications, polymer-clay nanocomposites have attracted a great deal of attention as attested by the huge volume of literature that has accumulated over the last decade (e.g., Lepoittevin et al., 2002; Jeon et al., 2003; Burgentzlé et al, 2004; Horrocks et al., 2005**;** Kashiwagi et al., 2005; Patel et al., 2006; Ruiz-Hitzky and van Meerbeek, 2006; Tjong, 2006**;** Zhang et al., 2006; Ibarra et al., 2007; Liff et al., 2007; Sun et al., 2007). Indeed, more than 90% of the publications on nanoclays and organoclays relate to their use in the synthesis and development of polymer nanocomposites. A similar situation applies to the patent literature.

Table 2.4. Improvements in the properties of polymers due to incorporation of organoclays

Property	**Reference** (selective)
Mechanical behaviour	Huang et al. (2004); Huang and Netravali (2007)
Tensile strength	Ng et al.(2001); Rong et al.(2001); Siegel et al. (2001); Chan et al. (2002)
Impact strength	Deshmane et al.(2007)
Break elongation	Dean et al. (2007)
Tensile/flexural strength	Usuki et al.(1993); Manias et al. (2001)
Stiffness/strength/toughness	Pinnavaia and Beall (2000)
Storage stability	Subramani et al. (2007)
Elastic modulus	Yasmin et al. (2003)
Flame retardancy	Ludueña et al. (2007) ; Pinnavaia and Beall (2000); Wei et al. (2002); Lu et al. (2001); Nam et al. (2001); Fornes et al. (2001)
Heat distortion temperature (HDT)	Gilman (1999); Gilman et al. (2000); Pinnavaia and Beall (2000); Kashiwagi et al. (2005)
Solvent resistance	Giannelis et al. (1999); Kornmann et al. (2001)
Gas barrier	Park et al. (2003); Anon. (2005); Yeh et al. (2004); Ragauskas (2004); Brody (2003); Sun et al. (2007); Burgentzlé et al. (2004)
Electrical conductivity (diminished)	Ludueña et al. (2007)

Polymer-clay nanocomposites, initially developed for the aerospace industry, now feature in almost every area of modern industrial production and enterprise, such as automobiles, household appliances, medicine, weaponry, civil infrastructure, and packaging (Huang and Netravali, 2007; Ray et al., 2007). Packaging and the associated food industry are the biggest users of these materials, despite concerns about their environmental impact. Table 5 shows the applications of polymer-clay nanocomposites in a number of industries and the corresponding estimates of market size.

Table 2.5. Applications of polymer-clay nanocomposites and estimated market size (from Argonne National Laboratory, USA).

Technological application	Estimated market size (by 2009)
Polymer-clay nanocomposites	>450 × 10^6 kg
Packaging	166 × 10^6 kg
Automotive	157 × 10^6 kg
Building and construction	68 × 10^6 kg
Coatings	16 × 10^6 kg
Industrial	22 × 10^6 kg
Others	30 × 10^6 kg

The high demand for polymer-clay nanocomposites, and environmental concerns about their use, have stimulated research into using biodegradable (plant-derived) polymers, such as soy protein and starch. Since these biopoylmers are also renewable and recycleable, the products have been referred to as 'green' nanocomposites (Lepoittevin et al., 2002; Chabba and Netravali, 2004, 2005a, 2005b; Lodha & Netravali, 2005; Huang and Netravali, 2007; Dean et al., 2007; Ludueña et al., 2007).

2.5.2 Nanomaterials as supports in enzyme immobilization

Enzymes are natural biocatalysts of nanometre dimensions (Kim et al., 2006). Because enzymes are highly selective and efficient, the processes that they catalyze give rise to relatively little greenhouse gas emission and waste. Enzyme immobilization on solid supports has been used for many decades in order to facilitate catalyst recycling, continuous operation, and product purification. Various methods for enzyme immobilization have been studied, such as membrane encapsulation, encapsulation with glycolipids, incorporation into polymers, and sol-gel entrapment (Moelans et al., 2005). Immobilized enzymes also show great stability, allowing the operation to be carried out at extreme pH and temperature conditions, or in the presence of organic solvents (Wu et al., 2005).

The low efficiency of immobilized enzymes in large-scale bioprocessing, however, is often an obstacle to their use (Bai et al., 2006; Kim et al., 2006). In order to improve catalytic efficiency, many support materials with varied composition, shape, structure, and surface modification have been investigated. Many organic polymeric materials, however, are susceptible to microbial attack, are unstable in organic solvents, and difficult to dispose

(Crespo et al., 2005). On the other hand, inorganic support materials such as silica gel, alumina, and zeolites are promising because of their thermal and mechanical stability, non-toxicity, and high resistance to microbial attack and organic solvents (Bai et al., 2006). Furthermore, hard solids are generally more stable than soft materials (Wang, 2006).

Nanomaterials are more promising candidates for enzyme immobilization than conventional supports because they can carry a high enzyme load, while substrate diffusion is relatively unhindered (Kim et al., 2006; Wang, 2006). Enzymes immobilized on nanoparticles also show a high mobility and activity, suggesting that the molecules are not rigidly attached to the support materials (Wang, 2006). Moreover, the good match between the pore dimension of nanomaterials and enzyme molecular size has a stabilizing effect on the immobilized enzyme (Vamvakaki and Chaniotakis, 2007). Zhou and Dill (2001) reported the first theoretical study linking protein stabilization and confinement into nano-cages. They found that confinement of a protein into a cage of 2–6 times the diameter of the native protein greatly increases its stability towards irreversible unfolding or denaturation. On this basis, such materials as porous carbon, mesoporous silica and aluminosilicates have been shown to be suitable for protein adsorption and stabilization (Vamvakaki and Chaniotakis, 2007).

We should point out that the term ‘mesopores’ refer to a class of pores whose widths are between 2 and 50 nm which, therefore, fall within the nanoscale range. Accordingly, mesoporous materials, especially mesoporous silica have attracted much interest as possible supports for enzyme immobilization because the size of most enzyme molecules (3–6 nm) is comparable with the diameter of mesopores (Moelans et al., 2005; Kim et al., 2006; Wang, 2006). Having physical features closely similar to those of mesoporous silica, allophane ‘nanoballs’ seem well suited for enzyme immobilization (cf. Table 2.6). The same would apply to montmorillonite but little information is available on this point. Li & Hu (2003) and Liu et al. (2005) have immobilized enzymes on montmorillonite nanoclays using layer-by-layer deposition and core-shell nanoclustering techniques.

Table 2.6. Range of pore diameters for some mesoporous silisa-based materials and allophane (adapted from Moelans *et al*., 2005).

Material	**Pore range** (diameter in nm)	**Reference**
MCM-41	2–10	Kresge *et al.* (1992)
		Van Der Voort *et al*. (1998)
MCM-48	2–10	Kresge *et al*. (1992)
		Van Der Voort *et al*. (1998)
		Huo *et al*. (1996)
SBA-15	5–30	Zhao *et al*. (1998a)
		Zhao *et al*. (1998b)
		Kim & Stucky (2000)
SBA-16	5–30	Zhao *et al*. (1998b)
		Kim & Stucky (2000)
MSU-n	2–15	Bagshaw *et al*. (1995)
		Bossiere *et al*. (1999)
HMS	2–10	Tanev *et al*. (1995)
		Tanev *et al*. (1994)
MCF	20–40	Bagshaw (1999)
		Liu & Pinnavaia (2002)
Allophane	2–50	Montarges-Pelletier *et al.* (2005)

2.5.3 Other uses

Organoclays and other layer silicates (laponite, hectorite and saponite) have long been used as rheological modifiers and additives in paints, inks, greases, and cosmetics to enhance performance, thermal stability, colour retention, and coverage. Organoclays can also usefully serve as carriers and delivery systems for the controlled release of drugs. By this means, therapeutic activity is maximized, while negative side effects are minimized (Patel et al., 2006). Montmorillonite, in particular, has long been used to adsorb bacterial toxins associated with gastrointestinal disturbance and hydrogen ions produced in acidosis as well as steroidal metabolites associated with pregnancy (Carretero et al., 2006; Droy-Lefaix and Tateo, 2006). All three physiological conditions give rise to a host of common symptoms, including nausea,

vomiting, and diarrhoea which are also typical side effects caused by anticancer drugs (Dong and Feng, 2005).

An important application of organoclays over recent years has been in wastewater treatment. Here the long-chain quaternary ammonium cations (QACs) in the montmorillonite interlayers act as an organic phase into which organic pollutants in water can partition. As might be expected, partitioning efficiency increases as the water solubility of the organic substance decreases (Beall, 2003; Theng et al.,2008). Organoclays exhibit a synergistic effect when used in combination with other adsorbents (e.g., granular activated charcoal) in such processes as reverse osmosis. Sorption by organoclays is superior to other wastewater treatment technologies, especially when the wastewater contains substantial amounts of oil, grease, or humic acid (Patel et al., 2006; Hedley et al., 2007). Humic acid is a major contaminant of potable water, and difficult to remove using conventional flocculation techniques. If not removed, humic acid can give rise to unacceptable levels of carcinogenic trihalomethanes when the water is chlorinated (Beall, 2003).

2.6 Allophane: a natural nanoclay

Allophane is a non-crystalline ('short-range order') aluminosilicate which, together with imogolite, occurs widely in soils derived from volcanic ash (Andisols). The unit particle of imogolite is a slender hollow tubule with an outer and inner diameter of about 2 and 1 nm, respectively (Fig. 2.2, left). Its unit formula is usually written as $(OH)_3Al_2O_3SiOH$, showing an Al/Si ratio of 2.0, and indicating the sequence of ions from the periphery to the centre of the tubule where the orthosilicate group shares three oxygens with aluminium. Unlike imogolite, allophane has no fixed chemical composition in that its Al/Si ratio can vary between 1 and 2. Irrespective of composition and origin, however, the unit particle of allophane is a hollow spherule with an outer diameter of 3.5–5.0 nm. The 0.7–1.0 nm thick spherule wall is composed of an outer Al octahedral (gibbsitic) sheet and an inner Si sheet. Defects in the wall structure give rise to perforations of ~ 0.3 nm in diameter (Parfitt, 1990; Brigatti et al. 2006; Hashizume and Theng, 2007) (Fig. 2.2, right).

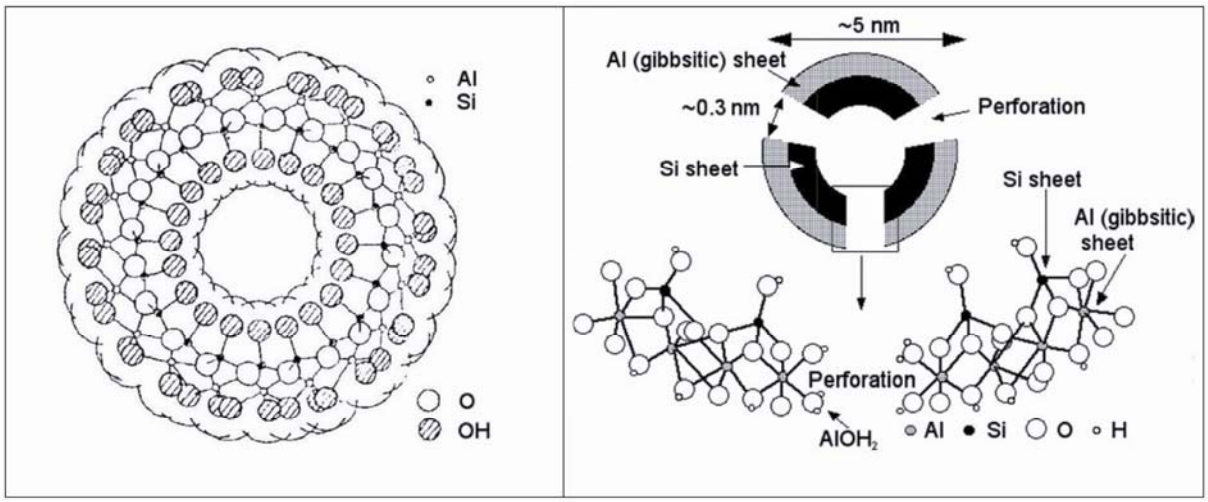

Figure 2.2. Cross-section of an imogolite tubule (left) (from McLaren and Cameron, 2000) and diagram of a unit particle of allophane (right) (from Hashizume and Theng, 2007).

Allophane has a high specific surface area. A value of about 1000 m^2g^{-1} is calculated for the external (interspherule) and internal (intraspherule) area on the basis of unit particle size and density, while 700–900 m^2g^{-1} is measured by retention of ethylene glycol and ethylene glycol monoethyl ether (Hall et al., 1985; Wada, 1989). Allophane has a variable (pH-dependent) surface charge attributable to the protonation and deprotonation of $(OH)Al(H_2O)$ groups exposed at perforations along the spherule wall. The point of zero net charge of allophane is about pH 6 (Mora et al., 1994; Hashizume and Theng, 2007). The chemical properties of allophane-rich soils reflect the surface charge characteristic of this nanoclay.

2.6.1 Allophane in Chile

Soils derived from volcanic ash (Andisols) occur in many parts of the world. They are especially widespread in Pacific-rim countries, such as Japan, Indonesia, Philippines, New Zealand, Western USA, Mexico, Central America, and Chile (Brady and Weil, 2002). In Chile volcanic soils cover about 60% (5.1 million ha) of agricultural land (Mora, 1992; Escudey et al., 2001; Matus et al., 2006).

Figure 2.3 shows a soil map of south-central Chile. On the basis of the USDA soil classification system, four soil orders may be distinguished: Andisols, Alfisols, Inceptisols, and Ultisols (Matus et al., 2006). The Andisols are rich in organic matter (1–25% w/w), have a high specific surface area, and a pH-dependent cation exchange capacity (CEC) (Mora, 1992; Escudey et al., 2001; Jara et al., 2005; Matus et al., 2006; Redel et al., 2007). Their clay fraction makes up 35–60% of the soil, and is dominated by allophane (Besoain and

Sepúlveda, 1985; Escudey et al., 2001). Having an Al:Si ratio of ~2:1, the allophane is apparently composed of fragments with an imogolite structure over a short range, often referred to as 'proto-imogolite allophane' or 'imogolite-like allophane' (Parfitt, 1990; Brigatti et al., 2006).

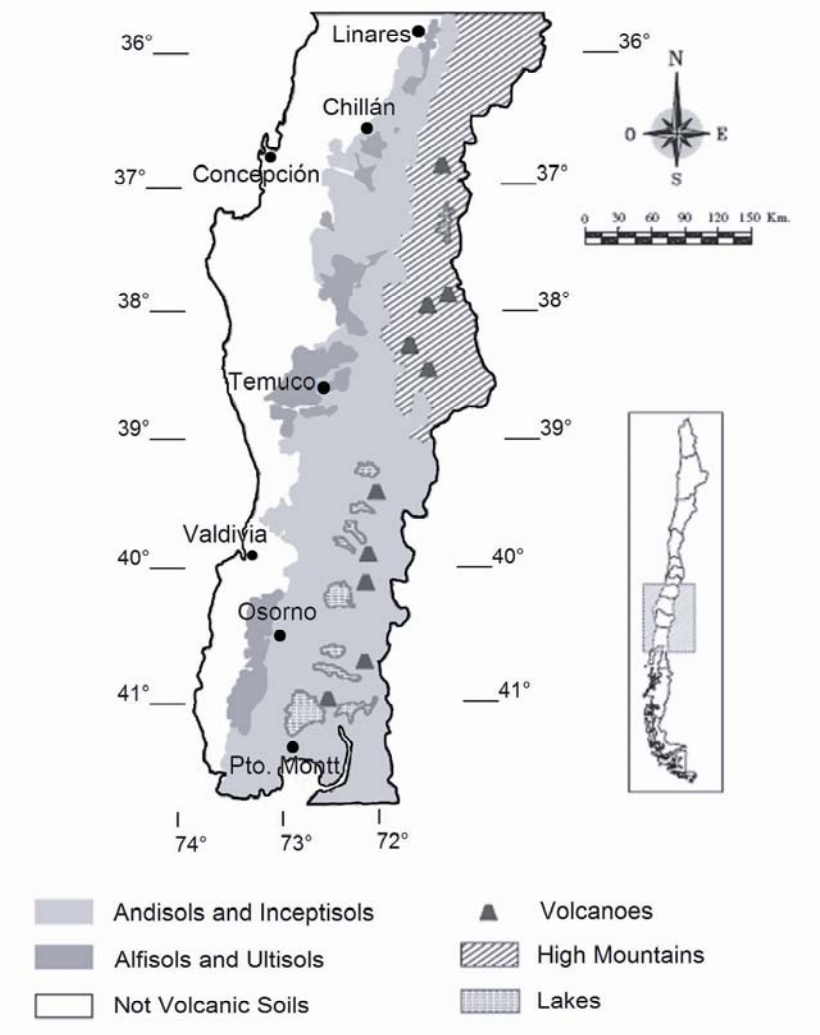

Figure 2.3. Distribution of volcanic soils in south-central Chile (from Matus et al., 2006)

We have extracted nanoclays from Andisols of the Temuco, Pemehue and Piedras Negras Series, located in southern Chile. Figure 2.4 compares the scanning electron microscopy (SEM) image of the clay fraction, separated from an Andisol from south-central Chile with that of an allophane from New Zealand. The similarity of the two images is striking. Figure 2.5 shows transmission electron microscopy (TEM) images of allophane and

other nanoclays separated from some Chilean Andisols. The allophane particles show up as non-crystalline hollow spherules with a diameter of 3–5 nm, giving no electron diffraction patterns (Figs. 2.5a, 2.5b, 2.5d). Some crystalline nanoparticles with a diameter of ≤ 50 nm also occur (Figs. 2.5c, 2.5e), while some nanoclay particles are less than 10 nm in diameter (Fig. 2.5f). These observations indicate that the method described by Li and Hu (2003) can be used to extract nanoclays with a particle size of less than 50 nm for varied practical applications.

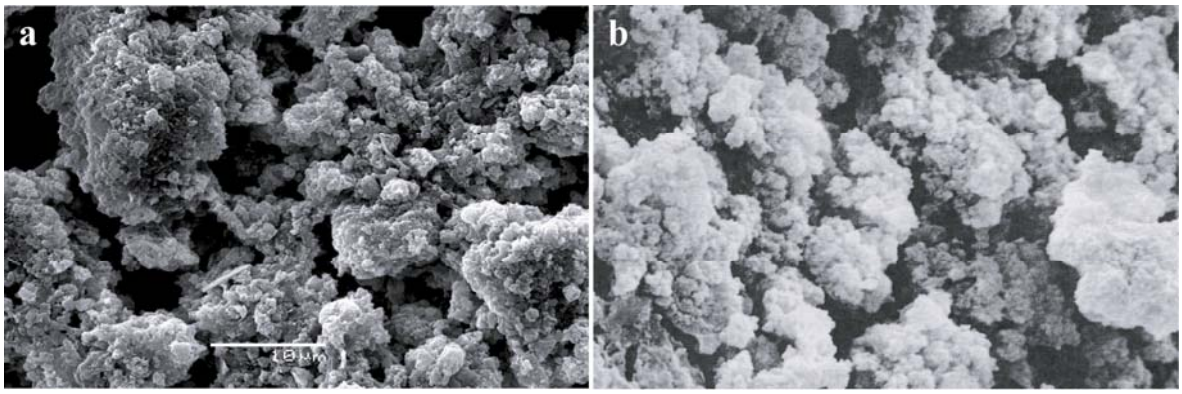

Figure 2.4. (a) Scanning electron microscopy (SEM) image of the clay fraction of an Andisol from Piedras Negras Series in southern Chile (unpublished data); (b) SEM image of allophane from Mangaturuturu River, New Zealand (from Browne and Soong, 1997; bar = 10 μm).

The physical characteristics and fractal geometry of allophane aggregates are similar to those of synthetic mesoporous silica-based materials (e.g., MCM–41, MCM–48, SBA–15, HMS, MSU, MCF) showing a high surface area (830–1500 $m^2\ g^{-1}$), high pore volume (1 ml g^{-1}), and well-ordered pore structure (2–40 nm) (Woignier et al., 2005, 2006, 2007). Mesoporous silicas have found applications in biocatalysis and enzyme immobilization because they are stable at high temperatures, while their pore diameter matches the size of enzyme molecules (Moelans et al., 2005; Kim et al., 2006; Wang, 2006). Likewise, allophane would have potential applications in biocatalysis and enzyme immobilization (Table 2.6). In keeping with this expectation, preliminary studies by our research group indicate that natural nanomaterials can serve as supports in enzyme immobilization. For example, acid phosphatase immobilized on an allophanic clay fraction from soil is 33% more active than the free enzyme (Rosas et al., 2008). This and similar findings with enzymes immobilized on different nanomaterials (Li and Hu, 2003; Liu et al., 2005; Kim et al., 2006; Wang, 2006) have led us to develop suitable methods for extracting allophane from Chilean Andisols, and explore its practical applications.

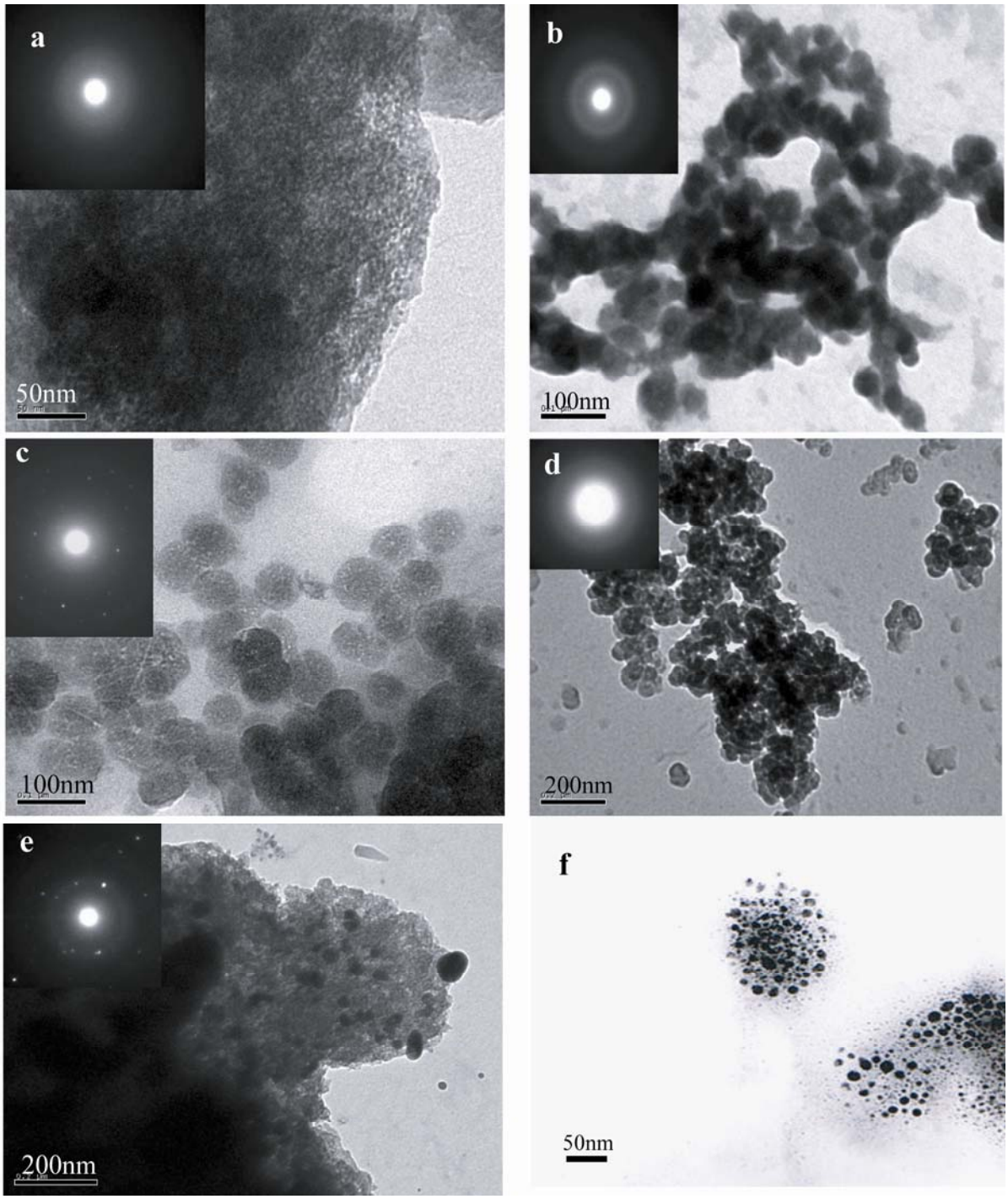

Figure 2.5. TEM images and electron diffraction patterns (insets) of nanoclays separated from different Andisols in southern Chile (unpublished data): (a) Temuco Series with immobilized enzyme, (b) Pemehue Series, (c) Piedras Negras Series with organic matter and immobilized enzyme, (d) Piedras Negras Series without organic matter and with immobilized enzyme, (e) Piedras Negras Series with organic matter, and (f) Pemehue Series with immobilized enzyme.

2.6.2 Applications of allophane

Besides being a suitable support material for enzyme immobiliztion, allophane is an efficient adsorbent of toxic substances (heavy metals, phenolics) and plant nutrients (phosphates and sulfates) (Mora et al., 2005). In Chile, Diez et al. (1999) were the first to report that allophanic soils (containing humic-allophane complexes) were much more effective in removing phenolic compounds and colour from bleached kraft mill effluents than conventional activated carbon. Allophanic soils were subsequently shown to be equally effective in cleaning up untreated kraft mill effluents under both aerobic (Navia et al., 2005) and anaerobic (Vidal et al., 2001) conditions. Acid allophanic soils are also useful for the tertiary treatment of wastewater (Diez et al., 2005). Indeed, the capacity of these materials to remove chlorophenols from water was comparable to that of activated carbon. Similarly, Yuan and Wu (2007) found that allophane was superior to a commercial montmorillonite-based adsorbent (Phoslock^{TM}) in taking up phosphate from water and meat effluent. The strong propensity of allophane for sorbing arsenate (Violante and Pigna, 2002; Arai et al., 2005) offers potential for the development of an environmentally friendly method of sequestering arsenic in drinking water as well as for the remediation of As-contaminated soils.

In terms of plant nutrition, however, allophanic soils are problematic in that they can strongly adsorb and retain sulphate and phosphate (Mora et al., 2005). Borie and Rubio (2003) reported that more than 50% of the phosphorus in Chilean Andisols was organically bound and not available to plants. Jara et al. (2006) have examined the influence of adding low-molecular-weight organic acids (LMMOAs) on the capacity of allophane to adsorb phosphate and sulphate. By competing with phosphate and sulphate for the same adsorption sites on allophane, LMMOAs reduced the adsorption of these inorganic ligands to allophane. Similarly, the adsorption of sulphate to allophanic soils was greatly decreased in the presence of organic and inorganic ligands, while phosphate inhibited the adsorption of LMMOAs and sulphate by allophanic soils. These studies provide useful information on the mutual influence of organic and inorganic ligands on adsorption/desorption reactions in soil environments, particularly in the rhizosphere where the concentration of LMMOAs is relatively high. The ability of different plant-derived acids to desorb allophane-bound phosphate in the rhizosphere merits detailed investigation because of its importance to plant nutrition and growth.

2.7 Conclusions

The advent of nanotechnology has stimulated research into the properties and potential applications of natural nanoclays, notably montmorillonite and allophane. Montmorillonite intercalated with long-chain quaternary ammonium ions ('organoclays') have long been used in a variety of industries (cosmetics, grease, paint, paper), and as adsorbents of organic contaminants. The single, most important application of organoclays over recent years, however, is in the formulation and synthesis of polymer-clay nanocomposites. On the other hand, relatively little information is available on the industrial and environmental applications of allophane despite its known efficiency in removing heavy metals, phenolic compounds, colour, arsenate, and phosphate from water and wastewater. Because of its mesoporous structure, allophane is also well-suited to serving as a support material for enzyme immobilization. Indeed, our studies indicate that the activity of allophane-immobilized phosphatase is greater than that of the free enzyme.

This review shows that natural nanoclays have a great potential for industrial and environmental applications. More research is required to improve our understanding of the surface properties and reactivity of these nanosize soil materials, and the mechanisms underlying their interactions with external solutes.

3

Nanoclays from an Andisol: extraction, properties and carbon stabilization

Nanoclays from an Andisol: extraction, properties and carbon stabilization

Marcela Calabi-Floody[1,6], James S. Bendall[2], Alejandra A. Jara[5,6], Mark E. Welland[2], Benny K.G. Theng[3], Cornelia Rumpel[4] and María de la Luz Mora[5,6*]

[1]Programa de Doctorado en Ciencias de Recursos Naturales Universidad de La Frontera, Av. Francisco Salazar 01145, P.O. Box 54-D, Temuco, Chile.l [2]Nanoscience Centre, University of Cambridge, Cambridge CB3 0FF, United Kingdom, [3]Landcare Research, Private Bag 11052, Palmerston North 4442, New Zealand, [4]Laboratoire de Biogéochimie et Ecologie des Milieux Continentaux (BIOEMCO, UMR Université Paris VI et XII-CNRS-INRA-IRD), Campus AgroParisTech, Thiverval-Grignon, France, e-mail: rumpel@grignon.inra.fr [5]Departamento de Ciencias Químicas y Recursos Naturales, Universidad de La Frontera, Av. Francisco Salazar 01145, P.O. Box 54-D, Temuco, Chile. [6]Scientific and Technological Bioresource Nucleus (BIOREN-UFRO), Universidad de La Frontera. Av. Francisco Salazar 01145, P.O. Box 54-D, Temuco, Chile. e-mail: mariluz@ufro.cl

3.1 Abstract

Soils contain an abundance of nanosize particles. Because of their tendency to aggregate and associate with organic colloids, however, soil nanoparticles are difficult to obtain and characterize. Here we report on a simple and rapid method of extracting mesoporous nanomaterials from the clay fraction of an Andisol with narrow size distribution. The clay and nanoclay were characterized by elemental analysis, pyrolysis GC/MS, electron and atomic force microscopy, infrared spectroscopy, and electrophoresis. The nanoclay dominantly consists of hollow allophane spherules forming globular aggregates of about 100 nm in diameter. The nanoclay contains more organic matter (carbon and nitrogen) with a larger proportion of polysaccharides and nitrogen containing compounds, and has a lower isoelectric point, than the clay. Treatment with hydrogen peroxide causes a large decrease in the organic matter contents of both nanoclay and clay. The aggregates of allophane nanoparticles retain a significant amount (~12 %) of carbon against intensive peroxide treatment. Thus, besides playing an important role in carbon stabilization, these naturally

occurring nanomaterials are potentially useful for developing a low-cost carbon sequestration technology.

Keywords: allophane, allophane-organic complexes, Andisol, carbon stabilization, clays, nanoclays

3.2. Introduction

Increased burning of fossil fuels and intensive deforestation have released an increasing amount of greenhouse gases into the environment (Glasby, 2006; Schulp et al., 2008; Thomson et al., 2008; Angulo-Brown et al., 2009). It has been suggested that nanoparticles, with their large surface-to-volume ratio, could be highly effective in carbon sequestration (Khedr et al., 2006). Many functional nanoparticles have been synthesized as candidates for environmental applications (Garrido-Ramírez et al., 2010). However, synthetic nanomaterials, especially those with a narrow size distribution, can be expensive and difficult to obtain. For this reason, much effort is being directed at developing simple methods for designing and synthesizing low-cost nanomaterials (Bendall et al., 2008, 2010; Plank et al., 2009). Nanoparticles occur widely in the natural environment (Yuan, 2004; Klaine et al., 2008). In this respect, soils can potentially provide an abundance of inexpensive nano-size materials (Parfitt et al., 1983, 1988; Besoain and Sepúlveda, 1985; Wada, 1987; Theng and Yuan, 2008; Calabi-Floody et al., 2009).

Soils contain about three times more carbon than the above-ground vegetation, and approximately 75% of the terrestrial carbon pool. As such, soils play a key role in the global carbon cycle (Schlesinger, 1986). The clay fraction of soils derived from volcanic ash (Andisols) contains a range of inorganic nanoparticles, among which allophane is the most abundant (Wada, 1987; Theng and Yuan, 2008). Allophane is a non-crystalline or 'short-range order' aluminosilicate with an Al/Si ratio between 1 and 2. Irrespective of chemical composition and origin, the unit particle of allophane is a hollow spherule (Fig. 3.1) with an outer diameter of 3.5–5.0 nm (Abidin et al., 2007; Creton et al., 2008). The 0.7–1.0 nm thick spherule wall is composed of an outer Al octahedral (gibbsitic) sheet and an inner Si sheet. Defects in the wall structure give rise to perforations of ~ 0.3 nm in diameter (Parfitt, 1990; Brigatti et al., 2006; Hashizume and Theng, 2007).

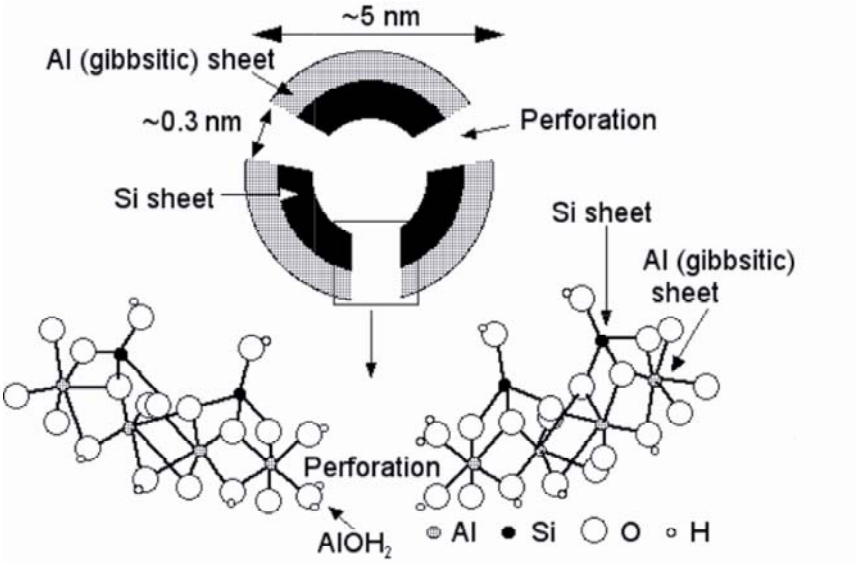

Figure 3.1. Diagram showing the structure and size of an allophane 'nano-ball' (from Hashizume and Theng, 2007)

The external (interspherule) and internal (intraspherule) surface area of allophane, calculated on the basis of unit particle size and density, is about 1000 $m^2 g^{-1}$, while values of 700–900 $m^2 g^{-1}$ are obtained by retention of ethylene glycol and ethylene glycol monoethyl ether (Hall et al., 1985; Wada, 1989). Allophane spherules ('nano-balls') tend to form porous nano-size aggregates (Calabi-Floody et al., 2009; Garrido-Ramírez et al., 2010) with physical characteristics similar to those of synthetic mesoporous silica.

The stability of organic matter in soil has been ascribed to interactions with inorganic nanoparticles, and physical protection within micropores of clay domains and interlayers (Theng et al., 1992; Chenu and Plante, 2006; Lehmann et al., 2008; Theng and Yuan, 2008). More recently, Monreal et al. (2010) have shown that the organic matter in a cultivated Black Chernozem is stabilized in nano-size structures. Because of their strong interaction with organic matter, nanoclays are difficult to isolate from soil.

Here we describe the extraction and spatial arrangement (i.e., form, shape, size) of clays and nanoclays from an Andisol in Southern Chile. The organic matter, associated with the clay and nanoclay particle size fraction, was characterized using various instrumental techniques, and their stability against treatment with hydrogen peroxide was determined. The results of this investigation can provide insight into the long-term stabilization of organic matter in volcanic ash soils.

3.3 Materials and Methods

3.3.1 Soil preparation and clay extraction

The soil used was an Andisol of the Piedras Negras Series in Southern Chile (40º20´S 72º35´W). Five samples of about 1 kg each were taken from the top 20 cm of the soil horizon. The samples were pooled, passed through a 2 mm mesh sieve, and dried in air (2−3 days at room temperature). A portion of the air-dried material was used for clay fractionation. Thus, 20 g of soil was ultrasonically dispersed in water by applying 7500 J g^{-1}, using a Sonics Vibra Cell model VC 750 equipment. The soil suspension was placed in a one-liter measuring cylinder, from which the clay fraction (< 2 μm equivalent spherical diameter), was obtained (390 g clay from 1 kg of soil) by sedimentation under gravity, following Stokes' law. The separated clay suspension was concentrated by evaporation (of the water) in a rotary evaporator at 60 ^{o}C. A portion of the concentrated suspension was set aside for subsequent nanoclay extraction, while another portion was freeze-dried for further analysis.

3.3.2 Nanoclay extraction

The nanoclay fraction was extracted using a modified method as described by Li and Hu (2003). Briefly, 5 g of the clay was suspended in 100 mL of 1 M NaCl, ultrasonicated at 4280 J g^{-1}, (selected from 3000 to 5000 J g^{-1} range tested) for 3 minutes, and centrifuged in a Sorvall Instrument RC-SB refrigerated superspeed centrifuge at 654*g* for 40 min and 25 ^{o}C. The centrifugation speed was the same as used by Li and Hu (2003). The average diameter of the particles was less that 100 nm when the first-round supernatant was discarded in order to remove mineral impurities. The pellet was suspended in 50 mL of deionized water with moderate stirring for 40 min and centrifuged again. The supernatant was collected, while the pellet was resuspended (in deionized water) and centrifuged. This procedure was repeated 11 more times. The collected supernatants, containing the nanoclay, were dialyzed (1000 kDa membrane) against deionized water until the conductivity of the water reached 0.5−0.8 μS cm^{-1}. The dialyzed material was freeze-dried to yield solid nanoclay.

3.3.3 Hydrogen peroxide treatment and organic matter removal

A portion of the clay and nanoclay was treated with 30% hydrogen peroxide (H_2O_2) to partially remove the associated organic matter. Peroxide treatment was selected (over potassium dichromate oxidation) because we wanted to preserve the integrity of the clay and nanoclay minerals, and isolate the refractory (recalcitrant) organic matter (Theng et al., 1992;

Plante et al., 2004; Eusterhues et al., 2005; Monreal et al., 2010). The procedure involved adding H_2O_2 to the clay or nanoclay suspension (2 mg mL^{-1} suspension concentration) at a H_2O_2:suspension ratio of 1:2, acidifying to pH 2 with 0.1 M HCl, and heating at 60 °C for 16 h with stirring. The suspensions were neutralized by adding NaOH (0.1 M) and dialyzed (1000 kDa membrane) against deionized water to remove excess H_2O_2.

3.3.4 Structural and chemical characterization

3.3.4.1 Elemental composition and chemical characterization of soil organic matter

The carbon and nitrogen contents of the clay and nanoclay fractions, before and after peroxide treatment, were determined on samples that had been dried at 60 ºC for 2 h. using a dry combustion method and an Analysis EuroEA3000 series instrument. The molecular composition of the organic matter, associated with the clay and nanoclay fractions, was determined by analytical pyrolysis, using samples that had been freeze-dried and ground to a fine powder. Curiepoint pyrolysis was carried out with a pyrolysis unit (GSG Curiepoint Pyrolyser 1040 PSC) coupled to a gas chromatograph (Hewlett Packard HP 5890) and a mass spectrometer (Hewlett Packard HP 5889; electron energy 70 eV). Briefly, 0.5−1 mg of sample was loaded into tubular ferromagetic wires, and inductively heated to their Curie temperature of 650°C (0.15 s) in the pyrolysis unit. The pyrolysis products were transferred to the GC system using a splittless mode with He as carrier gas, and then separated on a 60 m fused silica capillary column with a wax stationary phase (SolGelWax, SGE, 0.32 mm i.d., film thickness 0.5 μm). The temperature of the GC oven was programmed from 30 to 280 °C at 2 °C/min. The final temperature was held for 15 min. The pyrolysis products were identified using the library (Wiley) and assigned to polysaccharide-derived compounds, lignin-derived compounds, N-containing compounds and compounds of unspecified origin. The peak areas were integrated on the Total Ion Current (TIC) trace using the GC ChemStation program (Agilent Technologies). The total area was calculated as the sum of the identified peaks.

3.3.4.2 Transmission electron microscopy (TEM)

A drop of the clay or nanoclay suspension (1 μg mL^{-1}) was evaporated on a carbon-coated copper grid. TEM images were obtained with a Jeol-1200 EXII instrument operating at 120 kV, equipped with a Gatan 782 camera for image digitization. Electron diffraction (ED) was made at 60 cm from the focus.

3.3.4.3 Scanning electron microscopy (SEM)

SEM was carried out using a Leo 1530 VP (Karl Zeiss Ltd) field-emission microscope. The samples of clay and nanoclay were suspended in water (1 μg mL^{-1}) and sonicated at 150 kW for 5 min using a sonic probe. Ten μL of the suspension was deposited on a freshly cleaned silicon wafer and allowed to evaporate in a closed Petri dish under ambient conditions. Images were obtained at 15 kV and 6×10^{-5} torr vacuum.

3.3.4.4 Atomic force microscopy (AFM)

Samples of clay and nanoclay for AFM examination were prepared as described above except that the suspension was deposited on a mica surface. Images were obtained in air at a 4x4 μm scan size, using a Veeco EnviroScope instrument. All images were obtained by analysing 5 different samples with parallel height in tapping mode. The vertical height data were recorded digitally for surface microtopographic analysis.

3.3.4.5. Fourier-transform infrared (FTIR) spectroscopy

The samples were freeze-dried before analysis. The FTIR spectra of the clay and nanoclay, before and after peroxide treatment, were recorded with a Tensor 27 Brucker spectrometer. The samples were pressed into KBr discs at a sample:KBr ratio of 1:100. The resolution of each spectrum was 5 cm^{-1}, and the number of scans was 32.

3.3.5 Electrophoretic mobility

Electrophoretic mobility measurements were made at 25 ^{o}C using a Zetasizer Nano ZS apparatus (Malvern Instruments) with a re-usable dip cell (Malvern EZ 1002). The associated software allowed zeta potentials to be derived from electrophoretic mobility data, using the Smoluchowski and Hückel equations (Hunter, 1981). Briefly, 1 mg of the clay or nanoclay (before and after treatment with H_2O_2) was suspended in 1 mL of 0.001 M NaCl by immersion in an ultrasonic bath for 5 min. Measurements were carried out over a range of pH values (between 3 and 10), adjusted by careful addition of either 0.01 M HCl or 0.01 M NaOH.

3.4 Results and discussion

3.4.1 Elemental composition and chemical characterization of soil organic matter

The carbon and nitrogen contents of the clay and nanoclay fractions, before and after peroxide treatment, are shown in Table 3.1. Although peroxidation led to a large decrease in C

and N contents, an appreciable amount of C and N was retained especially by the nanoclay fraction, indicating physical and physico-chemical stabilization of organic matter in nano-structures as Monreal et al. (2010) have proposed.

Table 3.1. The content of soil carbon and nitrogen, form both clay and nanoclay fractions, before and after treatment to remove organic matter by mean oxidation with H_2O_2.

	Carbon (%)	**Nitrogen (%)**
Nanoclays untreated	28.8 (0.21)	1.9 (0.26)
Nanoclays treated	11.8 (0.08)	1.0 (0.10)
Clays untreated	19.1 (0.10)	1.2 (0.09)
Clays treated	1.3 (0.03)	0.8 (0.06)

Numbers in brackets denote ± standard deviation values.

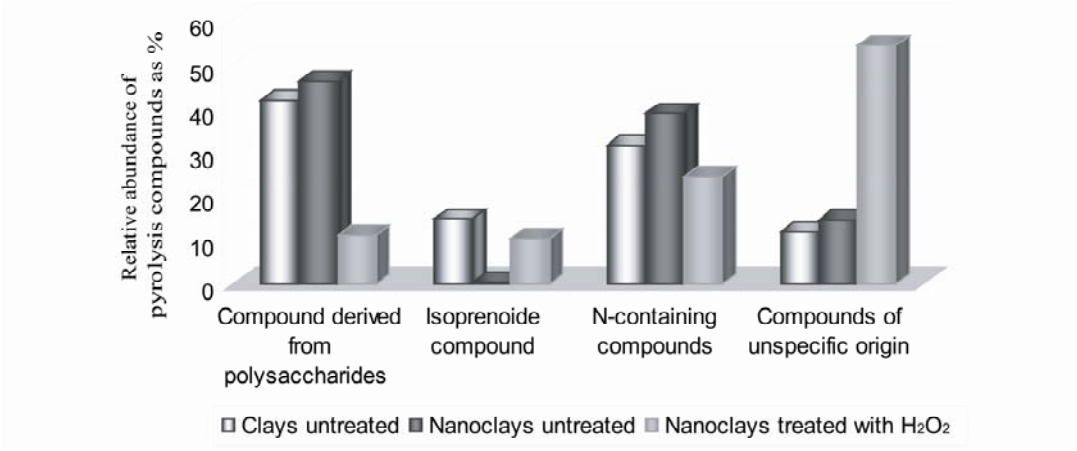

Figure 3.2. Relative abundance of pyrolysis products from untreated clay, and from nanoclay before and after peroxide treatment

The results of the pyrolysis GC/MS analysis (Fig. 3.2) show that, relative to the clay fraction, the nanoclay was enriched in polysaccharide-derived and N-containing compounds as well as in compounds of unspecified origin but depleted in isoprenoid compounds. These results are in line with those obtained by Montreal et al. (2010) and may be explained by the adsorption of strongly humified organic material to the smallest soil particles (Rumpel et al.,

2004). Peroxide treatment of the nanoclay caused a reduction in the abundance of compounds derived from polysaccharides, and a marked enrichment in compounds of unspecified origin most probably derived from black carbon. These results confirm the strong interaction between nanoclays and organic matter indicated by both electron and atomic force microscopy. They are also consistent with the observed reduction in the nitrogen content of the nanoclay (from 1.9 at 1.0%) following peroxide treatment (Table 3.1). Black carbon compounds in soil are known to be stabilized by interaction with minerals (Brodowski et al., 2005), contributing to the long-term storage of carbon in soil (Rumpel et al., 2008).

3.4.2 Electron microscopy

Transmission electron microscopy (TEM) images of the untreated nanoclay in close-up and normal views show the dominant occurrence of allophane nano-balls with an outer diameter of about 5 nm (Fig. 3.3a; arrows) in accordance with previous findings for allophane (Wada, 1967, 1989; Hall et al., 1985; Brigatti et al., 2006; Hashizume and Theng, 2007; Woignier et al., 2008) and soils with an allophane content of 5−11% in the clay fraction (Matus et al., 2008; Mora and Barrow, 1996; Mora and Canales, 1995; Vistoso et al., 2009). The hollow allophane spherules in the nanoclay fraction form rounded aggregates of about 100 nm in diameter (Fig. 3.3b; arrow) whereas those in the clay fraction tend to coalesce into 500−600 nm globular clusters (Fig. 3.3c). The electron diffraction (ED) patterns of the nanoclay (Figs. 3.3a and 3.3b; insets) show diffuse rings consistent with the presence of non-crystalline allophane. On the other hand, the ED pattern of the clay (Fig. 3.3c, inset) shows that the material contains crystalline particles in addition to allophane. The arrow in Fig. 3.3c indicates a particle with a platy morphology, representing a layered silicate mineral (Mella and Kühne, 1985).

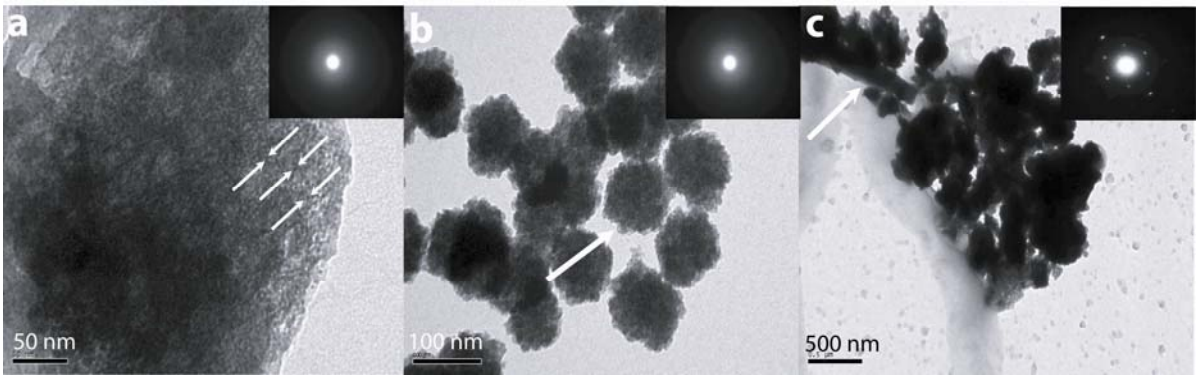

Figure 3.3. Transmission electron micrographs and electron diffraction patterns: (**a**) close-up of nanoclay; (**b**) nanoclay; and (**c**) clay.

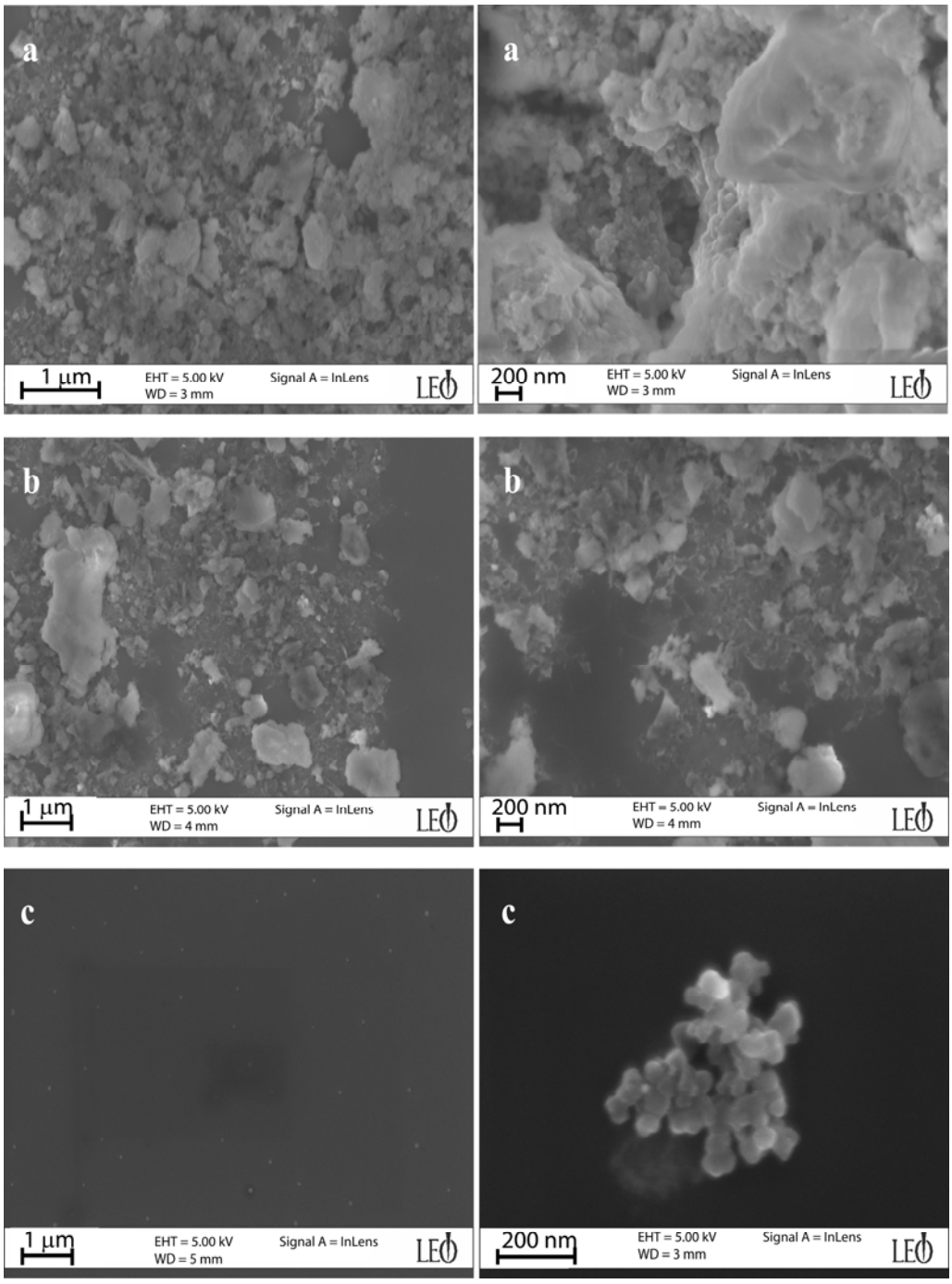

Figure 3.4. Scanning electron micrographs sequence of: (**a**) untreated nanoclay; (**b**) untreated clay; and (**c**) nanoclay after peroxide treatment**.**

The scanning electron microscopy (SEM) images of the nanoclay and clay, before peroxide treatment, show the presence of meso- and micro-porous particles (Fig. 3.4), capable of retaining much water (Okada et al., 2008). The aggregates of nanoclay (Fig. 3.4a) appear to be smaller and more porous than those of the clay (Fig. 3.4b). Peroxide treatment of the nanoclay causes a high reduction in aggregate size from 100 nm (Fig.3. 3b) to less than 50 nm

(Fig. 3.4c). These aggregates (Fig. 3.4c) look "cleaner" and have a sharper outline in comparison with their untreated counterparts. This would suggest that peroxide treatment causes the removal of encrusted and occluded organic matter.

3.4.3 Atomic force microscopy

Atomic force microscopy (AFM) of the nanoclay, before peroxide treatment, confirms the presence of allophane nano-balls (short arrows), and the abundance of aggregates (Fig. 3.5a). It also shows the presence of organic matter strands together with slender imogolite tubules (long arrows). Treatment with peroxide gave rise to smaller and cleaner allophane and imogolite structures (Fig. 3.5b). The AFM image of the clay fraction, before treatment with peroxide, shows strands of organic matter forming an interparticle network, and a coating around individual aggregates (Fig. 3.5c). Interestingly, these features are not clearly visible in the AFM image of the nanoclay although its C content (28.8 %) is much higher than that of the clay (19.1 %) (Table 3.1). This might be because the organic matter in the nanoclay is intimately associated with allophane particle surfaces. Indeed, the nanoclay fraction could retain a substantial proportion of the organic matter against repeated treatments with H_2O_2 (Table 3.1). Thus, the nanoclay fraction appears to be a privileged site for the accumulation of stabilized organic matter (Eusterhues et al., 2005; Lehmann et al., 2008; Monreal et al., 2010), and may be regarded as a carbon sink. By the same token, the nanoclay fraction has the potential of sequestering carbon in soil, and reducing CO_2 emission from soil.

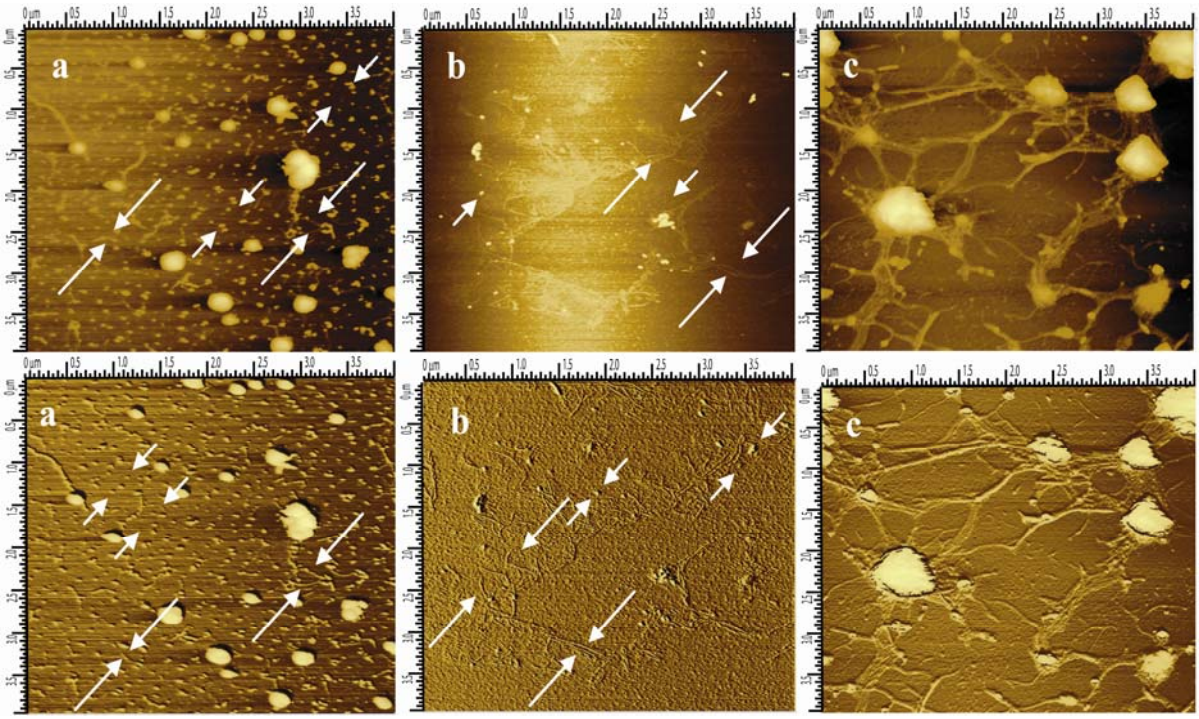

Figure 3.5. Atomic force microscopy images (top row) and phase images (bottom row): (**a**) untreated nanoclay; (**b**) nanoclay after peroxide treatment; and (**c**) untreated clay.

The AFM microtopographic analysis of the untreated nanoclay shows the presence of allophane-organic matter aggregates with a diameter of about less than 100 nm and a height of 3−5 nm (Fig. 3.6a). Peroxide treatment of the nanoclay causes a decrease in maximum aggregate height from 103.3 to 12 nm (Fig. 3.6b). No marked changes, however, occur in the average height of the small aggregates. This is indicative of strong interaction between organic matter and nanoclay (Mora and Canales, 1995). The aggregates of untreated clay are bigger than their nanoclay counterpart (Fig. 3.6c).

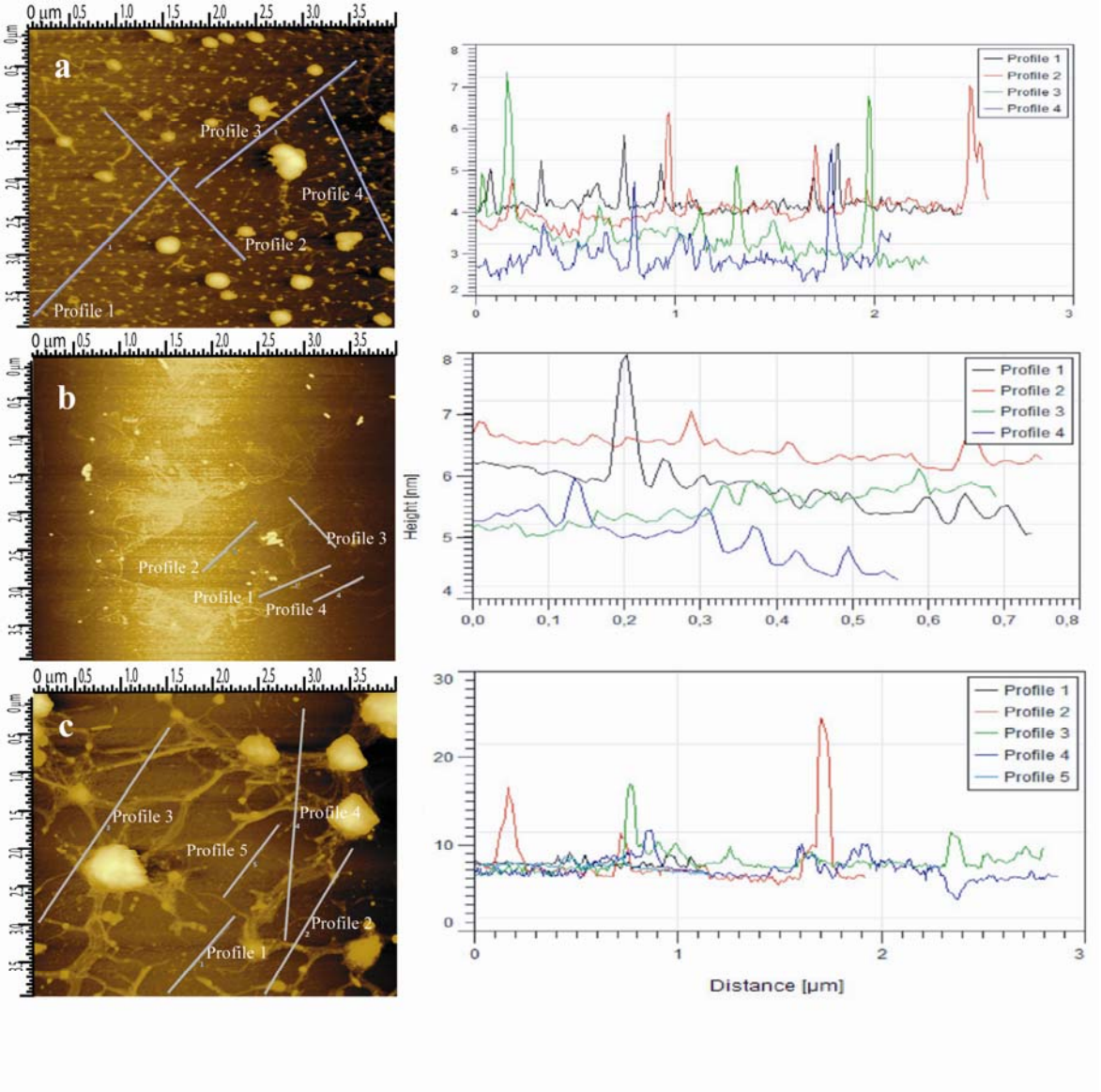

Figure 3.6. Atomic force microscopy images and height profiles: (**a**) untreated nanoclay; (**b**) nanoclay after peroxide treatment; and (**c**) untreated clay. The profiles outlined in the AFM images correspond to the horizontal axes in the corresponding graphs, showing the height of nanoparticles from each profile transect.

Both the electron and atomic force micrographs of the nanoclay show the dominant presence of allophane aggregates with a diameter of less than 100 nm for the untreated material and about 50 nm after peroxide treatment. Thus, our method of extracting nanoclays is simpler and faster than that proposed by Li and Hu (2003) who had to shake the clay suspension (in 1 M NaCl) for 48 h prior to separating the nanoclay fraction.

3.4.4 Fourier-transform infrared (FTIR) spectroscopy

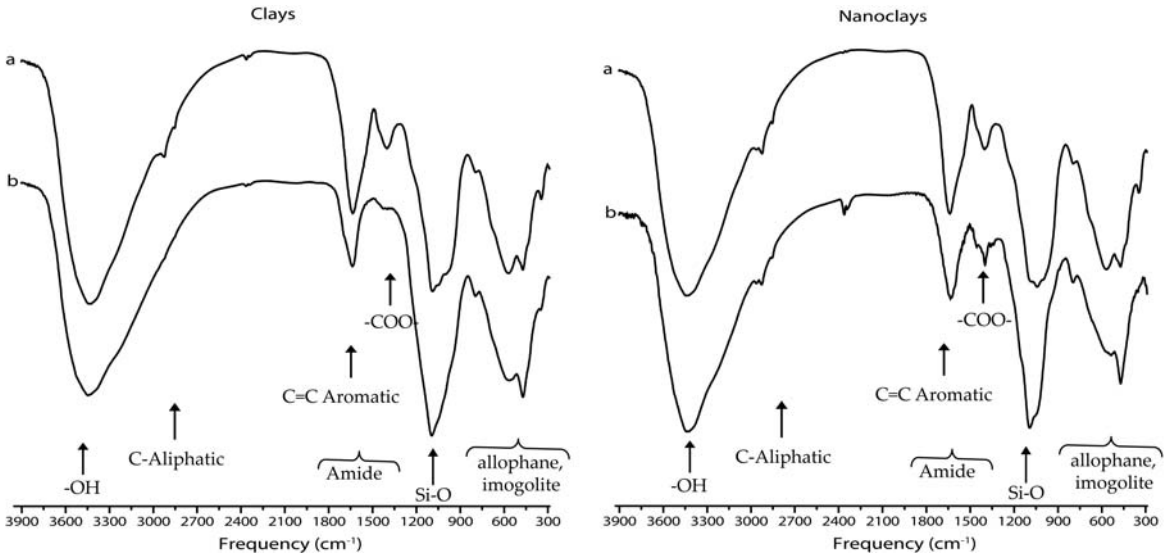

Figure 3.7. Fourier-transform IR spectra of clay and nanoclay: (**a**) before peroxide treatment; (**b**) after peroxide treatment.

3.4.4.1 Clay and nanoclay before peroxide treatment

The FTIR spectra of the freeze-dried clay and nanoclay, before treatment with H_2O_2, are shown in Fig. 3.7, curves (a). The broad band at about 3432 cm^{-1} is attributed to the stretching vibration of OH groups in the structure of allophane and imogolite (Wada, 1967; Wada et al., 1988). The shoulders near 2963, 2922 and 2854 cm^{-1} are assigned to aliphatic groups in organic matter (Bellamy, 1966; Senesi et al., 2003). The presence of polymethylene correlates with aliphatic C-H deformation vibration near 1450 cm^{-1} (Bellamy, 1966; Tatzber et al., 2007). These features are more evident in the spectrum of the nanoclay (28.8% C) than that of the clay (19.1% C). Aromatic type structures in clay and nanoclay fractions give rise to C=C vibrations in the 1600−1500 cm^{-1} region and a strong band near 1637 cm^{-1}. Bands near 1390 cm^{-1} are due to symmetric stretching of carboxylate (COO^-) ions, while those close to 1230 cm^{-1} arise from C–O stretching and OH deformation of carboxyl (COOH) groups in organic matter. The bands at 1590–1517 cm^{-1} are due to amide II, and those at 1660–1630 cm^{-1} to amide I, indicative of protein (Santín et al., 2009). As would be expected, the amide bands in the spectrum of the nanoclay fraction (1.9% N) are more intense than in that of the clay (1.2% N). The infrared results together with those obtained by analytical pyrolysis (see above) are consistent with the hypothesis that much of the organic matter, associated with mineral surfaces in soil, is microbially derived (Rumpel et al., 2010).

Allophane and imogolite are indicated by the broad band near 3432 cm^{-1} attributed to the stretching vibration of OH groups, and bands at 1090−940 cm^{-1} due to Si–O stretching vibration of orthosilicate anions and Si-O-Al groups (Wada, 1967; Wada et al., 1988; He et al., 1995; Musić et al., 1999; Abidin et al., 2007). Allophane also shows bands in the range of 670 to 430 cm^{-1} (Wada et al., 1988), whereas imogolite has bands at 500, 420, and 350 cm^{-1} (Abidin et al., 2007). Thus, FTIR spectroscopy confirms the presence of allophane and imogolite in both clay and nanoclay.

3.4.4.2 Clay and nanoclay after peroxide treatment

The FTIR spectra of the peroxide-treated clay and nanoclay (Fig. 4.7, curves b) are essentially similar to those of the untreated counterparts (Fig. 4.7, curves a). Peroxide treatment reduces the carbon content of the clay from 19.1 to 1.3%, and that of the nanoclay from 28.8 to 11.8% (Table 4.1). Accordingly, the relative intensity of the organic matter bands at 2963, 2922 and 2854 cm^{-1}, and near 1500 and 1230 cm^{-1} in the spectrum of the treated clay is much reduced, while the corresponding bands in the spectrum of the treated nanoclay show only a slight decrease in relative intensity. The spectrum of the peroxide-treated nanoclay also shows vibrations in the 1647−1506 cm^{-1} region due to aromatic carbon, while bands in the 1489−1316 cm^{-1} region may be assigned to phenolic aldehyde (Bellamy, 1966). The infrared data indicate the presence in the treated nanoclay of recalcitrant carbon compounds of unspecified origin (e.g., phenol, naphthalene, phenanthrene) in accordance with the results from pyrolysis GC/MS (Fig. 3.2).

Because of their extensive surface, exposing numerous $Al(H_2O)OH$ reactive sites (Eq. (1)), allophanic nanoclay aggegrates can bind a large amount of organic matter. The fraction of this mineral-bound organic matter resists oxidation by hydrogen peroxide may be regarded as stabilized soil organic matter (Eusterhues et al., 2005). Thus, allophanic nanoclays in Andisols play an important role in carbon sequestration and consequent stabilization.

The typical imogolite peak at 350 cm^{-1} decreases in intensity, while that at 990 cm^{-1} disappears, becoming a broad band centering around 1000 cm^{-1}, suggesting that peroxide treatment has an adverse effect on imogolite structures.

3.4.5 Electrophoretic mobility

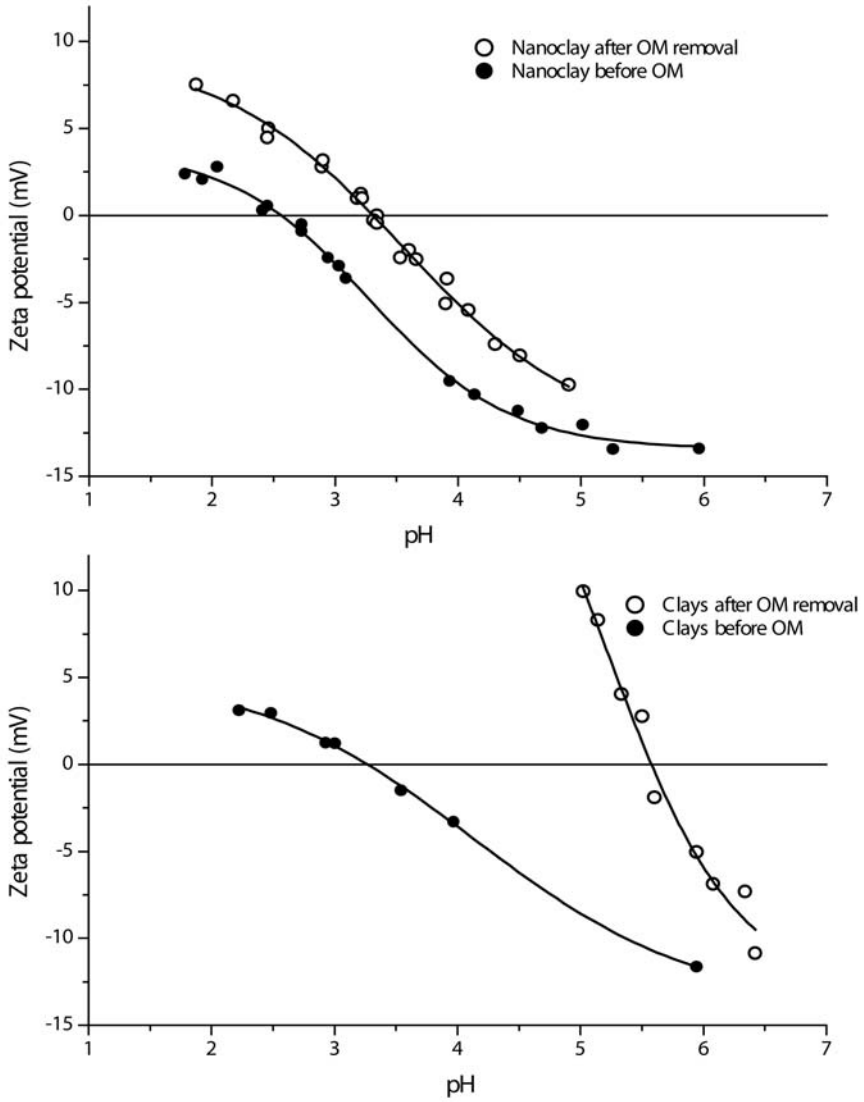

Figure 3.8. Zeta potentials as a function of suspension pH for (**a**) nanoclay before and after peroxide treatment; and (**b**) clay before and after peroxide treatment.

Fig. 3.8 clearly shows that the zeta potential of the nanoclay and clay, before and after peroxide treatment, becomes more negative (or less positive) as the pH of the suspension increases. This observation may be explained in terms of the increase in the negative surface charge of allophane with a rise in pH. Theng et al. (1982) have suggested that $Al(H_2O)(OH)$ groups, exposed at defect sites in the walls of allophane spherules, can gain or lose protons depending on the ambient solution pH, and hence are responsible for the pH-dependent charge characteristics of the mineral.

Peroxidation increases the isoelectric point (IEP) of the nanoclay from 2.6 to 3.3 (Fig. 3.8, top). A much larger increase (from 3.3 to 5.6) is observed for the clay fraction (Fig. 3.8,

bottom). The low IEP of the nanoclay, as compared to the corresponding value for the clay fraction, reflects its relatively high organic matter content (Table 3.1). This is because the negative surface charge of allophane increases with the amount of organic matter (humic substances) adsorbed (Yuan et al., 2000; Jara et al., 2005). Following Theng et al. (2005), we propose that ligand exchange occurs between surface hydroxyls of allophane and carboxyl groups of organic matter:

$$[\text{allophane–Al}(H_2O)(OH)]^0 + HOOC.R \rightarrow [\text{allophane–Al}(H_2O)(OOC).R]^{-1} + H_2O \quad (1)$$

where R denotes organic matter. Bolan et al. (1999) have suggested that phenoxy groups in soil organic matter may also be involved in ligand exchange.

According to Eq. (1) the overall charge of the system becomes more negative (or less positive) as its organic matter content increases. Mora et al. (1994) and Harbour et al. (2007) have reported similarly for a range of soil fractions containing different amounts of organic matter. Thus, chemisorption through ligand exchange promotes organic matter stabilization, and the formation of recalcitrant humic substances.

3.5 Conclusions

We have modified Li and Hu's (2003) procedure for extracting nanoclays from soil. By using ultrasonication (4.280 J g^{-1}, 3 min.) to disperse the clay fraction of an Andisol, we can significantly reduce the time required for nanoclay extraction.

The extracted nanoclay consists of spherical aggregates of allophane with a diameter of about 100 nm and an average height of 3−5.5 nm. Removal of the weakly associated organic matter by treatment with H_2O_2 causes a significant reduction in the height of the largest nanoclay aggregates (from 103.3 to 12 nm). Nanoclay aggregates also appear to have a larger mesopore volume than clay aggregates.

The organic matter content of the nanoclay is much higher than that of the clay. Accordingly, the isoelectric point of the nanoclay (pH 2.6) is lower than that of the clay (pH 3.3), and peroxide treatment shifts the isoelectric point to higher pH values. A significant amount (11.8%) of carbon is so strongly held by nanoclay surfaces as to resist repeated treatments with hydrogen peroxide. About 50% of this carbon is identifiable with black carbon-derived compounds, suggesting that allophanic nanoclays in volcanic ash soils play an important role in carbon stabilization.

We are fine-tuning the methodology of nanoclay extraction with a focus on finding the optimal energy required for clay dispersion and characterizing the various nanosize clay-organic complexes.

3.6 Acknowledgements

We gratefully acknowledge CONICYT (National foundation for Science and Technology), Chile for financial support under FONDECYT Grant Numbers 1061262 and 11070241 and ECOSSUD-CONICYT C08U01. We also thank colleagues at the Nanoscience Centre, University of Cambridge, UK for their assistance and input.

4

Natural nanoclays as support materials to increase the phosphate availability to the plants

Natural nanoclays as support materials to increase phosphate availability to the plants

Marcela Calabi-Floody[1,4], Gabriela Velásquez[1], Alejandra A. Jara[2,4] Surinder Saggar[3] and María Luz Mora[2,4*]

[1]*Programa de Doctorado en Ciencias de Recursos Naturales Universidad de La Frontera.* [2]*Departamento de Ciencias Químicas y Recursos Naturales, Universidad de La Frontera.* [3]*Principal Sientist & Research Leader Glabal changes processes, Landcare Research, Palmerston North 4442, New Zealand.* [4]*Scientific and Technological Bioresource Nucleus (BIOREN-UFRO), Universidad de La Frontera. Av. Francisco Salazar 01145, P.O. Box 54-D, Temuco, Chile. e-mail: mariluz@ufro.cl*

4.1 Abstract

The high phosphorus (P) retention of acid Andisols results in the fixation of P applied in fertilizer resulting in reducing P availability to crops. It is, thereofore, necessary to develop technologies to improve available P status of soils. The catalysis of P fixed in organic compounds by enzymes has the potential to improve P availability. But the stability of enzyme in soils is a concern. Recently the use of nanomaterials as immobilization support has been shown to improve enzymatic stability and catalytic activity against other materials. Results of our previous study show that acid phosphatase immobilized on allophanic clays from Andisols of Southern Chile increase its catalytic efficiency by 33%. The objectives of this study were: i) to evaluate allophanic and montmorillonite clays and nanoclays as support materials to stabilize acid phosphatase and ii) to evaluate the organic P mineralization of decomposed cattle dung with clay and nanoclay phosphatase complexes. Clays and nanoclays extracted from an Andisol and pure montmorillonite were characterized by scanning electron microscopy (SEM) and atomic force microscopy (AFM). The enzymatic activities were measured with ρ-nitrophenylphosphate (ρ-NPP) as substrate. The kinetics parameters (V_{max} and K_m) were calculated according to Michaelis–Menten equation. The P mineralization was determined by colorimetric analysis. The SEM analysis showed the presence of nanoclay aggregates. Clay and nanoclay from montmorillonite or allophanic soil were support materials suitable for acid phosphatase immobilization. Our results suggest that with enzyme immobilization on allophanic or montmorillonite materials both the specific activity and V_{max} were increased. The P mineralization was governed by water-soluble P_i present on cattle

dung, due to this high initial P_i concentrations to evaluate the effect free and immobilized acid phosphatase application show a little influence on organic P mineralization. However, more research is required to improve P mineralization in animal.

Keywords: Nanoclays, Andisols, phosphorous, phosphatase acid, enzyme immobilization

4.2 Introduction

Inorganic phosphorous (P) fertilization for decades had played a key role to incease crop productivity. However, the use of these chemicals has economic and environmental implications. Soils derived from volcanic ash (Andisols) occur in many parts of the world including Chile, New Zealand, Japan. In Chile, Andisols cover around 60% (5.1 million ha) of agricultural land (Mora, 1992; Escudey et al., 2001; Matus et al., 2006) supporting the bulk of agricultural production. The Andisols have the capacity to immobilize P thus decreasing its availability to plants. More than 50% of P incorporated is fixed as organic P (Borie and Rubio, 2003). Thus, organic P content in Andisols from Southern Chile is high (923 to 3000 mg P kg^{-1}) (Escudey et al., 2001). Additionally, the animal wastes such as dung also contain high amounts of P (Toor et al., 2005) present both in inorganic (orthophosphate and pyrophosphate) and organic (phospholipids, DNA, phosphonates and phytate) forms (Fuentes et al., 2006). Fuentes et al. (2009) studied P dynamic of dairy cattle dung from southern Chile containing 7.6 ± 0.3 g kg^{-1} total P of which 25% was water soluble and 38% was organic P.

In Andisols there is a potential to mobilize the fixed organic P by enhancing the catalysis of orgnic P through enzymes. The use of phytase enzymes to catalyze the hydrolysis of myo-inositol hexakisphosphate in soil suspension was studied by George et al., (2007) and Giaveno et al., (2010) who obtained release of P. Our research group has shown that acid phosphatase immobilized on allophanic clays from Andisols can increase the enzyme activity by 33% (Rosas et al. 2008). Hence catalysis of organic P by enzymes immobilized on allophanic clays could have the potential to enhance P availability and uptake. Furthermore, nanomaterials have been used to stabilize enzymes and increase their catalytic activity (Calabi-Floody et al., 2009; Moelans et al., 2005; Kim et al., 2006; Wang, 2006).

Natural nanomaterials occur widely in the environment. Nanoclays is a real alternative to get materials with nanometric size. In soils derived from volcanic ashes as Andisols, different structures of nanoparticles are possible to find within clay fraction such as aluminosilicate with nano-ball (allophane) and nano-tube (imogolite) morphology (Wada,

1987; Creton et al, 2008; Abidin et al, 2007a, 2007b; Calabi-Floody et al., 2009, 2011). These nanoparticles form stable microaggregates with pores within the nanoscale range with similar physical characteristics to silica nanomaterials, which have had great results in biocatalysis (Moelans et al., 2005; Kim et al., 2006; Wang, 2006), because it improve the catalytic efficiency of the enzyme. The objectives of this study were: i) to evaluate allophanic and montmorillonite clays and nanoclays as support materials to stabilize acid phosphatase and ii) to evaluate the organic P mineralization of decomposed cattle dung with clay and nanoclay phosphatase complexes.

4.3 Materials and Methods

4.3.1 Support materials

The clay and nanoclay materials extracted from an allophanic soil and montmorillonite were used as support materials. The soil used was an Andisol of the Piedras Negras Series of Southern Chile (40º20´S 72º35´W) and Montmorillonite was supplied by AppliChem (A6918, LOT 7W007719). These materials were characterized by scanning electron microscopy (SEM), atomic force microscopy (AFM), zeta potential techniques as reported in Calabi-Floody et al., (2011), The total specific surface area was determined gravimetrically for with the retention of ethylene glycol monoethylether (EGME), using the procedure of Heilman et al. (1965).

4.3.2 Optimal Complexes

4.3.2.1 Preparation of support enzyme complexes

Complexes were prepared following the method used by Rao and Gianfreda, (2000) and Rosas et al., (2008) as outlined in Figure 4.1. Briefly, 20 mg of support material (from allophanic and montmorillonite clay and nanoclay) and 30 µg of protein in 1 mL of 0.1 M Na-acetate buffer at pH 5.0 were mixed. The mixtures were incubated at 30 °C for 1 h and centrifuged at 10,000 g for 40 min. The supernatant was removed and the pellets formed at the base of the centrifuge tube were washed twice with 1 mL 0.1 M Na-acetate buffer at pH 5.0 and then resuspended in an equal volume of the buffer. There were two control treatments: i) free enzyme solution and ii) free support materials. The controls, supernatants and washings were tested for enzyme activity.

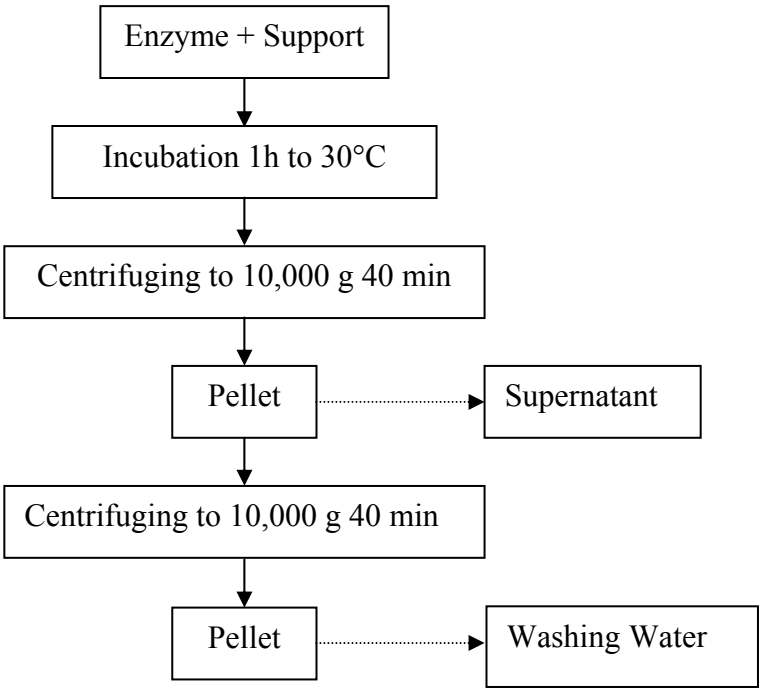

Figure 4.1. Scheme of enzyme immobilization.

4.3.2.2 Adsorption Kinetics

All the samples were incubated at 30 °C for 0.5, 1, 2, 4 and 6 h and enzyme adsorption was calculated as difference between amount of enzyme incorporated and amount of enzyme present in the supernatant.

4.3.2.3 Adsorption Isotherms

According to adsorption experiment the enzyme uptake was determined by the equation:

$$q_s = (C_i - C_s)\, V_s / W_s$$

where q_s is the mass of enzyme adsorbed by the support material (μg mg^{-1}), C_i is the initial concentration of solute (μg mL^{-1}), C_s is the solution-phase enzyme concentration at the end of the adsorption experiment (μg mL^{-1}), V_s is the volume of solution (mL), and W_s is the mass of the support (mg). The acid phosphatase adsorption was described using the empirical Freundlich-type isotherm, which works well for heterogeneous sorbents (Sposito, 1980):

$$C_s = K_f \times C_e^{1/n}$$

where C_s is the mass of acid phosphatese adsorbed per mass of support (μg mg^{-1}); Ce is the concentration of acid phosphatase remaining in solution (μg mL^{-1}) after equilibration; K_f is the Freundlich distribution coefficient (mg mL^{-1}); and 1/*n* is an exponential empirical parameter that accounts for non-linearity in adsorption behavior (Sposito,1984).

4.3.3 Evaluation of enzyme immobilization.

A drop of the clay or nanoclay suspension (1 μg mL^{-1}) was air dried and used to obtain for confocal laser-scanning microscopy (CLSM) images by means of FLUORVIEW 1000 CLSM with a 100X-40X and 10X objective lens and these images were used to determine the immobilization of the enzyme. This method allows obtaining image sharpness, contrast and three-dimensional (3D) studies, hence is a potential technique to study the enzyme bioencapsulation.

To avoid autofluorescence overlapping between organic mater content from natural nanoclays and acid phosphatase also was used a synthetic allophane provided from our research group according to the methodology proposed by Jara et al., (2005).

4.3.4 Phosphatase assay

The activity of free and immobilized phosphatase in allophanic and montmorillonite clays and nanoclays was assayed with 1 ml of 6 mM *p*-nitrophenylphosphate (*p*-NPP) in 0.1 M Na-acetate buffer at pH 5.0 and 30 °C. After 20 min incubation, 4 mL of 1 M NaOH were added and the concentration of *p*-nitrophenol was determined by measuring of the absorbance at 405 nm with a spectrophotometer. To avoid interference by turbidity, the samples were centrifuged at 14,000 *g* for 4 min prior to measurement.

4.3.5 Kinetic and stability tests

The kinetics of free and immobilized phosphatase was determined as reported above by using suitable amounts of enzyme at 30 °C and pH 5.0 and *p*-NPP concentrations ranging from 0 to 6 mM. Apparent V_{max} and K_m values were calculated by a non-linear regression analysis according to the Michaelis–Menten equation.

4.3.6 Phosphate mineralization in aerobic degraded cattle dung

The dairy cattle dung collected and aerobically degraded as described by Fuentes et al. (2009) was used as an organic P substrate. Briefly, the dung was degraded aerobically for 105 days at 60% of moisture, C:N ratio 22, 300 mL min^{-1} kg^{-1} of air flow at 20 °C. The dung had

85% water content, 85%, pH 6–7, C:N ratio 17.7 ± 0.3, total P 7.6 ± 0.3 g kg^{-1}, Al 3.3 ± 0.1 g kg^{-1}, Ca 9.9 ± 0.2 g kg^{-1}, Fe 2.9 ± 0.4 g kg^{-1}.

Three hundred mg of cattle dung was added to 24 mL of pure and sterilized water and then either the complex (20 mg support materials + 30 µg acid phosphatase, in 1 mL buffer) or free enzyme (30 µg acid phosphatase in 1 mL buffer) were added. The treatments were: C (control), AC (allophanic clays), AN (alophanic nanoclays), MC (montmorillonite clays), MN (montimorillonite nanoclays), AC-P (alophanic clays acid pphosphatase complexes), AN-P (alophanic nanoclays acid pphosphatase complexes), MC-P (montmorillonite clays acid pphosphatase complexes) and MN-P (montmorillonite nanoclays acid pphosphatase complexes). These were incubated for 18 days at room temperature. During the incubation the optimal pH was maintained at 5.0 by adding HCl acid. In the initials stages of incubation the amount of acid required to maintain the optimal pH was more (50 to 30 µL). However in later stages less acid (20 to 5 µL) was needed. The supernantant samples were collected at 0, 1, 4, 8, 12, 14, 16 and 18 d. Water soluble P concentration in the supernantant was determined by molybdate blue method (Olsen et al., 1962).

4.3.7 Statistical analysis

Each determination was made in triplicate and analyzed using analysis of variance (ANOVA). Significantly different means between treatments were separated with the Tukey's test at 0.05 significance level of probability.

4.4 Results and discussion

4.4.1 Characteristic of support materials

The SEM images show that the support materials used in this study have different morphology (Fig 4.2). The allophanic materials are predominately nanospherical (Fig 4.2a), and montmorillonite is layer (Fig 4.2b).

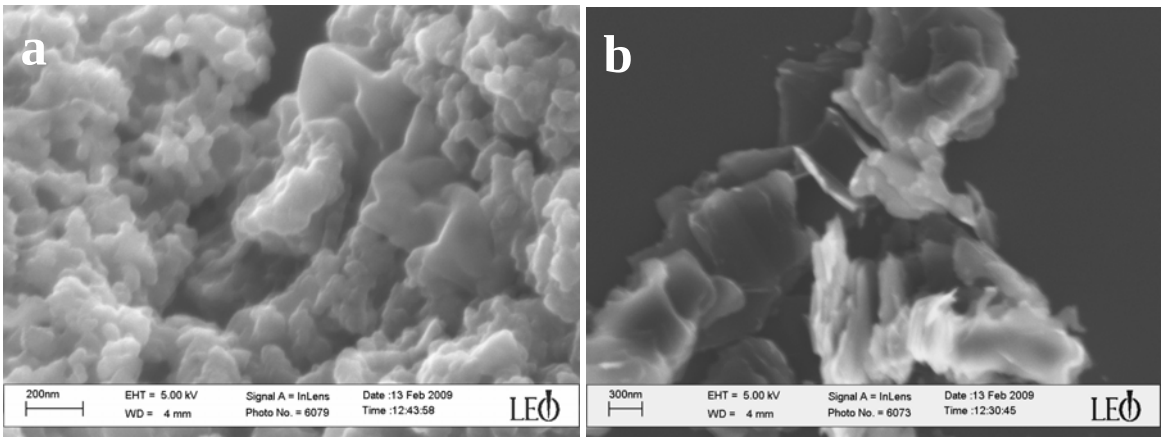

Figure 4.2. SEM images from allophanic clays (a) and montmorillonite clays (b).

The results of AFM microtopography also showed that montmorillonite nanoclays are heterogeneous (Fig. 4.3), and have a basal length between 25 at 700 nm, and an average height 1.7 nm with a maximal-height of aggregate around 45.5 nm. Although our AFM images are similar to those reported by Cadene et al. (2005), we extracted montmorillonite nanoclays with smaller particle sizes. Our results also showed that montmorillonite nanoclays are different from allophanic nanoclays (Fig 4.3), which consists of spherical aggregates of allophane with a diameter of about 100 nm and an average height of 3−5.5 nm (Calabi-Floody et al., 2011).

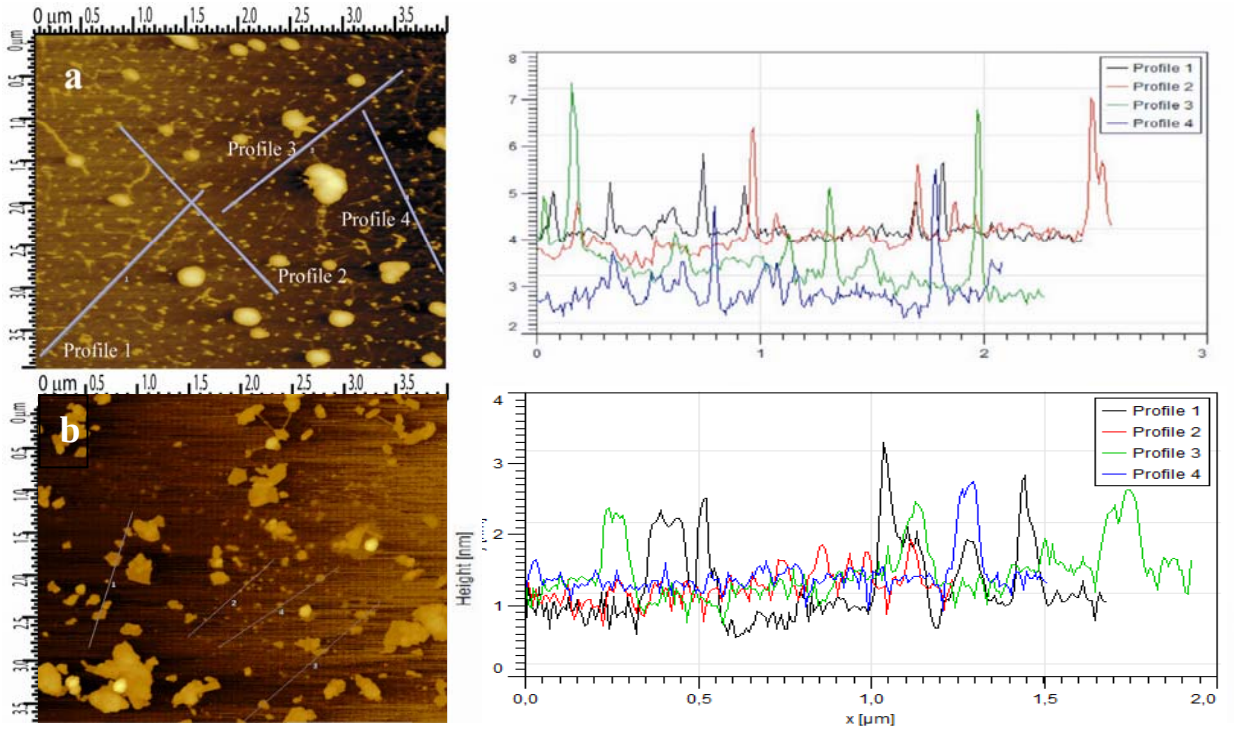

Figure 4.3. Atomic force microscopy images and height profiles: (**a**) allophanic nanoclays (image taken from Calabi-Floody et al., 2011) and (**b**) montmorillonite nanoclays.

The surface area of montmorillonite nanoclay (351 m^2 g^{-1}) was more than twice the montmorillonite clay area (149 m^2 g^{-1}) (Table 4.1). However, the difference in surface area between allophanic clay (364 m^2 g^{-1}) and nanoclay (384 m^2 g^{-1}) was very small. The organic matter content of the nanoclay fraction (28.3 % C) was higher than the clay fraction (19.1 % C) (Calabi-Floody et al., 2011). This could have a reduced the available surface area in allophanic materials.

Zeta potential is one of the important electrokinetic properties of clay minerals. The zeta potential is the electrical potential developed at the solid–liquid interface. Thus, the higher the zeta potential, it gives the higher surface potential of charged clay particle. For clay minerals, it is usually negative (it results from the charge on the particle surfaces), but it is strongly dependent on the pore fluid chemistry (Sposito 1989). Our results (Table 4.1) showed that montmorillonite materials have around 2 fold the electrical potential than allophanic materials, hence have larger surface potential of charged for enzyme immobilization.

Table 4.1. Surface characteristics from support materials

	Surface area [m^2g^{-1}]	Zeta-Potential [mV]
Allophanic clay	364	-8,6
Allophanic nanoclay	384	-12,6
Montmorillonite clay	149	-24,3
Montmorillonite nanoclay	351	-22,9

4.4.2 Complexes determination

4.4.2.1 Determination of incubation time

The adsorption kinetic for acid phosphatase on allophanic and montmorillonite support materials did not show any difference in the amount of adsorbed enzyme over time (Fig. 4.4). Therefore 1 hour incubation was used to prepare complexes. However, the results of kinetic studies suggest that the enzyme adsorption was different in different support materials. For example, allophanic clays adsorbed around 80% of the enzyme (Fig 4.4a), and nanoclays adsorbed around 70% (Fig. 4.4b), while montmorillonite support materials adsorbed 100% (Fig. 4.4c,d). The lower adsorption in allophanic support materials compared to

montmorillonite appears to be from organic matter in natural allophanic materials reducing the effective surface area and reactive sites. Giaveno et al. (2010) also reported a decrease in enzyme sorption with increased soil organic P. The differences in the amount of enzyme adsorbed can also be explained based on the zeta potential of the support materials (Table 4.1). Montmorillonite materials are more electro negative than allophanic materials providing higher surface potential of charged particles (Table 4.1). At the pH of the phosphatase assays (pH 5) their electrical potential is closer to 0 (phosphatase IEP=5.18; Sugiura et al., 1981). However, as the pH in the enzyme microenvironment is about 1 or 2 units lower than the bulk solution (Dick and Tabatabai, 1987; Rao et al., 2000), the enzyme is more positively charged than expected from its IEP. This would explain a greater attraction to negatively charged mineral surfaces as obtained here.

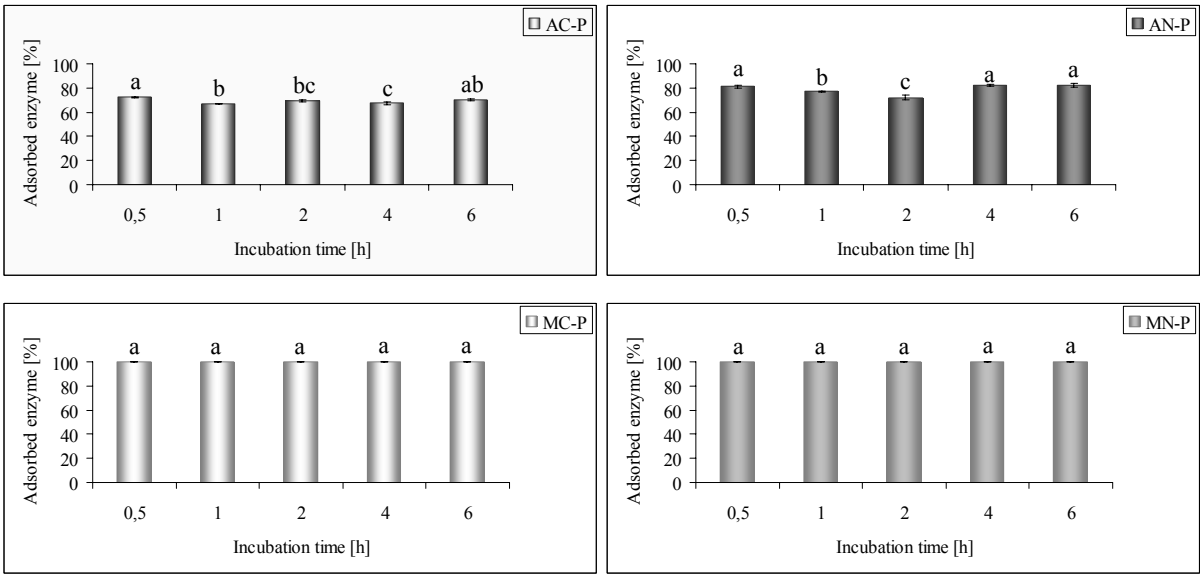

Figure 4.4. Adsorption kinetics of the acid phosphatase (30 µg P) applied at 20 mg support materials. AC-P: complex of the phosphatase immobilized on 20 mg allophanic clays, AN-P: complex of the phosphatase immobilized on 20 mg allophanic nanoclays, MC-P: complex of the phosphatase immobilized on 20 mg montmorillonite clays, MN-P: complex of the phosphatase immobilized on 20 mg montmorillonite nanoclays. Different letters mean statistical differences ($P \leq 0.05$ Tukey's test).

4.4.2.2 Determination of the enzyme amount

The adsorption isotherms for acid phosphatase on allophanic materials are presented in the Fig. 4.5 (montmorillonite results are not shown because of 100% adsorption). These isotherms were adequately described by the Freundlich equation (R^2 0.991 and 0.989 for clay

and nanoclay, respectively) (Table 4.2), and suggest that the support materials did not reach saturation in the enzyme range studied. The results of the Freundlich parameters (Table 4.2) show that both the adsorption capacity (K_f) and enzyme coverage (1/n) on support material were higher in clay than nanoclay. A higher adsorption on nanoclay materials than the clay materials is expected because of their higher surface area. However, in this study allophanic clay adsorbed ~10% more than the nanoclays because the higher organic mater content in nanoclay appears to have saturated the active sites.

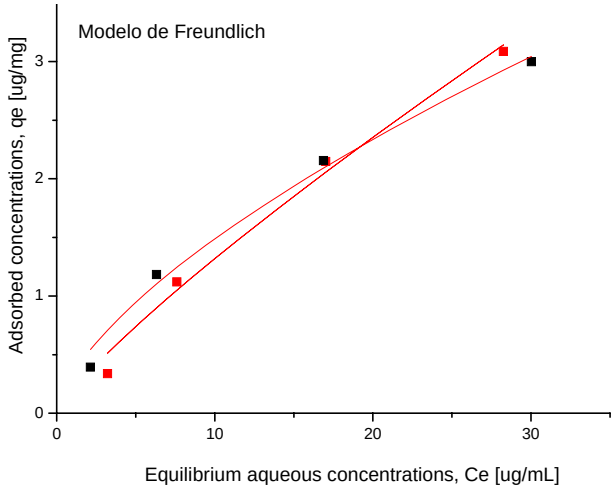

Figure 4.5. Adsorption isotherms of the acid phosphatase on allophanic clays and nanoclays. The enzyme amount applied was 10, 30, 60 and 90 µg enzyme by 20 mg of support.

Table 4.2. Freundlich adsorption parameters obtained from acid phosphatase on allophanic clay and nanoclay adsorption isotherms at pH 5.

	K_f	1/n	r^2
Allophanic clay	0,193	0,836	0,9893
Allophanic nanoclay	0,332	0,652	0,9909

Based on the similarities in adsorption isotherms of clay and nanoclay (Fig. 4.5) the specific activity (Figs. 4.6a,b) was used to determine the optimal amount of enzyme required for the preparation of the complexes. However, for Montmorillonite the clay complexes specific activity increased linearly (Fig. 4.6c) while the nanoclay complexes showed highest activities at 30 and 60 µg enzyme mL^{-1} (Fig. 4.6d). Therefore, 30 µg enzyme mL^{-1} was used to prepare the complexes.

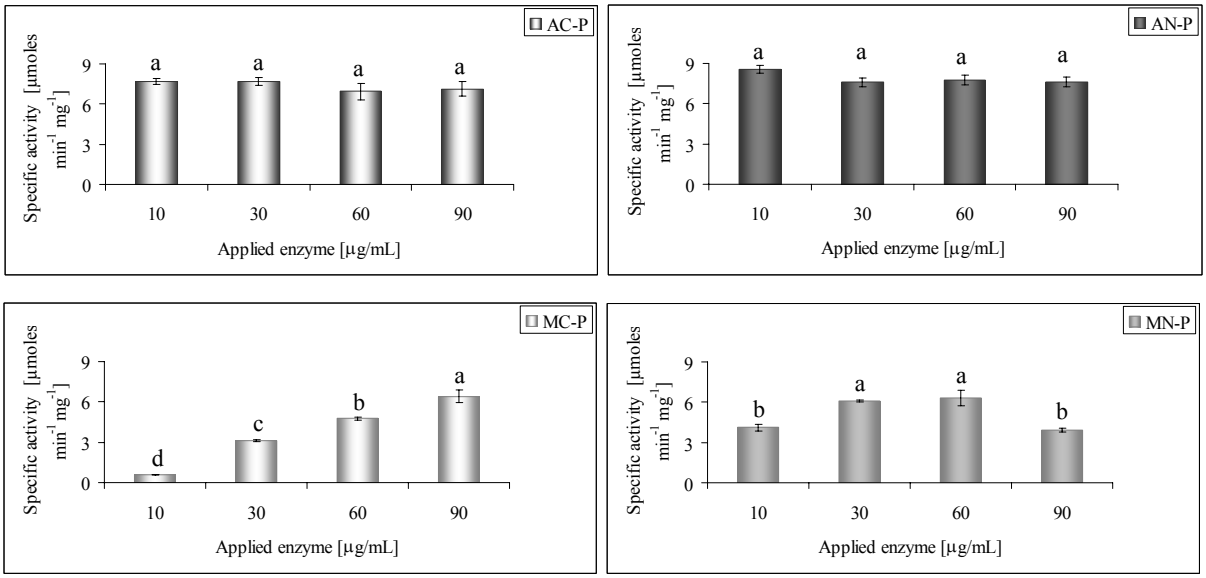

Figure 4.6. Specific activity of acid phosphatase at different levels of enzyme. Free (P) and immobilized in allophanic clays (AC-P complex) and nanoclay (AN-P complexes), and montmorillonite clays (MC-P complex) and nanoclay (MN-P complexes). Different letters means statistically different at different enzyme amount ($P \leq 0.05$ Tukey's test).

4.4.3 Evaluation of enzyme immobilization

The confocal images showed that free phosphatase have an autofluorescence mainly at 520 nm (green area in visible spectrum) (Fig 4.7a), while the complexes allophanic nanoclays acid phosphatase emitted autofluorescence at 461 nm, 520 nm and 572 nm (blue, green and red channel, respectively) (Fig 4.7b). Because of an overlap in the autofluorescence of the sample it was not possible to identify the enzyme in the complex. The images of allophanic nanoclays (Fig 4.7c) showed that allophanic nanoclay with organic matter had autofluorescence emission at same wavelength that complex. However, allophanic nanoclays after treatment to removal organic matter showed a weak autofluorescence signals. These results suggest that confocal microscopy technique could not be used to assess support materials containing organic matter.

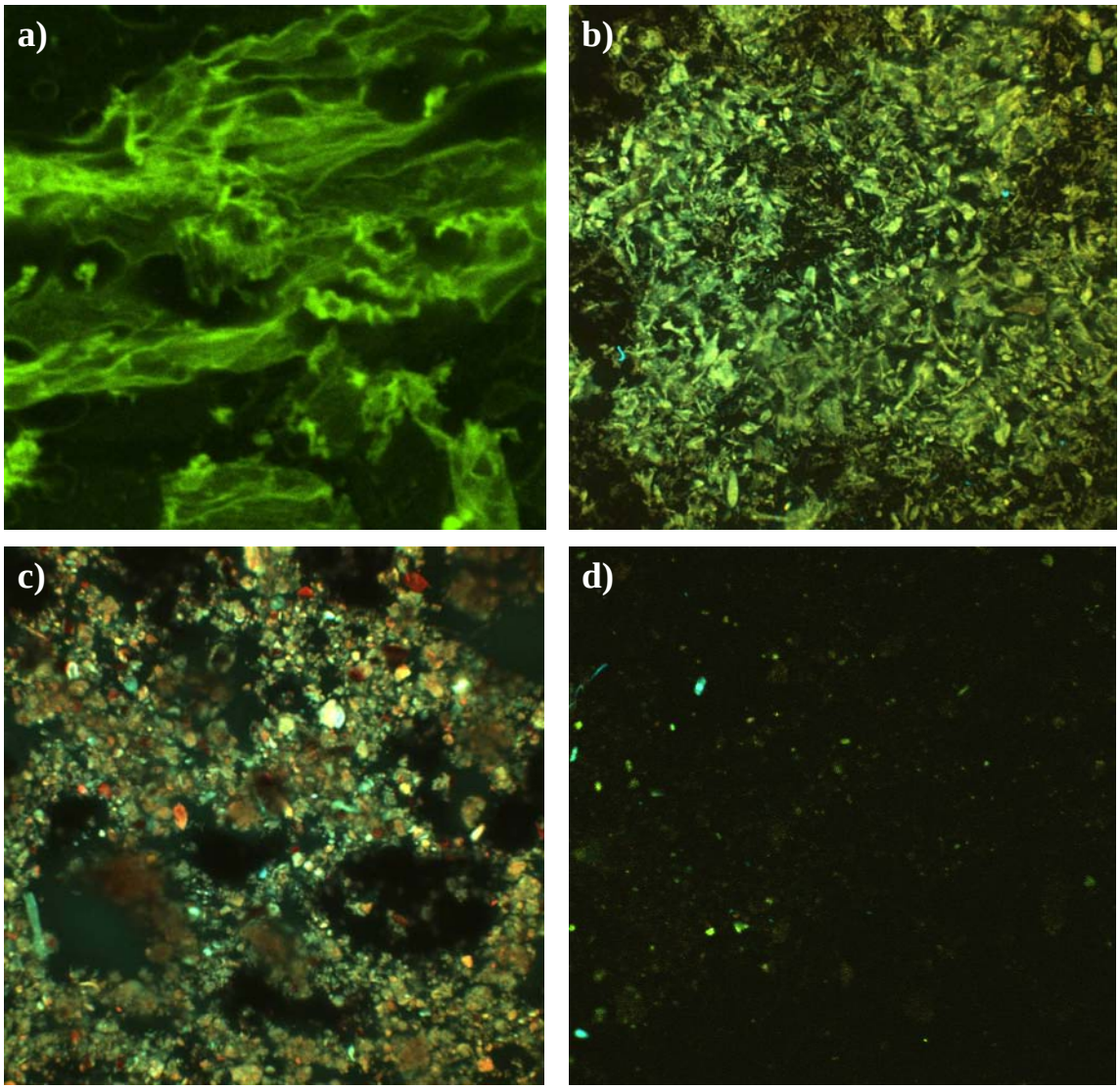

Figure 4.7. Fluorescence images of the confocal microscopy. a) Natural allophanic nanoclays with organic matter, b) natural allophanic nanoclays treated with H_2O_2, c) acid phosphatase in phosphate buffer pH 5.0 and d) natural allophanic nanoclays phosphatase complex.

To elucidate the mechanism of the phosphatase immobilization synthetic allophane and motmorrillonite nanoclay without organic matter were used. No autoflouorescence was observed from synthetic allophane (Fig 4.8a), and the synthetic allophane complex showed an autofluorescence at 520 nm (Fig. 4.8b) that was located within microaggregates of allophane. These results suggest that the phosphatase is stabilized by encapsulation. Similar pattern was obtained with montmorillonite nanoclay complex (Fig 4.8d,e,f). To confirm phosphate encapsulation within aggregates of montmorillonite a 3D projection was modeled (Fig 4.9). The images of a cross-sectional area clearly showed that fluorescence corresponding to phosphatase occluded in the microaggregates of montmorillonite.

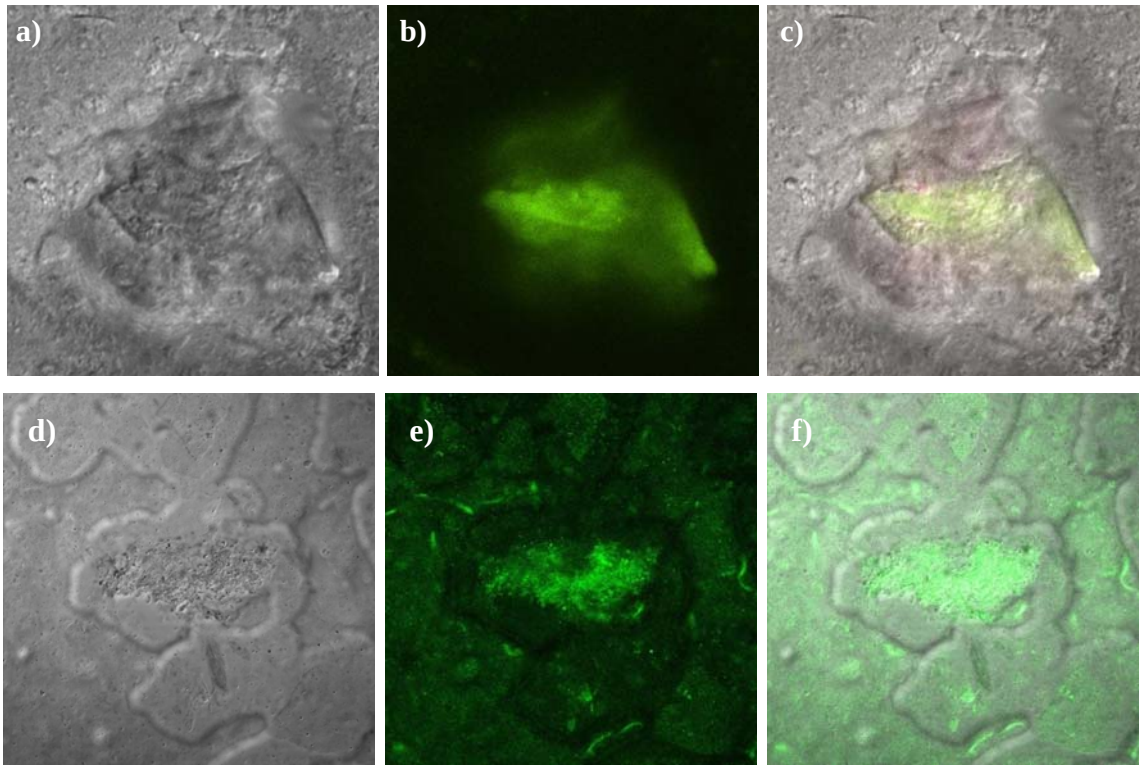

Figure 4.8. Confocal images from complexes. a) differential interference contrast image (Nomarksi) of the allophane synthetic complexes b) fluorescence image of the phosphatase acid immobilized in synthetic allophane, c) Overlap of the images a) and b), d) differential interference contrast image (Nomarksi) of the montmorillonite nanoclays phosphatase complexes e) fluorescence image of the phosphatase acid immobilized in montmorillonite nanoclays, and f) Overlap of the images d) and e).

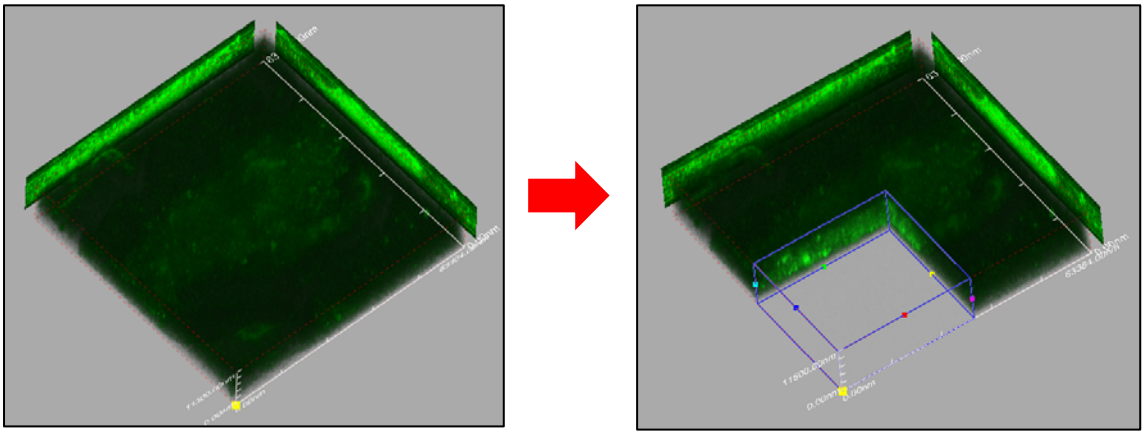

Figure 4.9. 3D projection of the montmorillonite nanoclays phosphatase complexes

4.4.4 Phosphatase assay

Results of phosphatase assay obtained in this study (Fig. 4.10) show that acid phosphatase immobilized on support materials (allophanic and montmorillonite clays and

nanoclays) increased enzyme activity from 4 to 48% with nanoclays complexes having the highest specific activity. Our findings are in line with previous research from our laboratory (Rosas et al., 2008) who obtained a 33% increase in the activity of phosphatase immobilized on allophane. Other researchers (Wei et al., 2001; Allison, 2006) also found increased activity of acid phosphatase immobilized on silica mesopoures or amorphous clays as allophane.

Our results from enzyme activity measurements confirm the previous findings and show that the nanomaterials have greater potential for enzyme immobilization than conventional supports because have the capacity to carry high enzyme load without reducing the substrate diffusion. This results in a high mobility and activity of the enzymes immobilized on nanoclay.

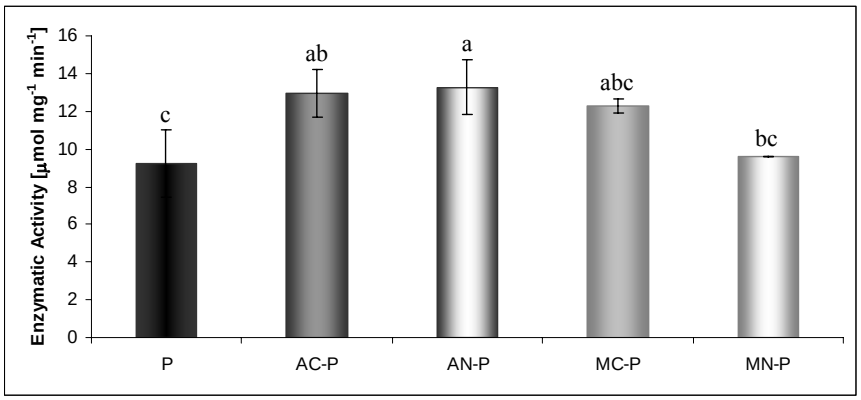

Figure 4.10. Specific activity of acid phosphatase free (P) and immobilized in allophanic clays (AC-P complexes) and nanoclays (AN-P complexes), and montmorillonite clays (MC-P complexes) and nanoclays (MN-P complexes). Different letters means statistically different ($P \leq 0.05$ Tukey's test).

The kinetic parameters (Fig. 4.11 and Table 4.3) showed that the enzymatic immobilization on allophanic clay and nanoclay increased V_{max} by 33 and 38%, respectively. The montmorillonite clay complexes increased V_{max} by 28%. However, when the enzyme was immobilized in nanoclay montmorillonite V_{max} did not change. However, the substrate affinity decreased in the immobilized enzyme (K_m = 0.14 to 0.20) compared to the free enzyme (Km = 0.11). This decrease was more in nanoclay supports than clays (Table 4.3). Also the enzyme effectiveness based on kinetic parameter (V_{max}/K_m) was better in clay than nanoclay. The increase in V_{max} suggest that enzyme were adequately immobilized in all support materials but this enzyme immobilization may have decreased effectiveness for montmorillonite nanoclay complex by 40%.

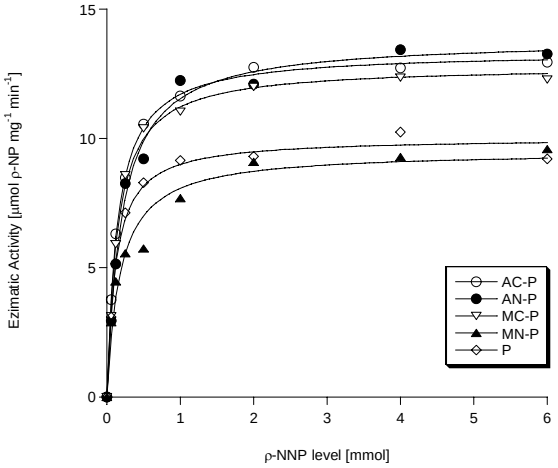

Figure 4.11. Michaelis-Menten plots of free (P) and immobilized acid phosphatase on (AC-P) allophanc clays, (AN-P) allophanic nanoclays, (MC-P) montmorillonite clays and (MN-P) montmorillonite nanoclays.

Table 4.3. Kinetic parameters of acid phosphatase free and immobilized on allophanic clay and nanoclays

	P	**AC-P**	**AN-P**	**MC-P**	**MN-P**
$\mathbf{V_{max}}$	10.0	13.3	13.8	12.8	9.5
$\mathbf{K_m}$	0.11	0.14	0.20	0.14	0.18
$\mathbf{V_{max}/K_m}$	87.9	95.0	69.6	90.6	53.4
$\mathbf{r^2}$	0.995	0.999	0.996	0.889	0.984

4.4.5 Phosphorous mineralization from the aerobic degraded cattle dung

We first assessed the interaction between the clay and nanoclay materials and cattle dung, and then analyzed the effect of immobilized enzyme on cattle dung based on changes in P_i resulting from P mineralization. The changes in P_i concentration in the cattle dung alone or in the presence of montmorillonite clay and nanoclay showed an increase in P_i only up to 8 days without further change (Fig. 4.12). The initial changes in Pi in the presence of allophanic materials followed the same trend but they showed a decrease for the remaining period of incubation (Fig. 4.12). This decrease resulted in 30 and 40% lower P_i concentration which could be attributed to high affinity of allophanic materials to P_i resulting in P_i fixation.

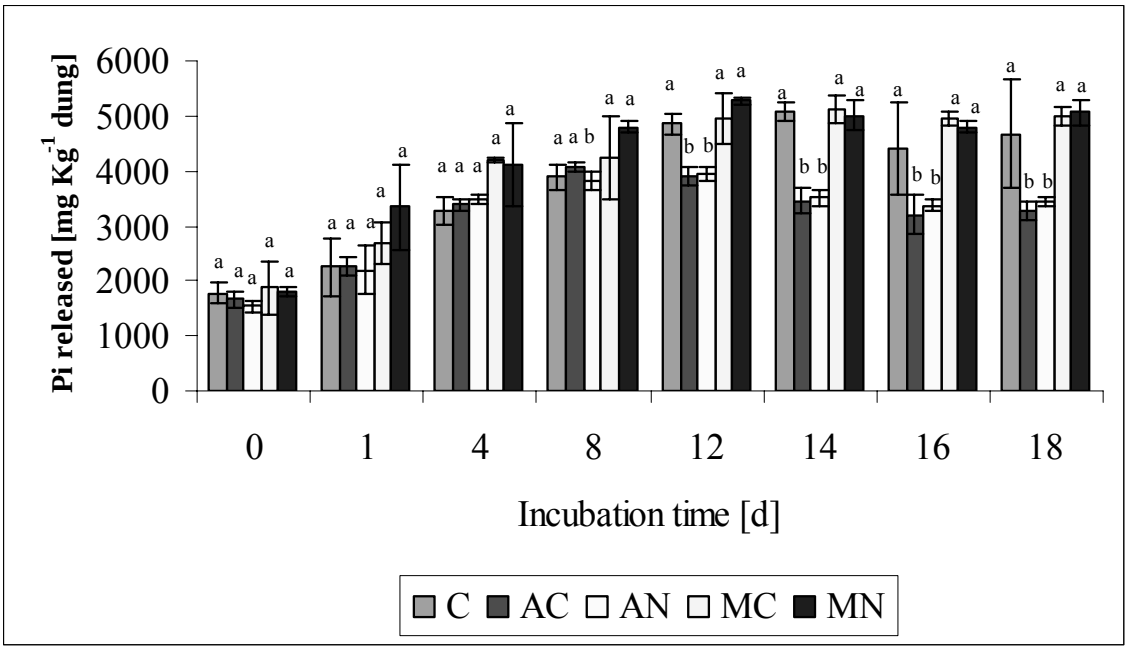

Figure 4.12. Water-soluble P_i found in solution on the different controls. C: aerobic degraded cattle dung control; AC: allophanic clays control; AN: allophanic nanoclays control; MC: montmorillonite clays control and NM montmorillonite nanoclays control. Different letters means statistically different at the same incubation time ($P \leq 0.05$ Tukey's test).

The changes in P_i in the dung treated with free and immobilized enzyme were similar to those observed in the dung and the dung in presence of support materials but without the treatment of enzyme (Fig. 4.13). These results suggest little influence of acid phosphatase alone or immobilized on support materials in enhancing P_i availability. It is also seen that there was large replicate variability in P_i in all the treatments resulting in statistically insignificant differences. This variability could be attributed to very high original P_i values in the decomposed dung used in the study and the large dilutions required to achieve the P_i concentrations in the analytical solutions within the analytical limits of the instruments. Furthermore these high Pi concentrations (1.7 to 4.5 g P_i Kg^{-1} dung) in the dung may have had hampered the enzyme performance. It is therefore recommended that in future such studies should ensure low P_i levels of organic materials such as dung by extracting the water soluble P_i before the application of enzymes free or immobilized on support materials.

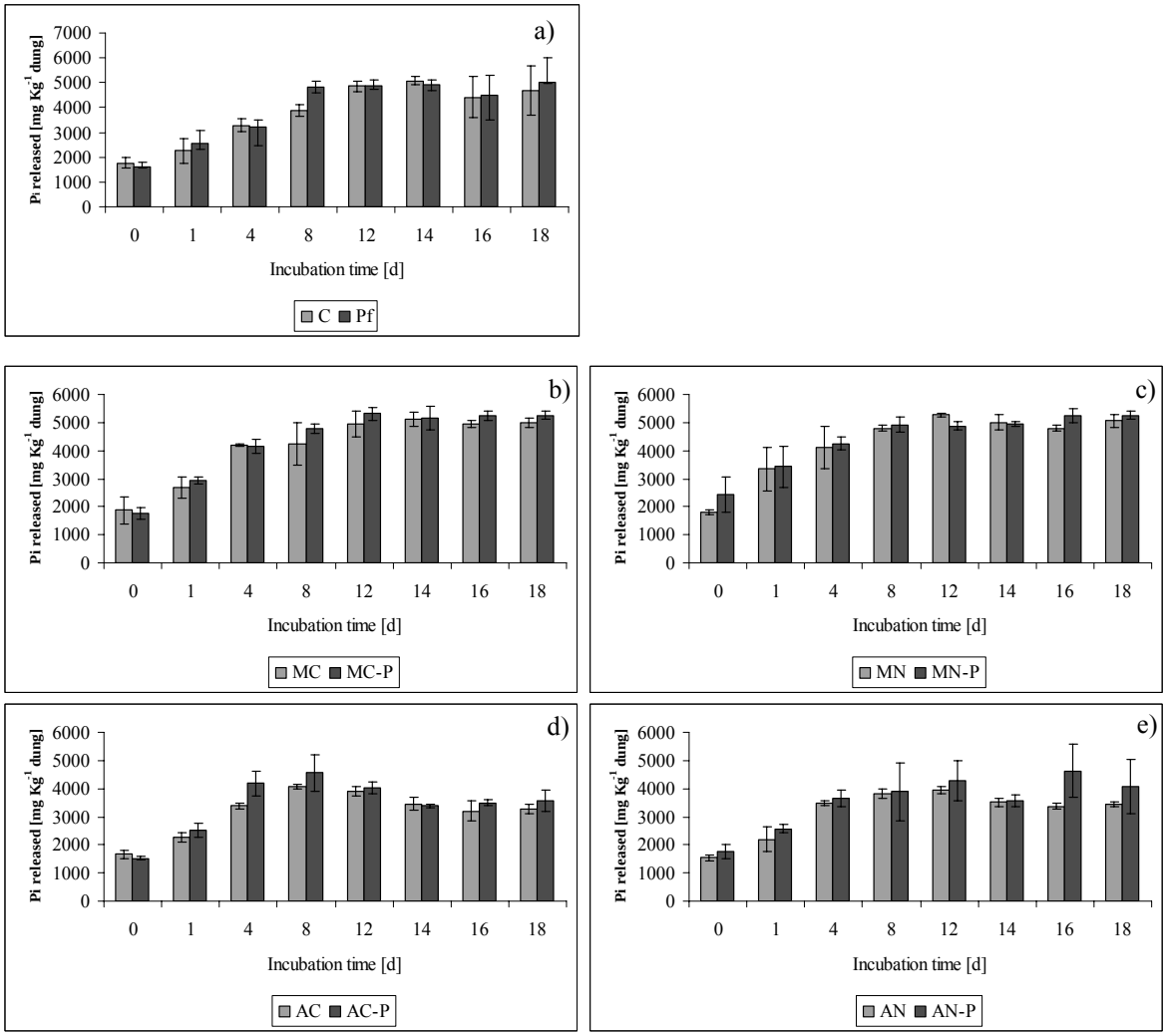

Figure 4.13. The effect of free (P_f) and immobilized enzyme on P mineralization from cattle dung. (a) C: dung control; P: free enzyme, (b) MC: MMT clays control; MC-P: phosphatase-MMT clays, (c) MN: MMT nanoclays control, MN-P: phosphatase-MMT nanoclays, (d) AC: Allophanic clays control; AC-P: phosphatase-allophanic clays complexes and (e) AN: Allophanic nanoclays control; AN-P: phosphatase-allophanic nanoclays complexes.

4.5 Conclusion

The confocal studies and kinetic parameters used in this study showed that acid phosphatase was stabilized on natural nanomaterials (allophane and montmorrillonite nanoclays) mainly by encapsulation.

Our results show that acid phosphatase immobilization increased the specific activity (between 4 to 48 %) when allophanic or montmorillonite clays and nanoclays were used as support materials and increased V_{max} (between 38 and 28 %). These studies confirm that allophanic and montmorillonite clay and nanoclay support materials were suitable for acid

phosphatase immobilization. Among these support materials, clay and nanoclay from Andisol were better the montmotillonite materials. The former materials showed a higher increase in of both specific activity (40 and 48 %, respectively) and V_{max} (33 and 38 %, respectively) of the enzyme compared to free enzyme.

The P mineralization was governed by water-soluble P_i present on cattle dung. The high initial P_i concentrations of the decomposed dung used here and large variability in P_i concentrations among the replicates plus analytical limitations little influence of addition of free or immobilized enzyme on organic P mineralization was detected. However, more research involving initially low P_i containing organic materials is required to further assess the effectiveness of free or support material immobilized enzyme addition on P mineralization in animal wastes their implications on bioavailability of P_i in the rhizosphere.

4.6 Acknowledgement

We gratefully acknowledge CONICYT (National foundation for Science and Technology), Chile for financial support under FONDECYT Grant Numbers 1061262, 1100625 and 11070241. We also thank colleagues at the Nanoscience Centre, University of Cambridge, UK for their assistance and input.

5

General discussion and conclusions

5.1 General discussion

In the present thesis, the methodology for nanoclays extraction from clays was modified according to the methodology proposed by Li and Hu (2003), and adjusted for an Andisol of the Piedras Negras Series in Southern Chile (40º20´S 72º35´W) (Chapter 3) and montmorillonite clays (AppliChem A6918, LOT 7W007719) (Chapter 4). Later, the extracted clays and nanoclays were structurally and chemically characterized for biotechnological applications (Chapter 3). In a second part of this thesis, clays and nanoclays were evaluated as support materials for acid phosphatase immobilization (Chapter 4) and these complexes (phosphatase-support materials) were studied on the phosphorous mineralization in aerobic stabilized cattle dung (Chapter 4).

5.1.1. Extraction and characterization of clays and nanoclays

The microscopic techniques showed that our modified methodology was suitable for nanoclays extraction, simpler and faster than the original methodology proposed by Li and Hu (2003) who had to shake the clay suspension (in 1 M NaCl) for 48 h prior to separating the nanoclay fraction, whereas we only sonicated for 3 minutes the clay suspension (Chapter 3).

The TEM images showed nanoclays presence in both allophanic and montmorillonite samples. Allophanic nanoclays extracted are more homogeneous materials with predominant sizes < 100 nm in samples with organic matter (OM) and < 50 nm in samples treated with H_2O_2. We could appreciate a high occurrence of allophane nanoparticles (outer diameter around 5 – 3 nm) with two morphology types: like gel or condensed aggregates, which are commonly reported for natural allophanic materials (Montarges-Pelletier et al., 2005). Likewise, we observed imogolite fibers which are in agreement with other studies (Wada, 1967; Ohashi et al, 2002; Montarges-Pelletier et al, 2005; Woignier et al, 2008). The montmorillonite nanoclays are more heterogeneous with at least one of its dimension within nanoscale range.

The SEM analysis showed difference in size between clays and nanoclays from allophanic soil with OM and treated with H_2O_2 (Chapter 3). The SEM images showed that nanoclay aggregates with OM (Chapter 3) have high amount of mesoporous with different sizes, these can absorb water from surrounding environment (Okada et al., 2008). Thus, providing an aqueous microenvironment which could be useful for biotechnological applications (Li and Hu, 2003), allowing an adequate mass transport for both substrates and products. Nanoclays treated with H_2O_2 exhibited nanoclay aggregates (Chapter 3) smaller and

cleaner than nanoclays with OM. The montmorillonite SEM images showed clearly the layered structure of this aluminosilicate (Chapter 4) which have Al and Mg atoms present in octahedral sites forming the central layer octahedral (O) of each clay sheet, Si atoms in tetrahedral sites form two layers (T) on either side of the octahedral layer, forming the configuration T–O–T (Cadene et al, 2005; Tyagi et al, 2006; Xia et al, 2009).

In the montmorillonite AFM images (Chapter 4) we can observe the well known structure of montmorillonite, and similar result of AFM image of individual montomotillonite particles reported by Cadene et al. (2005). However, we could obtain smaller particle size. The AFM analysis showed that montmorillonite nanoparticles are a heterogeneous material, confirming the result observed by SEM. The microtopography AFM revealed a basal long between 25 to 700 nm, and an average height of particle around 1.7 nm with a maximal-height of aggregate around 45.5 nm. This result confirmed that montmorillonite nanoclays are a nanomaterial, but not all its dimension are within nanometer scale.

The AFM analysis in the allophanic sample confirmed the presence of allophane and imogolite (Chapter 3), and the abundance of aggregates with similar size such as those observed by TEM. AFM images from allophanic clay samples showed clearly a high content of OM forming networks between particles, and inside the aggregates as coating, but we can not observed clearly the OM content in nanoclays. However, the elemental analysis showed that the nanoclays (28.8%) have around 20% higher OM content than clays (19.1%). This could be explained due to the strong interaction between OM and nanoclays. The analysis of AFM images of allophanic nanoclays after treatment to remove OM allowed identify smaller and cleaner allophane and imogolite nanoclays. By means microtopography AFM we confirmed nanoparticles presence with basal length and thickness of single particle aggregates in the nanoscale. The H_2O_2 treatment in nanoclays produced a decrease of maximal-height aggregates from 103.3 to 12 nm for nanoclays. The decreasing in aggregate size corroborates the decreasing C content of H_2O_2 treated nanoclays. We found that the extracted aggregates of nanoparticles retain a significant carbon amount (11.8%) against intensive peroxide treatment. Also, we showed by pyrolysis-GC/MS that the organic compounds persist on allophanic nanoclays after H_2O_2 treatment (Chapter 3).

The FTIR, IEP and elemental composition confirm the OM content, and showed that the content and types of OM are able to affect the structural and physicochemical properties of allophanic materials. The nanoclay are enriched in polysaccharide-derived and N-containing compounds as well as in compounds of unspecified origin, but depleted in isoprenoid compounds (Chapter 3) respect to clay fractions. These results may be explained

by the adsorption of strongly humified organic material to the smallest soil particles (Rumpel et al., 2004). Peroxide treatment of the nanoclay caused a reduction in the abundance of compounds derived from polysaccharides, and a marked enrichment in compounds of unspecified origin most probably derived from black carbon. The black carbon compounds in soil are known to be stabilized by interaction with minerals (Brodowski et al., 2005), contributing to the long-term storage of carbon in soil (Rumpel et al., 2008).

5.1.2 Phosphatase assay

Results of phosphatase assay obtained in this study (chapter 4) show that acid phosphatase immobilized on support materials (allophanic and montmorillonite clays and nanoclays) increased enzyme activity from 4 to 48% with nanoclays complexes having the highest specific activity. Huang et al. (2005) used different support materials from soil colloids to acid phosphatase immobilization reporting a high reduction in the enzymatic activity between 28 to 61%. In addition, Rao et al. (2000) obtained high deactivation values (37 to 77 %) after acid phosphatase immobilization on montmorillonite clay, tannic acid and organo-mineral complex. Therefore, our results showed an improvement in enzyme immobilization. Thus, allophanic and montmorillonite clays and nanoclays are suitable as material support.

The kinetic parameters obtained from Michaelis-Menten equation (Chapter 4) showed an increased in V_{max}, and suggest that the enzyme immobilization in the nanoclay supports can be within microaggregate pore, while in clays could be more in the surface. The confocal studies confirmed that the mainly mechanism was encapsulation.

5.1.3 Phosphorous mineralization from aerobic stabilized cattle dung

We analyzed the effect of immobilized enzyme on cattle dung based on changes in P_i resulting from P mineralization. The changes in P_i concentration in the dung treated with free and immobilized enzyme showed an increase in P_i only up to 8 days without further change (Chapter 4), these results were similar that obtained in the incubation of cattle dung alone, suggesting that the changes in the P_i concentration were governed by the high water soluble P concentration in degraded cattle dung (Chapter 4). These results suggest little influence of acid phosphatase alone or immobilized on support materials in enhancing P_i availability. It is also seen that there was large replicate variability in P_i in all the treatments resulting in statistically insignificant differences. This variability could be attributed to very high original P_i values in the decomposed dung used in the study and the large dilutions required to achieve the P_i concentrations in the analytical solutions within the analytical limits of the instruments.

Furthermore these high Pi concentrations (1.7 to 4.5 g P_i Kg^{-1} dung) in the dung may have had hampered the enzyme performance. It is therefore recommended that in future such studies should ensure low P_i levels of organic materials such as dung by extracting the water soluble P_i before the application of enzymes free or immobilized on support materials.

5.2 General conclusions

In this study we have been able to significantly reduce the time required for extracting nanoclay (from the clay fraction) of an Andisol, by modifying the methodology of Li and Hu (2003), changing the 48 h shaking by 3 min ultrasonication and allowed to obtain nanoclays of reduced size, and suitable nanoparicles to enzymatic immobilization.

The nanomaterial obtained from Andisols is homogeneous, showing particle aggregates with a diameter of about 100 nm and an average height of 3−5.5 nm. In contrast, montmorillonite nanoclays were heterogeneous in shape and size (height around 1.7 nm), showing some nanoparticles with only one of its dimension within the nanometer scale. Physicochemical and structural properties of the allophanic samples showed that the organic matter governs the behavior of studied fractions, highlighting a strong influence on the structure and size of the Andisols particles before and after H_2O_2 treatment to remove organic matter.

The C content of the nanoclay (28.3%) is higher than of the clay (19.1%). After H_2O_2 treatment a significant amount (11.8%) of carbon is so strongly held by nanoclay surfaces as to resist repeated treatments with hydrogen peroxide. About 50% of this carbon is identifiable like black carbon-derived compounds, suggesting that allophanic nanoclays in volcanic ash soils play an important role in carbon stabilization.

The confocal studies and kinetic parameters used in this study showed that acid phosphatase was stabilized on natural nanomaterials (allophane and montmorrillonite nanoclays) mainly by encapsulation.

Our results show that acid phosphatase increased the specific activity (between 4 to 48%) and V_{max} (between 28 and 38%) when allophanic or montmorillonite materials were used as support. We determined that the allophanic nanoclays structure were more suitable

than montmorillonite nanoclays to immobilized acid phosphatase, showing that acid phosphatase immobilized in allophanic nanoclays increased the specific activity by 91% more than the montmorillonite nanoclays used as support materials.

The P mineralization was governed by water-soluble P_i present on cattle dung. The high initial P_i concentrations of the decomposed dung used and large variability in P_i concentrations among the replicates showed a little influence of addition of free or immobilized enzyme on organic P mineralization.

More research involving initially low P_i containing organic materials is required to further assess the effectiveness of free or support material immobilized enzyme addition on P mineralization in animal wastes their implications on bioavailability of P_i in the rhizosphere.

5.3 Outlook

In this research we found that nanoclays from an Andisol of the southern Chile have a stabilize effect in the carbon sequestration. However, more studies are needed to evaluate the real importance of the allophanic nanoclays, in the global carbon sequestration and stabilization in the Andisols of the Southern Chile.

In this thesis we also shown that allophanic and montmorillonite materials are adequate for enzyme immobilization increasing their specific activity. However, more research is required in order to evaluate P mineralization in animal wastes and their implications on bioavailability of Pi in the rhizosphere.

6

Reference

References

Abidin, Z., Matsue, N., and Henmi, T. (2007a). Differential formation of allophane and imogolite: experimental and molecular orbital study. Journal of Computer-Aided Materials Design, 14, 5-18.

Abidin, Z., Matsue, N., and Henmi, T. (2007b). Nanometer-scale chemical modification of nano-ball allophane. Clays and Clay Minerals, 55, 443-449.

Acevedo, F., Pizzul, L., Castillo, M.dP., González, M.E., Cea, M., Gianfreda, L., Diez, M.C., 2010. Degradation of polycyclic aromatic hydrocarbons by free and nanoclay-immobilized manganese peroxidase from Anthracophyllum discolor. Chemosphere 80, 271–278.

Allison, S., (2006). Soil minerals and humic acids alter enzyme stability: implications for ecosystems processes. Biogeochemistry, 81: 161–373.

Angulo-Brown, F., Sánchez-Salas, N., Barranco-Jiménez, M.A., Rosales, M.A., 2009. Possible future scenarios for atmospheric concentration of greenhouse gases: A simplified thermodynamic approach. Renewable Energy 34, 2344–2352.

Anon., (2005). Barrier to success. Brand, 4: 42–48.

Arai, Y., Sparks, D.L., Davis, J.A., (2005). Arsenate adsorption mechanisms at the allophane-water interface. Environmental Science & Technology, 39: 2537–2544.

Baeza G., 2002. Dinámica del reciclaje de N, P y S provenientes de excretas animales en un andisol acidificado. Tesis doctoral. Universidad de Santiago de Chile.

Bagshaw, S.A., (1999). Morphosynthesis of macrocellular mesoporous silicate foams. Chemical Communications, 767–768.

Bagshaw, S.A., Prouzet, E., Pinnavaia, T.J., (1995). Templating of mesoporous molecular sieves by nonionic polyethylene oxide surfactants. Science, 269: 1242–1244.

Bai, Y.X., Li, Y.F., Yang, Y., Yi, L.X., (2006). Covalent immobilization of triacylglycerol lipase onto functionalized nanoscale SiO_2 spheres. Process Biochemistry, 41: 770–777.

Barnett, G. M. 1994. Phosphorus forms in animal manure. Biores. Technol. 49: 139-147.

Beall, G.W., (2003). The use of organo-clays in water treatment. Applied Clay Science, 24: 11–20.

Bellamy, L.J., 1966. The Infra-red Spectra of Complex Molecules. John Wiley and Sons, New York, pp. 1–425.

Bendall, J.S., Paderi, M., Ghigliotti, F., Li Pira, N.L., Lambertini, V., Lesnyak, V., Gaponik, N., Visimberga, G., Eychmüller, A., Sotomayor Torres, C.M., Welland, M.E., Gieck, C.,

Marchese, L., 2010. Layer-by-layer all-inorganic quantum dot-based LEDs: A simple procedure with robust performance. Adv. Funct. Mater. 20, 3298−3302.

Bendall, J.S., Visimberga, G., Szachowicz, M., Plank, N.O.V., Romanov, S., Sotomayor-Torres, C.M., Welland, M.E., 2008. An investigation into the growth conditions and defect states of laminar ZnO nanostructures. J. Mater. Chem. 18, 5259−5266.

Besoain, E., Sepúlveda, G., 1985. Minerales secundarios. In: Tosso, J. (Ed.). Suelos Volcanicos de Chile, First edition. Instituta de Investigaciones Agropecuarias. Ministerio de Agricultura, Santiago, Chile, pp. 153−214.

Biondi, E., Branciamore, S., Fusi, L., Gago, S., Gallori, E., (2007). Catalytic activity of hammerhead ribozymes in a clay mineral environment: Implications for the RNA world. Gene, 389: 10–18.

Boissiere, C., Van der Lee, A., El Mansouri, A., Larbot, A., Prouzet, E., (1999). A double step synthesis of mesoporous micrometric spherical MSU-X silica particles. Chemical Communications, 2047–2048.

Bolan, N.S., Naidu, R., Syers, J.K., Tillman, R.W., 1999. Surface charge and solute interactions in soils. Adv. Agron. 67, 88−141.

Borie, F., Rubio, R., (2003). Total and organic phosphorus in Chilean volcanic soils. Gayana Botanica (Chile), 60: 69–78.

Borkowski, R.E., Drucker, J., Bennett, P. And Robertson, J. (2008). Ledge-flow-controlled catalyst interface dynamics during Si nanowire growth. Nature materials, 2140, 1-4.

Brady, N.C., Weil, R.R., (2002). The Nature and Properties of Soils, Thirteenth Edition. Prentice Hall, Upper Saddle River, NJ. 960 pp.

Briceño M, Escudey M, Galindo G, Borchardt D y Chang A 2004 Characterization of Chemical phosphorus forms in volcanic soils using ^{31}P-NMR spectroscopy. Communications in Soil Science and Plant Analysis 35(9-10), 1323-1337.

Brigatti, M.F., Galan, E., Theng, B.K.G., (2006). Structures and mineralogy of clay minerals. Pp 19–86 in: Handbook of Clay Science (F. Bergaya, B.K.G. Theng & G. Lagaly, editors). Elsevier, Amsterdam.

Brodowski, S., Amelung, W., Haumaier, L., Abetz, C., Zech, W., 2005. Morphological and chemical properties of black carbon in physical soil fractions as revealed by scanning electron microscopy and energy-dispersive X-ray spectroscopy. Geoderma 128, 116–129.

Brody, A.L., (2003). “Nano, nano” food packaging technology. Food Technology, 57: 52–54.

Browne, G.H., Soong, R., (1997). An occurrence of allophane from Mangaturuturu River, Tongariro National Park, North Island, New Zealand. New Zealand Journal of Geology and Geophysics, 40: 253–256.

Burgentzlé, D., Duchet, J., Gérard, J.F., Jupin, A., Fillon, B., (2004). Solvent-based nanocomposite coatings I. Dispersion of organophilic montmorillonite in organic solvents. Journal of Colloid and Interface Science, 278: 26–39.

Cadene, A., Durand-Vidal, S., Turq, P. and Brendle, J. (2005). Study of individual Na-montmorillonite particles size, morphology, and apparent charge. Journal of Colloid and Interface Science, 285, 719-730.

Calabi-Floody, M., Bendall, J.S., Jara, A.A., Welland, M.E., Theng, B.K.G., Rumpel, C., Mora, M.L., (2010). Nanoclays from an Andisol: Extraction, properties and carbon stabilization. Geoderma, doi:10.1016/j.geoderma.2010.12.013.

Calabi-Floody, M., Theng, B.K.G., Reyes, P., Mora, M.L., (2009). Natural nanoclays: applications and future trends – a Chilean perspective. Clay Miner. 44: 161–176.

Calabi-Floody, M., Jara, A. & Mora, M. L. Allophane nanoclays: The potential use to increase the catalytic efficiency of acid phosphatase enzyme. *J. Soil Sci. Plant Nutr. Special Issue* 8, 174 (2008).

Carretero, M.I., Gomes, C.S.F., Tateo, F., (2006). Clays and human health. Pp 717–741 in: Handbook of Clay Science (F. Bergaya, B.K.G. Theng & G. Lagaly, editors). Elsevier, Amsterdam.

Causserand, C., Kara, Y., Aimar, P., (2001). Protein fractionation using selective adsorption on clay surface before filtration. Journal of Membrane Science, 186: 165–181.

Chabba, S., Netravali, A.N., (2004). 'Green' composites using modified soy protein concentrate resin and flax fabrics and yarns. JSME International Journal Series A, 47: 556–560.

Chabba, S., Netravali, A.N., (2005a). 'Green' composites Part 1: characterization of flax fabric and glutaraldehyde modified soy protein concentrate composites. Journal of Materials Science, 40: 6263–73.

Chabba, S., Netravali, A.N., (2005b). 'Green' composites Part 2: characterization of flax yarn and glutaraldehyde/poly(vinyl alcohol) modified soy protein concentrate composites. Journal of Materials Science, 40: 6275–6282.

Chan, C.M., Wu, J.S., Li, J.X., Cheung, Y.K., (2002). Polypropylene/calcium carbonate nanocomposites. Polymer, 43: 2981–2992.

Chen, T.K., Tien, Y.I., Wei, K.H., (2000). Synthesis and characterization of novel segmented polyurethane/clay nanocomposites. Polymer, 41: 1345–1353.

Chenu, C., Plante, A.F., 2006. Clay-size organo-mineral complexes in a cultivation chronosequence: revisiting the concept of the 'primary organo-mineral concept'. Eur. J. Soil Sci. 57, 596–607.

Choong, C.L., Bendall, J.S. and Milne W.I. (2009). Carbon nanotube array: A new MIP platform. Biosensors and Bioelectronics, doi:10.1016/j.bios.2008.11.025

Churchman, G.J., Gates, W.P., Theng, B.K.G., Yuan, G., (2006). Clays and clay minerals for pollution control. Pp 625–675 in: Handbook of Clay Science (F. Bergaya, B.K.G. Theng & G. Lagaly, editors). Elsevier, Amsterdam.

Cotterell, B., Chia, J.Y.H., Hbaieb, K., (2007). Fracture mechanisms and fracture toughness in semicrystalline polymer nanocomposites. Engineering Fracture Mechanics, 74: 1054–1078.

Crespo, J., da Silva, Queiroz, N., Nascimento, da Graca, M., Soldi, V., (2005). The use of lipases immobilized on poly(ethylene oxide) for the preparation of alkyl esters. Process Biochemistry, 40: 401–409.

Creton, B., Bougeard, D., Smirnov, K.S., Guilment, J., Poncelet, O., 2008. Structural model and computer modeling study of allophane. J. Phys. Chem. C. 112, 358–364.

Dean, K., Yu, L., Wu, D.Y., (2007). Preparation and characterization of melt-extruded thermoplastic starch/clay nanocomposites. Composites Science and Technology, 67: 413–421.

Deshmane, C., Yuana, Q., Perkins, R.S., Misra, R.D.K., (2007). On striking variation in impact toughness of polyethylene-clay and polypropylene-clay nanocomposite systems: The effect of clay-polymer interaction. Materials Science and Engineering A, 458: 150–157.

Dick, W.A., Tabatabai, M.A., (1987). Kinetics and activities of phosphatase-clay complexes. Soil Science 143(1): 5–15.

Diez, M.C., Mora, M.L., Videla, S., (1999). Adsoption of phenolic compounds and color from bleached Kraft mill effluent using allophanic compounds. Water Research, 33: 125–130.

Diez, M.C., Quiroz, A., Ureta-Zañartu, S., Vidal, G., Mora, M.L., Gallardo, F., Navia, R., (2005). Soil retention capacity of phenols from biologically pre-treated Kraft mill wastewater. Water, Air & Soil Pollution, 163: 325–339.

Dong, Y., Feng, S.S., (2005). Poly(d,l-lactide-co-glycolide)/montmorillonite nanoparticles for oral delivery of anticancer drugs. Biomaterials, 26: 6068–6076.

Droy-Lefaix, M.T., Tateo, F., (2006). Clays and clay minerals as drugs. Pp 743–752 in: Handbook of Clay Science (F. Bergaya, B.K.G. Theng & G. Lagaly, editors). Elsevier, Amsterdam.

Drozdov, A.D., Christiansen, J.C., (2007). Cyclic deformation of ternary nanocomposites: Experiments and modelling. International Journal of Solids and Structures, 44: 2677–2694.

Ensminger, L.E. and Gieseking, J.E. (1942). Resistance of clay-adsorbed proteins to proteolytic hydrolysis. Soil Sci, 53, 205-209.

EPA, (2007). Nanotechnology White Paper. U.S. Environmental Protection Agency Report EPA 100/B-07/001, Washington DC.

Escudey, M., Galindo, G., Förter, J.E., Briceño, M., Diaz, P., Chang, A., (2001). Chemical forms of phosphorus of volcanic ash-derived soils in Chile. Communications in Soil Science and Plant Analysis, 32: 601–616.

Eusterhues, K., Rumpel, C., Kögel-Knabner, I., 2005. Stabilization of soil organic matter isolated via oxidative degradation. Org. Geochem. 36, 1567–1575.

Fairhurst, A.J., Warwick, P. and Richardson, S. (1995). The influence of humic acid on the adsorption of europium onto inorganic colloids as a function of pH. Colloids and surfaces. A, Physicochemical and engineering aspects, 99, 187-199.

Fornes, T.D., Yoon, P.J., Keskkula, H., Paul, D.R., (2001). Nylon 6 nanocomposites: effect of matrix molecular weight. Polymer, 42: 9929–9940.

Fuentes, B., Bolan, N., Naidu, R., Mora, M.L., (2006). Phosphorus in organic waste-soil systems. J. Soil Sc. Plant. Nutr., 6(2): 64 – 83

Fuentes, B., Jorquera, M., Mora, M.L., (2009). Dynamics of phosphorus and phytate-utilizing bacteria during aerobic degradation of dairy cattle dung. Chemosphere, 74: 325–331.

Fukushima, Y., Inagaki, S., (1987). Synthesis of an intercalated compound of montmorillonite and 6-polyamide. Journal of Inclusion Phenomena and Macrocyclic Chemistry, 5: 473–482.

Garrido-Ramírez, E.G., Theng, B.K.G., Mora, M.L., 2010. Clays and oxide minerals as catalysts and nanocatalysts in Fenton-like reactions – A review. Appl. Clay Sci. 47, 182–192.

Gianfreda, L., Bollag, J.M., (2002). Isolated enzymes for the transformation and detoxification of organic pollutants. En: Burns RG y Dick R (editores). Enzymes in the environment activity, ecology and applications. New York: Marcell Dekker. Pp. 495–538.

Giannelis, E.P., Krishnamoorti, R., Manias, E., (1999). Polymer-silicate nanocomposites: model systems for confined polymers and polymer brushes. Advanced Polymer Science, 138: 107–147.

Giaveno, C., Celi, L., Richardson, A.E., Simpson, R.J., Barberis, E., (2010). Interaction of phytases with minerals and availability of substrate affect the hydrolysis of inositol phosphates. Soil Biology & Biochemistry, 42: 491 – 498.

Gilman, J.W., (1999). Flammability and thermal stability studies of polymer layered-silicate (clay) nanocomposites. Applied. Clay Science, 15: 31–49.

Gilman, J.W., Jackson, C.L., Lomakin, S., Morgan, A.B., Harris, R., Manias, E., Giannelis, E.P., Wuthenow, M., Hilton, D., Phillips, S.H., (2000). Flammability properties of polymer-layered silicate nanocomposites. Polypropylene and polystyrene nanocomposites. Chemistry of Materials, 12: 1866–1873.

Glasby, G.P., (2006). Drastic reductions in utilizable fossil fuel reserves: An environmental imperative. Environ. Dev. Sustain. 8: 197−215.

Goldoni, A., Robertson, J., (2007). In situ Observations of Catalyst Dynamics during Surface-Bound Carbon Nanotube Nucleation Nano Letter, 7: 602-608.

Gomes, C.S.F., Silva, J.B.P., (2007). Minerals and clay minerals in medical geology. Applied Clay Science, 36: 4–21.

Guggenheim, S., Adams, J.M., Bain, D.C., Bergaya, F., Brigatti, M.F., Drits, V.A., Formoso, M.L.L., Galan, E., Kogure, T., Stanjek, H., (2006). Summary of recommendations of nomenclature comittees relevant to clay mineralogy: report of the Association Internationale pour l'Etude des Argiles (AIPEA) Nomenclature Committee for 2006. Clay Minerals, 41: 863–877.

Hall, P.L., Churchman, G.J., Theng, B.K.G., (1985). The size distribution of allophane unit particles in aqueous suspensions. Clays and Clay Minerals, 33: 345–349.

Harbour, P., Dixon, D.R., and Scales P.J. (2007). The role of natural organic matter in suspension stability 1. Electrokinetic–rheology relationships. Colloids and surfaces. A, Physicochemical and engineering aspects, 295: 38–48.

Hashizume, H., Theng, B.K.G., (2007). Adenine, adenosine, ribose and 5'-AMP adsorption to allophane. Clays and Clay Minerals, 55: 599–605.

He, H., Barr, T.L., Klinowski, J., 1995. ESCA and solid-state NMR studies of allophane. Clay Miner. 30, 201–209.

Hedley, C.B., Yuan, G., Theng, B.K.G., (2007). Thermal analysis of montmorillonites modified with quaternary phosphonium and ammonium surfactants. Applied Clay Science, 35: 180–188.

Heilman, M.D., Carter, D.L., González, C.L., (1965). The Ethylene Glycol Monoethyl Ether (EGME) Technique for Determining Soil-Surface Area. Soil Sci., 100: 409–413.

Holister, P., Weener, J.W., Román, C., Harper, T., (2003). Nanoparticles. Cientifica, 3: 1–11.

Horrocks, A.R., Kandola, B.K., Davies, P.J., Zhang, S., Padbury, S.A., (2005). Developments in flame retardant textiles – a review. Polymer Degradation and Stability, 88: 3–12.

Huang, M., Yu, J., Ma, X., (2004). Studies on the properties of montmorillonite reinforced thermoplastic starch composites. Polymer, 45: 7017–7023.

Huang, Q., Liang, W., Cai, P., (2005). Adsorption, desorption and activities of acid phosphatase on various colloidal particles from an Ultisol. Colloids and Surfaces B: Biointerfaces, 45: 209–214.

Huang, X., Netravali, A.N., (2007). Characterization of flax fiber reinforced soy protein resin based green composites modified with nano-clay particles. Composites Science and Technology, 67: 2005–2014.

Hunter, R.J., 1981. Zeta Potential in Colloid Science. Academic Press, London.

Huo, Q., Margolese, D.I., Stucky, G.D., (1996). Surfactant control of phases in the synthesis of mesoporous silica-based materials. Chemistry of Materials, 8: 1147–1160.

Ibarra, L., Rodriguez, A., Mora, I., (2007). Ionic nanocomposites based on XNBR-OMg filled with layered nanoclays. European Polymer Journal, 43: 753–761.

Jara, A., Goldberg, S., Mora, M.L. (2005). Studies of the surface charge of amorphous aluminosilicates using surface complexation models. Journal of Colloid and Interface Science, 292: 160–170.

Jara, A., Violante, A., Pigna, M., Mora, M.L., (2006). Mutual interactions of sulfate, oxalate, citrate, and phosphate on synthetic and natural allophanes. Soil Science Society of America Journal, 70: 337–346.

Jeon, H.S., Rameshwaram, J.K., Kim, G., Weinkauf, D.H., (2003). Characterization of polyisoprene-clay nanocomposites prepared by solution blending. Polymer, 44: 5749–5758.

Joussein, E., Petit, S., Delvaux, B., (2007). Behavior of halloysite clay under formamide treatment. Applied Clay Science, 35: 17–24.

Kashiwagi, T., Du, F., Douglas, J.F., Winey, K.I., Harris, R.H. Jr, Shields, J.R., (2005). Nanoparticle networks reduce the flammability of polymer nanocomposites. Nature Materials, 4: 928–933.

Khedr, M.H., Omar, A.A., Abdel-Moaty, S.A., 2006. Reduction of carbon dioxide into carbon by freshly reduced $CoFe_2O_4$ nanoparticles. Mater. Sci. Eng. A. 432, 26–33.

Khider, K., Akretche, D.E., Larbot, A., (2004). Purification of water effluent from a milk factory by ultrafiltration using Algerian clay support. Desalination, 167: 147–151.

Kim, J., Grate, J.W., Wang, P., (2006). Nanostructures for enzyme stabilization. Chemical Engineering Science, 61: 1017–1026.

Kim, J.M., Stucky, G.D., (2000). Synthesis of highly ordered mesoporous silica materials using sodium silicate and amphiphilic block copolymers. Chemical Communications, 1159–1160.

Klaine, S. J., Alvarez, P. J.J., Batley, G.E., Fernandes, T.F., Handy, R.D., Lyon, D.Y., Mahendra, S., McLaughlin, M. J. and Lead, J.R. (2008). Nanomaterials in the environment: behavior, fate, bioavailability, and effects- Critical Review. Environmental Toxicology and Chemistry, 27: 1825–1851.

Kornmann, X., Lindberg, H., Berglund, L.A., (2001). Synthesis of epoxy-clay nanocomposites: influence of the nature of the clay on structure. Polymer, 42: 1303–1310.

Kresge, C.T., Leonowicz, M.E., Roth, W.J., Vartuli, J.C., Beck, J.S., (1992). Ordered mesoporous molecular sieves synthesized by a liquid-crystal template mechanism. Nature, 359: 710–712.

Lee, L., Saxena, D., Stotzky, G., (2003). Activity of free and clay-bound insecticidal proteins from Bacillus thuringiensis subsp. israelensis against the mosquito Culex pipiens. Applied and Environmental Microbiology, 69: 4111–4115

Lehmann, J., Kinyangi, J., Solomon, D., 2008. Organic matter stabilization in soil microaggreagtes: implications from spatial heterogeneity of organic carbon contents and carbon forms. Biogeochem. 85, 45–57.

Lepoittevin, B., Devalckenaere, M., Pantoustier, N., Alexandre, M., Kubies, D., Calberg, C., Jérôme, R., Dubois, P., (2002). Poly(ε-caprolactone)/clay nanocomposites prepared by melt intercalation: mechanical, thermal and rheological properties. Polymer, 43: 4017–4023.

Li, Z., Hu, N., (2003). Direct electrochemistry of heme proteins in their layer-by-layer films with clay nanoparticles. Journal of Electroanalytical Chemistry, 558: 155–165.

Liff, S.M., Kumar, N., McKinley, G.H., (2007). High-performance elastomeric nanocomposites via solvent-exchange processing. Nature Materials, 6: 76–83.

Liu, Y., Liu, H., Hu, N., (2005). Core-shell nanocluster films of hemoglobin and clay nanoparticle: Direct electrochemistry and electrocatalysis. Biophysical Chemistry, 117: 27–37.

Liu, Y., Pinnavaia, T.J., (2002). Assembly of hydrothermally stable aluminosilicate foams and large-pore hexagonal mesostructures from zeolite seeds under strongly acidic conditions. Chemistry of Materials, 14: 3–5.

Lodha, P., Netravali, A.N., (2005). Characterization of stearic acid modified soy protein isolate resin and ramie fiber reinforced 'green' composites. Composites Science and Technology, 65: 1211–1225.

Lojou, E., Giudici-Orticoni, M.T., Bianco, P., (2005). Direct electrochemistry and enzymatic activity of bacterial polyhemic cytochrome c3 incorporated in clay films. Journal of Electroanalytical Chemistry, 579: 199–213.

Lu, J., Ke, Y., Qi, Z. Yi, X-S., (2001). Study on intercalation and exfoliation behaviour of organoclays in epoxy resin. Journal Polymer Science Part B: Polymer Physics, 39: 115–120.

Ludueña, L.N., Alvarez, V.A., Vazquez, A., (2007). Processing and microstructure of PCL/clay nanocomposites. Materials Science and Engineering A, 460(461): 121–129.

Macilwain, C., (1999). US plans large funding boost to support nanotechnology boom. Nature, 400: 95.

Maharsia, R.R., Jerro, H.D., (2007). Enhancing tensile strength and toughness in syntactic foams through nanoclay reinforcement. Materials Science and Engineering A, 454(455): 416–422.

Malucelli, G., Ronchetti, S., Lak, N., Priola, A., Dintcheva, N.T., La Mantia, F.P., (2007). Intercalation effects in LDPE/o-montmorillonites nanocomposites. European Polymer Journal, 43: 328–335.

Manias, E., Touny, A., Wu, L., Strawhecker, K., Lu, B., Chung, T.C., (2001). Polypropylene/montmorillonite nanocomposites. Review of the synthetic routes and materials properties. Chemistry of Materials, 13: 3516–3523.

Matus, F., Amigo, X., Kristiansen, S.M., (2006). Aluminium stabilization controls organic carbon levels in Chilean volcanic soils. Geoderma, 132: 158–168.

Matus, F., Garrido, E., Sepúlveda, N., Cárcamo, I., Panichini, M., Zagal, E., (2008). Relationship between extractable Al and organic C in volcanic soils of Chile. Geoderma 148, 180–188.

McLaren, R.G., Cameron, K.C., (2000). Inorganic soil colloids. Pp 159–167 in: Soil Science: Sustainable Production and Environmental Protection, Second Edition. Oxford University Press, New Zealand.

Medina, C., Santos-Martinez, M.J., Radomski, A., Corrigan, O.I., Radomski, M.W., (2007). Nanoparticles: pharmacological and toxicological significance. British Journal of Pharmacology, 150: 552–558.

Mella, A., Kühne, A., 1985. Sistemática y descripción de las familias, asociaciones y series de suelos derivados de materiales piroclasticos de la zona central-sur de Chile. In: Tosso, J. (Ed.), Suelos Volcanicos de Chile, First edition. Instituta de Investigaciones Agropecuarias. Ministerio de Agricultura, Santiago, Chile, pp. 549–712

Moelans, D., Cool, P., Baeyens, J., Vansant, E.F., (2005). Using mesoporous silica materials to immobilise biocatalysis-enzymes. Catalysis Communications, 6: 307–311.

Monreal, C.M., Sultan, Y., Schnitzer, M., 2010. Soil organic matter in nano-scale structures of a cultivated Black Chernozem. Geoderma, 159, 237–242.

Montarges-Pelletier, E., Bogenez, S., Pelletier, M., Razafitianamaharavo, A., Ghanbaja, J., Lartiges, B., Michot, L., (2005). Synthetic allophane-like particles: textural properties. Colloids and Surfaces A: Physicochemical and Engineering Aspects, 255: 1–10.

Mora M.L., Shene C., Violante A., Demanet R., Bolan N.S., (2005). The effect of organic matter and soil chemical properties on sulfate sorption in Chilean volcanic soils. P.444. In P.M. Huang et al (ed.) Soil abiotic and biotic iteractions and the impact on the ecosystem and human welfare.Science Publishers, Enfield, NH.

Mora, M.L., (1992). Ph.D. thesis, Universidad de Santiago de Chile.

Mora, M.L., Barrow, N.J., (1996). The effect of time of incubation on the relation between charge and pH of soil. Eur. J. Soil Sci. 47, 131–136.

Mora, M.L., Canales, J., (1995). Interactions of humic substances with allophanic compounds. Commun. Soil Sci. Plant Anal. 26, 2805–2817.

Mora, M.L., Escudey, M., Galindo, G.G., (1994). Sintesis y caracterización de suelos alofánicos. Boletín de la Sociedad Chilena de Química, 39: 237–243.

Musić, S., Santana, G.P., Šmit, G., Garg, V.K., 1999. ^{57}Fe Mössbauer, FT-IR and TEM observation of oxide phases precipitated from concentrated $Fe(NO_3)_3$ solutions. Croat. Chem. Acta 72, 87–102.

Nam, P.H., Maiti, P., Okamoto, M., Kotaka, T., Hasegawa, N., Usuki, A., (2001). A hierarchical structure and properties of intercalated polypropylene/clay nanocomposites. Polymer, 42: 9633–9640.

Navia, R., Fuentes, B., Lorber, K.E., Mora, M.L., Diez, M.C., (2005). In-series columns adsorption performance of Kraft mill wastewater pollutants onto volcanic soil. Chemosphere 60: 870–878.

Ng, C.B., Ash, B.J., Schadler, L.S., Siegel, R.W., (2001). A study of the mechanical and permeability properties of nano- and micron-TiO_2 filled epoxy composites Advanced Composites Letters, 10: 101–111.

Nowack, B., Bucheli, T.D., (2007). Occurrence, behavior and effects of nanoparticles in the environment. Environmental Pollution, 150: 5–22.

Ohashi, F., Wada , S .I., Suzuki, M., Maeda, M. and Tomura, S. (2002). Synthetic allophane from highconcentration solutions: nanoengineering of the porous solid. Clay Minerals, 37, 451-456.

Okada, K., Matsui, S., Isobe, T., Kameshima, Y., and Nakajima, A. (2008). Water-retention properties of porous ceramics prepared from mixtures of allophane and vermiculite for materials to counteract heat island effects. Ceramics International, 34, 345-350.

Parfitt, R.L. Childs, C.W. and Eden, D.N. (1988). Ferrihydrite and Allophane in Four Andepts from Hawaii and Implications for their Classification. Geoderma, 41, 223-241

Parfitt, R.L., (1990). Allophane in New Zealand – A review. Australian Journal of Soil Research, 28: 343–360.

Parfitt, R.L., Russell, M. and Orbell, G.E. (1983). Weathering sequence of soils from volcanic ash involving allophane and halloysite, new zealand. Geoderma, 29, 41-57.

Park, H.M., Lee, W.K., Park, C.Y., Cho, W.J., Ha, C.S., (2003). Environmentally friendly polymer hybrids. Journal of Materials Science, 38: 909–915.

Patel, H.A., Somani, R.S., Bajaj, H.C., Jasra, R.V., (2006). Nanoclays for polymer nanocomposites, paints, inks, greases and cosmetics formulations, drug delivery vehicle and waste water treatment. Bulletin of Materials Science, 29: 133–145.

Pinnavaia, T.J., Beall, G.W., (Editors) (2000). Polymer-Clay Nanocomposites. John Wiley & Sons, New York, 370 pp.

Plank, N.O.V., Howard, I., Rao, A., Wilson, M.W.B., Ducati, C., Mane, R.S., Bendall, J.S., Louca, R.R.M., Greenham, N.C., Miura, H., Friend, R.H., Snaith, H.J., Welland, M.E., 2009. Efficient ZnO nanowire solid-state dye-sensitized solar cells using organic dyes and core-shell nanostructures. J. Phys. Chem. C. 113, 18515–18522.

Plante, A.F., Chenu, C., Balabane, M., Mariott, A., Righi, D., 2004. Peroxide oxidation of clay-associated organic matter in a cultivation chronosequence. Eur. J. Soil Sci. 55, 471–478.

Porta, J., Lopez-Acevedo, M., Roquero, C., (2003). Edafología para la agricultura y el medio ambiente. Ediciones Mundi-Prensa, Madrid, España, 929 pp.

Qian, L., Hinestroza, J.P., (2004). Application of nanotechnology for high performance textiles. Journal of Textiles and Apparel, Technology and Management, 4: 1–7.

Ragauskas, A.J., (2004). Big opportunities with tiny technology. Pulp Paper, 78: 80.

Rahman, M.B.A., Tajudin, S.M., Hussein, M.Z., Rahman, R.N.S.R., Salleh, A.B., Basri, M., (2005). Application of natural kaolin as support for the immobilization of lipase from Candida rugosa as biocatalyst for effective esterification. Applied Clay Science, 29: 111–116.

Rao, M.A. and Gianfreda, L. (2000). Properties of acid phosphatase-tannic acid complexes formed in the presence of Fe and Mn. Soil Biology and Biochemistry, 32, 1921-1926.

Rao, M.A., Violante, A. and Gianfreda L. (2000). Interaction of acid phosphatase with clays, organic molecules and organo-mineral complexes: kinetics and stability. Soil Biology & Biochemistry, 32, 1007-1014.

Ray, V.V., Banthia, A.K., Schick, C., (2007). Fast isothermal calorimetry of modified polypropylene-clay nanocomposites. Polymer, 48: 2404–2414.

Rebollar, P.G., Mateos, G.G., (1999). El fósforo en nutrición animal. Necesidades, valoración de materias primas y mejora de la disponibilidad. En Curso de Especialización FEDNA: Avances en nutrición y alimentación animal. Fundación Española para el Desarrollo de la Nutrición Animal. Eds.: P.G. Rebollar, C. de Blas y G.G. Mateos. Madrid, España.

Redel, Y.D., Rubio, R., Rouanet, J.L., Borie, F., (2007). Phosphorus bioavailability affected by tillage and crop rotation on a Chilean volcanic derived Ultisol. Geoderma, 139: 388–396.

Rong, M.Z., Zhang, M.Q., Zheng, Y.X., Zeng, H.M., Walter, R., Friedrich, K., (2001). Structure-property relationships of irradiation grafted nano-inorganic particle filled polypropylene composites. Polymer, 42: 167–183.

Rosas, A., Mora, M.L., Jara, A., López, R., Rao, M.A., Gianfreda, L., (2008). Catalytic behavior of acid phosphatase immobilized on natural supports in the presence of manganese or molybdenum. Geoderma 145: 77–83.

Ruiz-Hitzky, E., van Meerbeek, A., (2006). Clay mineral- and organoclay-polymer nanocomposite. Pp 583–621 in: Handbook of Clay Science (F. Bergaya, B.K.G. Theng & G. Lagaly, editors). Elsevier, Amsterdam.

Rumpel, C., Chaplot, V., Chabbi, A., Largeau, C., Valentin, C., (2008). Stabilisation of HF soluble and HCl resistant organic matter in tropical sloping soils under slash and burn agriculture. Geoderma 145, 347–354.

Rumpel, C., Eusterhues, K., Kögel-Knabner, I., (2004). Location and chemical composition of stabilized organic carbon in topsoil and subsoil horizons of two acid forest soils. Soil Biol. Biochem. 36, 177–190.

Rumpel, C., Eusterhues, K., Kögel-Knabner, I., (2010). Non-cellulosic neutral sugar contribution to mineral associated organic matter in top-and subsoil horizons of two acid forest soils. Soil Biol. Biochem. 42, 379–382.

Santín, C., González-Pérez, M., Otero, X.L., Álvarez, M.A., Macías, F., (2009). Humic substances in estuarine soils colonized by *Spartina maritime*. Est. Coast Shelf Sci., 81: 481–490.

Schlesinger, W.H., (1986). Changes in soil carbon storage and associated properties with disturbance and recovery. In: Trabalka, J.R., Reichle, D.E., (Eds.). The Changing Carbon Cycle: A Global Analysis. Springer-Verlag, New York, pp. 194–220.

Schulp, C.J.E., Nabuurs, G.J., Verburg, P.H., (2008). Future carbon sequestration in Europe − effects of land use change. Agric. Ecosyst. Environ. 127, 251–264.

Senesi, N., D'Orazio, V., Ricca, G., (2003). Humic acids in the first generation of Eurosoils. Geoderma, 116: 325–344.

Shahwan, T., Erten, H.N., Unugur, S., (2006). A characterization study of some aspects of the adsorption of aqueous Co^{2+} ions on natural bentonite clay. Journal of Colloid and Interface Science, 300: 447–452.

Siegel, R.W., Chang, S.K., Ash, B.J., Stone, J., Ajayan, P.M., Doremus, R.W., Schadler, L.S., (2001). Mechanical behavior of polymer and ceramic matrix nanocomposites. Scripta Materialia, 44: 2061–2064.

Speir, T. W., Horswell, J., Van Schaik, A. P., Mclaren, R. G., Fietje, G. 2004. Composted biosolids enhance fertility of a sandy loam soil under dairy pasture. Biol. Fertil. Soil. 40: 349-358.

Subramani, S., Lee, J.Y., Kim, J.H., Cheong, I.W., (2007). Crosslinked aqueous dispersion of silylated poly(urethane–urea)/clay nanocomposites. Composites Science and Technology, 67: 1561–1573.

Sun, Q., Schork, F.J., Deng, Y., (2007). Water-based polymer/clay nanocomposite suspension for improving water and moisture barrier in coating. Composites Science and Technology, 67: 1823–1829.

Tan, K.H., (1998). Colloidal chemistry of inorganic soil constituents. Pp. 177–258 in: Principles of Soil Chemistry. Marcel Dekker, New York.

Tanev, P.T., Chibwe, M., Pinnavaia, T.J., (1994). Titanium-containing mesoporous molecular sieves for catalytic oxidation of aromatic compounds. Nature, 368: 321.

Tanev, P.T., Pinnavaia, T.J., (1995). A neutral templating route to mesoporous molecular sieves. Science, 267: 865–867.

Tang, Z.Y., Wu, L.H., Luo, Y.M., Christie, P., (2008). Size fractionation and characterization of nanocolloidal particles in soils. Environmental Geochemistry and Health DOI 10.1007/s10653-008-9131-7.

Tatzber, M., Stemmer, M., Spiegel, H., Katzlberger, C., Haberhauer, G., Mentler, A., Gerzabek, M.H., (2007). FTIR-spectroscopic characterization of humic acids and humin fractions obtained by advanced NaOH, $Na_4P_2O_7$, and Na_2CO_3 extraction procedures. J. Plant Nutr. Soil Sci. 170: 522–529.

Theng, B.K.G., Yuan, G., (2008). Nanoparticles in the Soil Environment. Elements, 4: 395-399.

Theng, B.K.G., Churchman, G.J., Gates, W.P., Yuan, G., (2008). Organically modified clays for pollution uptake and environmental protection. Pp 145–174 in: Soil Mineral-Microbe-Organic Interactions (Q. Huang, P.M. Huang & A. Violante, editors). Springer-Verlag, Berlin.

Theng, B.K.G., Russell, M., Churchman, G.J., Parfitt, R.L., (1982). Surface properties of allophane, halloysite, and imogolite. Clays Clay Miner. 30: 143–149.

Theng, B.K.G., Tate, K.R., Becker-Heidmann, P., (1992). Toward establishing the age, location, and identity of inert soil organic matter of a Spodosol. Z. Pflanzenern. Bodenkunde 155: 181–184.

Theng, B.K.G., Yuan, G., Hashizume, H., (2005). Clay minerals and polymers: from soils to nanocomposites. Clay Sci. 12 Supplement 1: 69–73.

Thomson, A.M., Izaurralde, R.C., Smith, S.J., Clarke, L.E., (2008). Integrated estimates of global terrestrial carbon sequestration. Global Environ. Change 18: 192–203.

Tjong, S.C., (2006). Structural and mechanical properties of polymer nanocomposites. Materials Science and Engineering: R-Reports, 53: 73–197.

Toor, G., Hunger, S., Peak, J.D., Sims, J.T., Sparks, D.L., (2006). Advances in the characterization of phosphorus in organic wastes: environmental and agronomic applications. Adv. Agron, 89 : 1–72.

Toor, G.S., Cade-Menun, B.J., Sims, J.T., (2005). Establishing a linkage between phosphorus forms in dairy diets, feces, and manures. J. Environ. Qual, 34: 1380–1391.

Traoré, O., Sinaj, S., Frossard, E., Van De Kerkhove, J. M. (1999). Effect of composting time on phosphate exchangeability. Nutr. Cycl. Agroecosys.55: 123-131.

Tyagi, B., Chudasama, C.D., Jasra, R.V., (2006). Determination of structural modification in acid activated montmorillonite clay by FT-IR spectroscopy Spectrochimica Acta Part A, 64: 273–278.

Usuki, A., Kojima, Y., Kawasumi, M., Okada, A., Fukushima, Y., Kurauchi, T., Kamigaito, O., (1993). Synthesis of nylon 6-clay hybrid. Journal of Materials Research, 8: 1179–1184.

Vamvakaki, V., Chaniotakis, N.A., (2007). Immobilization of enzymes into nanocavities for the improvement of biosensor stability. Biosensors and Bioelectronics, 22: 2650–2655.

Van Der Voort, P., Mathieu, M., Mees, F., Vansant, E.F., (1998). Synthesis of high-quality MCM-48 and MCM-41 by means of the GEMINI surfactant method. Journal of Physical Chemistry B, 102: 8847–8851.

Vidal, G., Navia, R., Levet, L., Mora, M.L., Diez, M.C., (2001). Kraft mill anaerobic color enhancement by a fixed-bed adsorption system. Biotechnology Letters, 23: 861–865.

Villegas, R.A.S., Espírito, Santo, J.L. Jr, Mattos, M.C.S., Aguiar, M.R.M.P., Guarino, A.W.S., (2007). Natural Brazilian clays: Efficient green catalysts for coordination of styrene. Catalysis Communications, 8: 97–100.

Violante, A., Pigna, M., (2002). Competitive sorption of arsenate and phosphate on different clay minerals and soils. Soil Science Society of America Journal, 66: 1788–1796.

Vistoso, E.M., Bolan, N.S., Theng, B.K.G., Mora, M.L., (2009). Kinetics of molybdate and phosphate sorption by some Chilean Andisols. J. Soil Sci. Plant Nutr. 9: 55–68.

Volzone, C., (2007). Retention of pollutant gases: Comparison between clay minerals and their modified products. Applied Clay Science, 36: 191–196.

Wada K. (1967). A structural scheme of soil allophane. The American Mineraiogist, 52: 690–708.

Wada, K., (1987). Minerals formed and mineral formation from volcanic ash by weathering. Chem. Geol. 60, 17–28.

Wada, K., (1989). Allophane and imogolite. In: Dixon J.B., Weed, S.B., (Eds.), Minerals in Soil Environments, Second edition. Soil Science Society of America, Madison, WI, pp. 1051–1087.

Wada, K., Wilson, M., Kakuto, Y. and Wada, S.I. (1988). Synthesis and characterization of a hollow spherical form of monolayer aluminosilicate. Clays Clay Miner., 36: 11–18.

Wang, K., Wang, C., Li, J., Su, J., Zhang, Q., Du, R., Fu, Q., (2007). Effects of clay on phase morphology and mechanical properties in polyamide 6/EPDM-g-MA/organoclay ternary nanocomposites. Polymer, 48: 2144–2154.

Wang, P., (2006). Nanoscale biocatalyst systems. Current Opinion in Biotechnology, 17: 574–579.

Wei, C.L., Zhang, M.Q., Rong, M.Z., Friedrich, K., (2002). Tensile performance improvement of low nanoparticle-filled polypropylene composites. Composites Science and Technology, 62: 1327–1340.

Woignier, T., Braudeau, E., Doumenc, H., Rangon, L., (2005). Supercritical drying applied to natural “gels”: allophanic soils. Journal of Sol-Gel Science and Technology, 36: 61–68.

Woignier, T., Pochet, G., Doumenc, H., Dieudonné, P., Duffours, L., (2007). Allophane: a natural gel in volcanic soils with interesting environmental properties. Journal of Sol-Gel Science and Technology, 41: 25–30.

Woignier, T., Primera, J., Duffours, L., Dieudonne´, P. and Raada, A. (2008). Preservation of the allophanic soils structure by supercritical drying. Microporous and Mesoporous Materials. 109, 370-375.

Woignier, T., Primera, J., Hashmy, A., (2006). Application of the DLCA model to "natural" gels: the allophanic soils. Journal of Sol-Gel Science and Technology, 40: 201–207.

Wu, S., Liu, B., Li, S., (2005). Behaviors of enzyme immobilization onto functional microspheres. International Journal of Biological Macromolecules, 37: 263–267.

Xia, M., Jiang, Y., Li, F., Sun, M., Xue, B. and chen, X. (2009). Preparation and characterization of bimodal mesoporous montmorillonite by sing single. Colloids and Surfaces A: Physicochem. Eng. Aspects, 338: 1–6.

Yasmin, A., Abot, J.L., Daniel, I.M., (2003). Processing of clay/epoxy nanocomposites by shear mixing. Scripta Materialia, 49: 81–86.

Yeh, J.M., Liou, S.J., Lai, M.C., Chang, Y.W., Huang, C.Y., Chen, C.P., Jaw, J.H., Tsai, T.Y., Yu, Y.H., (2004). Comparative studies of the properties of poly(methyl methacrylate)-clay nanocomposite materials prepared by in situ emulsion polymerization and solution dispersion. Journal of Applied Polymer Science, 94: 1936–1946.

Yuan, G. (2005). Environmental Nanomaterials: Occurrence, Syntheses, Characterization, Health Effect, and Potential Applications. Journal of Environmental Science and Health, Part A, 39:10, 2545 – 2548.

Yuan, G., Theng, B.K.G., Parfitt, R.L., Percival, H.J., (2000). Interactions of allophane with humic acid and cations. Eur. J. Soil Sci. 51, 35–41.

Yuan, G., Wu, L., (2007). Allophane nanoclay for the removal of phosphorus in water and wastewater. Science and Technology of Advanced Materials, 8: 60–62.

Zhang, Z., Zhao, N., Wei, W., Wu, D., Sun, Y., (2006). Synthesis and characterization of poly(butyl acrylate-comethyl methacrylate)/clay nanocomposites via emulsion polymerization. International Journal of Nanoscience, 5: 291–297.

Zhao, D.Y., Feng, J.L., Huo, Q.S., Melosh, N., Fredrickson, G.H., Chmelka, B.F., Stucky, G.D., (1998a). Triblock copolymer syntheses of mesoporous silica with periodic 50 to 300 angstrom pores. Science, 279: 548–552.

Zhao, D.Y., Huo, Q.S., Feng, J.L., Chmelka, B.F., Stucky, G.D., (1998b). Nonionic triblock and star diblock copolymer and oligomeric surfactant syntheses of highly ordered, hydrothermally stable, mesoporous silica structures. Journal of the American Chemical Society, 120: 6024–6036.

Zhou, H.X., Dill, K.A., (2001). Stabilization of proteins in confined spaces. Biochemistry, 40: 11289–11293.

Zhou, X., Huang, Q., Chen, S., Yu, Z., (2003). Adsorption of the insecticidal protein of Bacillus thuringiensis on montmorillonite, kaolinite, silica, goethite and Red soil. Applied Clay Science, 30: 87–93.

7

Appendix

7.1 Appendix 1

7.1.1 List of original papers of this thesis:

Calabi-Floody, M., Theng, B.K.G., Reyes, P., Mora, M.L., (2009). Natural nanoclays: applications and future trends - a Chilean perspective. Clay Minerals, 44(16): 1–176

Calabi-Floody, M., Bendall, J.S., Jara, A.A., Welland, M.E., Theng, B.K.G., Rumpel, C., Mora, M.L., (2010). Nanoclays from an Andisol: Extraction, properties and carbon stabilization. Geoderma, doi:10.1016/j.geoderma.2010.12.013.

Calabi-Floody, M., Jara, A.A., Velasquez, G., Saggar, S., Mora, M.L., (2010). Natural nanoclays as support materials to increase the phosphate availability to the plants. In process.

7.2 Appendix 2

7.2.1 Carbon compounds found in clays and nanoclays untreated, and nanoclays treated with H_2O_2

Table 7.2.1. Pyrolysis products identified in compounds by Py-GC/MS

Clays untreated	**Nanoclays untreated**	**Nanoclays treated with H_2O_2**
	Compounds	
Polysaccarides derived	**Polysaccarides derived**	**Polysaccarides derived**
2-methyl-Furan	2-Methyl-Furan	Benzofuran
2,4-dimethyl-Furan,	2,5-dimethylfuran	
2,5-dimethyl-Furan,	2-Vinylfuran	
2,3,5-trimethyl-Furan,	2-Furancarboxaldehyde	
	5-methyl-2-	
2-Vinylfuran	Furancarboxaldehyde	
2-Furancarboxaldehyde	1-(2-furanyl)-Ethanone	
5-methyl-2-Furancarboxaldehyde,	2-Cyclopenten-1-one	
	2-methyl-2-Cyclopenten-1-	
1-(2-furanyl)-Ethanone	one	
	2-hydroxy-3-methyl-2-	
2-methyl-Benzofuran	Cyclopenten-1-one	
2-Furancarbonitrile	Pentanal	
2-Cyclopenten-1-one	2,3-Pentanedione	
2-Methylcyclopentanone		
2-methyl- 2-Cyclopenten-1-one		
3-methyl-2-Cyclopenten-1-one		
2,3-Dimethyl-2-cyclopenten-1-		
one		
2,5-Dimethyl-2-cyclopentenone		

Isoprenoide	**Isoprenoide**	**Isoprenoide**
2-methyl-1,3-Pentadiene		1-Decene
3-methyl-Butanal		1-Tridecene
2,5-dimethyl-1,4-hexadiene		1-Tetradecanol
		pentadecane
		1H-Indene
		(E)-9-Octadecene
		(E)-3-Eicosene
		Phenanthrene

N-containing	**N-containing**	**N-containing**
Propanenitrile	Acetamide	Acetamide
2-Propenenitrile	1H-Indole	Acenaphthylene
2-Butenenitrile	Benzeneacetonitrile	Benzenamine
3-Butenenitrile	3-Butenenitrile	Pyrrole
Pyridine	Propanenitrile	2-Butenenitrile
2-Ethylpyridine	2-Propenenitrile	2-Pyrimidinamine
2-methyl-Pyridine,	Pyridine	Propanenitrile
3-Methylpyridine	2-ethyl-Pyridine	2-Propenenitrile
2,3-Dimethylpyridine	2-methyl-Pyridine	2-methyl-2-Propenenitrile
Methylpyrazine	3-methyl-Pyridine	Pyridine
3-Methylpyridazine	4-methyl-Pyridine	2-methyl-Pyridine
1H-Pyrrole	3-methoxy-Pyridine	3-Pyridinecarbonitrile
1-ethyl-1H-Pyrrole	Pyrazine	Benzyl nitrile
1-methyl-1H-Pyrrole,	ethyl-Pyrazine	2-methyl- Benzonitrile
3-methyl-1H-Pyrrole	2,3-dimethyl-Pyrazine	4-methyl-Benzonitrile
2,5-Dimethyl-1H-pyrrole	1H-Pyrrole	Hexadecanenitrile
1H-Pyrrole-2-carboxaldehyde	3-ethyl-1H-Pyrrole,	Heptadecanenitrile
	2-ethyl-4-methyl-1H-	
1,3-Diazine $$ Pyrimidine	Pyrrole,	4-Pentadienenitrile
1-methyl-2,5-Pyrrolidinedione	1-methyl-1H-Pyrrole	

	2-methyl-1H-Pyrrole 3-methyl-1H-Pyrrole 2,3-dimethyl-1H-Pyrrole 2,5-dimethyl-1H-Pyrrole 1H-Pyrrole-2-carboxaldehyde 1-(1H-pyrrol-2-yl)-Ethanone 2-Formyl-1-methylpyrrole 3,4-Dimethyl-1H-pyrrole-2,5-dione 1-methyl-2,5-Pyrrolidinedione,	
Unspecific origin	**Unspecific origin**	**Unspecific origin**
Phenol 3-methyl-Phenol 4-methyl-Phenol 1-phenyl-Ethanone Toluene Styrene Ethylbenzene isocyanato-Benzene Acetic acid DIMETHYLDISULFIDE	Phenol 4-methyl-Phenol Toluene Styrene 2-methyl-Benzoxazole Isocyanato-Benzene Acetic acid Propanoic acid 2-Butenoic acid (Z)-2-Butenoic acid methyl-ester-2-Butenoic acid,	Phenol Benzene Toluene Styrene 1,2-dimethyl-Benzene 1-propenyl-Benzene, 2-propenyl- Benzene Naphthalene 2-ethenyl- Naphthalene 1-methyl- Naphthalene 2-methyl- Naphthalene Acetic acid Thiophene Undecane Isoquinoline 9H-Fluorene

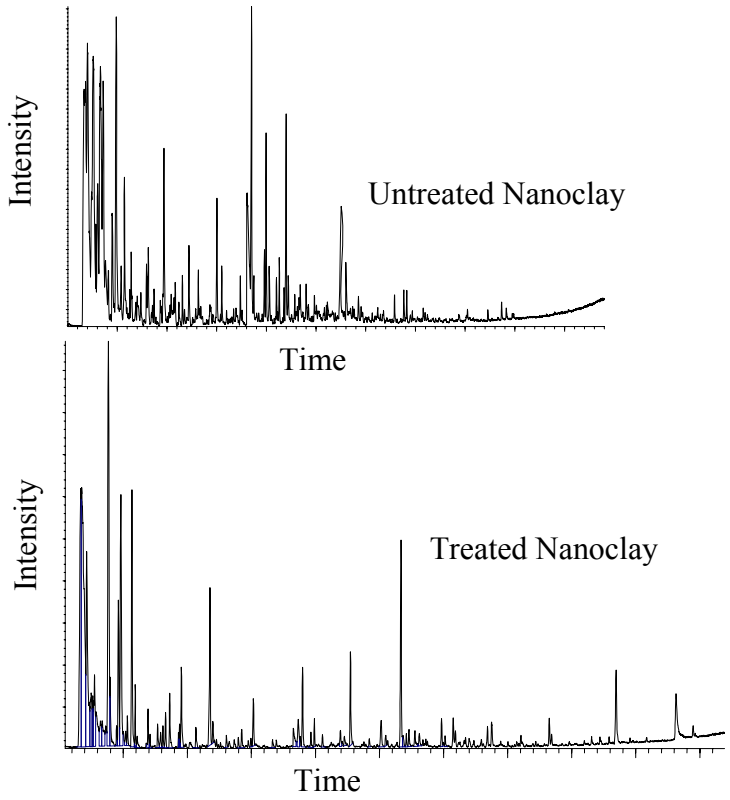

Figure 7.2.2. Pyrograms of nanoclays before and after treatment to remove organic matter.